NORADRENERGIC MECHANISMS OF PRECLINICAL ALZHEIMER'S DISEASE

By

Sarah Colette Kelly

A DISSERTATION

Submitted to
Michigan State University
in partial fulfillment of the requirements
for the degree of

Cell and Molecular Biology—Doctor of Philosophy

2018

ABSTRACT

NORADRENERGIC MECHANISMS OF PRECLINICAL ALZHEIMER'S DISEASE

By

Sarah Colette Kelly

Noradrenergic locus coeruleus (LC) neuron loss is a feature of Alzheimer's disease (AD). The LC is the primary source of norepinephrine (NE) in the forebrain, where it modulates attention and memory in vulnerable cognitive regions such as prefrontal cortex (PFC) and hippocampus. Furthermore, LC-mediated NE signaling is thought to play a role in blood-brain barrier (BBB) maintenance and neurovascular coupling, suggesting that LC degeneration may impact the high comorbidity of cerebrovascular disease (CVD) and AD. However, the extent to which LC projection system degeneration occurs in the earliest stages of AD and the physiological consequences of this phenomenon is not fully characterized to date. To address these issues, we analyzed LC tissue samples from University of Kentucky AD Center (UKADC) subjects who died with a premortem diagnosis of no cognitive impairment (NCI) and Braak stages 0-II at autopsy, NCI subjects with Braak stages III-V thought to be in a preclinical AD (PCAD) stage, and subjects with mild cognitive impairment (MCI) or mild AD. Paraffin-embedded pontine tissue blocks containing the LC were cut at 20μm, immunostained with tyrosine hydroxylase (TH, a marker for NE synthesis), and analyzed to estimate total TH-positive LC neuron number. We measured a significant ~40-55% loss of LC neuron numbers in MCI and AD compared to NCI, whereas the mild ~25% LC neuron loss observed in PCAD did not reach significance. However, the topographical, rostrocaudal extent of LC cell loss in PCAD was significantly different

from NCI and MCI. Moreover, LC cell loss correlated with premortem global cognition across the diagnostic groups. Studies were also performed to compare additional LC neuronal pathologies (phospho-tau and DNA/RNA oxidative damage markers) across the diagnostic groups. A significant ~15-30% increase in phospho-tau was observed in PCAD and MCI compared to NCI. DNA/RNA oxidative damage was significantly increased by ~25-40% in MCI and AD compared to NCI and PCAD. LC phospho-tau pathology correlated with Braak stage, whereas LC oxidative damage correlated with premortem global cognitive performance . Finally, while LC neuron number did not correlate with scores of global arteriosclerosis or microinfarcts, pontine arteriosclerosis severity was increased by two-fold in MCI and AD. To model the relationship between LC projection system degeneration and forebrain neuronal and vascular pathology *in vivo*, we stereotactically lesioned LC projection neurons innervating the PFC of the TgF344-19 rat model of AD (aged 6 months) using the noradrenergic immunotoxin, dopamine-β-hydroxylase IgG-saporin (DBH-sap), or an untargeted control IgG saporin (IgG-sap). DBH-sap lesioned animals performed significantly worse on the Barnes maze task and displayed increased amyloid and inflammatory pathology, as well as evidence for vessel remodeling and BBB leakage, compared to IgG-sap control animals. Taken together, these data compiled in my dissertation shed light on the multifactorial noradrenergic pathways contributing to neuronal and vascular pathologies during the onset of AD

Dedicated to the memory of James Lee Anderson

ACKNOWLEDGMENTS

I would first and foremost like to thank my advisor, Dr. Scott Counts, for his unfaltering support and guidance during my graduate career. Regardless of the activity, Scott has always given me advice and encouragement, and his support has helped shape me into the scientist and individual that I am today. I would also like to express my sincere gratitude to the members of my committee, Dr. Timothy Collier, Dr. Nicholas Kanaan, and Dr. Irving Vega, for their insights and collaboration. Furthermore, I would like to thank Dr. Susan Conrad for her role not only as a committee member but as an advocate for myself and the other students in the CMB program.

To the members of the Counts laboratory, past and present, I thank you for sharing your knowledge and supporting me throughout my graduate career. John Beck is the master of all things molecular, and I have learned so much from him over the years. I would like to especially thank my fellow graduate student Erin McKay, for not only her assistance with behavior and surgeries, but her friendship and advice. I would also like to acknowledge the TSMM staff from other labs, especially Tessa Grabinski, Brian Daley, Allyson Cole-Strauss, and Christopher Kemp for going outside the scope of their jobs to help me establish many new protocols and for their advice with troubleshooting.

The TSMM department has a small, but tight-knit group of students who are always willing to help others, and for that I will always be grateful. The “Who Cares” trivia team will always hold a special place in my heart. I would particularly like to thank Rhyomi Sellnow, Kelly Fader, and Nicole Polinski for always keeping my spirits up,

pushing me in my career, and being down to grab a Starbucks when an experiment didn’t go as planned.

Additionally, I would like to thank all sides of my family, the Kellys, the Andersons and the Millers as well as my friends outside of lab for their encouragement, support, and understanding during this journey. Finally, I would like to thank my husband Sean. His optimism, unwavering support, and humor has always kept me grounded. You have been my constant cheerleader, listened to every presentation no matter how boring, and always made the best cookies. The cats and I are lucky to have you in our lives.

PREFACE

At the time of writing this dissertation, both chapters describing the research of my Specific Aims are in preparation for publication and will be submitted in the near future. Images in the introduction to Chapter 2 were published by our laboratory in 2017 as part of an article in *Acta Neuropathologica Communications*.

TABLE OF CONTENTS

LIST OF TABLES

LIST OF FIGURES

KEY TO ABBREVIATIONS

AAALAC	Association for Assessment and Accreditation of Laboratory Animal Care
Aβ	β-amyloid
AChE	Acetylcholine Esterase
ACTA2	Alpha Actin 1
AD	Alzheimer's Disease
aMCI	Amnestic Mild Cognitive Impairment
APOE	Apolipoprotein
APP	Amyloid Precursor Protein
APPswe	APP Swedish mutation
BACE	β-APP cleaving enzyme
BBB	Blood-Brain Barrier
CAA	Cerebral Amyloid Angiopathy
CBF	Cerebral Blood Flow
CDR	Clinical Dementia Rating
CERAD	Consortium to Establish a Registry for Alzheimer's Disease
CNS	Central Nervous System
CSF	Cerebrospinal Fluid
CV	Cerebrovascular
CVD	Cerebrovascular Disease
Cytc1	Cytochrome C1
DA	Dopamine

DBH	Dopamine β-Hydroxylase
DBH-sap	Dopamine B-Hydroxyase Saporin
DLB	Dementia with Lewy Bodies
DOPEGAL	Dihydroxyphenylglycolaldehyde
EPM	Elevated Plus Maze
GCS	Global Cognitive Score
GFAP	Glia Fibrillary Acidic Protein
H&E	Hematoxylin and Eosin
HBAV	Healthy Brain Aging Volunteers
IACUC	Institutional Animal Care and Use Committee
Iba1	Ionized Calcium Binding Adaptor Molecule 1
IgG-sap	Untargeted IgG Saporin
IHC	Immunohistochemistry
L-DOPS	L-Dihydroxyphenylserine
LAAAD	L-Aromatic-Amino-Acid Decarboxylase
LC	Locus Coeruleus
MAO	Monoamine Oxidase
MCI	Mild Cognitive Impairment
Me5	Mesencephalic Tract of 5
MLF	Medial Longitudinal Fasciculus
MMSE	Mini-Mental State Examination
MTL	Medial Temporal Lobe
MV	Mesencephalic Vellum

MWM	Morris Water Maze
NB	Nucleus Basalis
NE	Norepinephrine
NET	Norepinephrine Transporter
NFT	Neurofibrillary Tangle
NIA	National Institute of Aging
NCI	No Cognitive Impairment
NMDA	N-methyl-D-aspartate
Nrf1	Nuclear Respiratory Factor 1
NVU	Neurovascular Unit
oh8dG	8-hydroxy-2’-deoxyguanosine
oh8G	8-hydroxyguanosine
PCAD	Preclinical Alzheimer's Disease
PD	Parkinson’s disease
PFC	Prefrontal Cortex
PMI	Post Mortem Interval
PS1dE9	Presinilin 1 Delta Exon 9
PSEN1	Presinilin 1
PSEN2	Presinilin 2
RROS	Rush Religious Orders Study
SCP	Spinocerebellar Peduncle
SD	Standard Deviation
SEM	Standard Error of the Mean

SVD	Small Vessel Disease
TBI	Traumatic Brain Injury
TBS	Tris Buffered Saline
TgF344	Transgenic Fisher 344-19 AD rat
TH	Tyrosine hydroxylase
TX	Triton X-100
UKADC	University of Kentucky Alzheimer's Disease Center
WLR	Wall to Lumen Ratio
WML	White Matter Lesion
WT	Wild Type

Chapter 1: Introduction and Dissertation Objectives

Introduction

There was once a long-held assumption that the vascular and neuronal architecture of the brain were independent systems. Until recently, the dichotomization of these major entities of the brain has precluded a comprehensive analysis of the pathologic mechanisms underlying multifactorial neurodegenerative diseases such as Alzheimer's disease (AD). For instance, it is now understood that the brain receives one fifth of the cardiac output and as well as one-fifth of the body's oxygen and glucose, even though the brain only accounts for 2% of the total body mass (Mergenthaler et al. 2013). Indeed, healthy brain function requires the delivery of oxygen, energy metabolites and nutrients through a vast, approximately 400-mile-long network of arteries, arterioles and capillaries via cerebral blood flow (CBF), coupled with efficient efflux and clearance of carbon dioxide, metabolic waste products, and potentially toxic cellular debris through venules and the rest of the venous system (Zlokovic 2008). This process is tightly regulated by the blood-brain barrier (BBB), which allows for the selective transport of nutrients into metabolically active areas of the brain, while excluding blood and neurotoxins. Therefore, dysregulation of the BBB can cause irreparable neuronal damage and, if severe or prolonged enough, extensive brain damage and death (Iadecola 2013). Significantly, there is evidence for cerebrovascular dysfunction in AD, including *in vivo* evidence such as decreased perfusion (Iturria-Medina et al. 2016; Chen et al. 2011) and reduced metabolic function(Mosconi, Andrews, and Matthews 2013; Chen and Zhong 2013) as well as postmortem observations that vascular lesions

such as microinfarcts and microbleeds are present in up to 84% of AD cases and correlate with antemortem cognitive function (Jellinger 2002; Schneider et al. 2007; Esiri et al. 2014; Attems and Jellinger 2014). Hence, understanding the role of CV pathology in neurodegeneration and AD will allow for a more comprehensive understanding of disease pathogenesis.

Notably, there are many known and proposed regulators of CBF dynamics and BBB regulatory function but the mechanisms underlying the progression of AD are unclear (reviewed in: (Zenaro, Piacentino, and Constantin 2017; Erickson and Banks 2013; Zlokovic 2008; Daneman and Prat 2015). In this regard, noradrenergic forebrain projection neurons of the locus coeruleus (LC) have been implicated in regulating BBB permeability, neurovascular coupling, and perfusion (Bekar, Wei, and Nedergaard 2012; Bekar, He, and Nedergaard 2008; Toussay et al. 2013). Located in the pontine brainstem, this population of neurons has been shown to degenerate in end-stage AD (Bondareff, Mountjoy, and Roth 1981a; Mann et al. 1980b) and, more recently, we demonstrated that LC degeneration begins even before the onset of amnestic mild cognitive impairment (aMCI), a putative prodromal stage of AD (Kelly et al. 2017; Theofilas et al. 2017; Arendt et al. 2015). LC projection neurons are the sole source of norepinephrine (NE) in cognitive areas of the brain such as neocortex and hippocampus, where they regulate attention and memory (Arnsten and Goldman-Rakic 1984, 1985; Aston-Jones and Cohen 2005; Aston-Jones and Bloom 1981; Szabadi 2013; Sara 2009b). Therefore, given the increased prevalence of vascular pathology found in the brains of patients with AD and related dementias, understanding the extent to which the loss of NE signaling is linked to vascular dysfunction in AD is an important

and understudied problem in the field. Here, we will review the literature leading us to connect LC cell loss to vascular dysfunction in AD pathogenesis.

Alzheimer's disease

Dr. Alois Alzheimer was credited as being the first to describe the disease while observing a patient, August Deter at the Frankfurt Psychiatric Hospital in November 1901 (Hippius and Neundorfer 2003; Alzheimer et al. 1995). He described the 50-year-old woman whom he had studied from her admission for paranoia, sleep and memory disturbance, aggression, and confusion, until her death 5 years later. His reports described distinctive plaques and neurofibrillary tangles (NFTs) in the brain histology, which we now know are composed of aggregated extracellular β-amyloid (Aβ) or intracellular hyper-phosphorylated tau proteins respectively. Since then, we have come to call the disease he described as Alzheimer's disease (AD).

AD is the most common dementing disorder and is the sixth leading cause of death in the United States (Alzheimer's 2018). Currently, 1 in 10 older adults (>65 years) in the US currently suffer from this debilitating disease, about 5.7 million people (Alzheimer's 2018). The elevated economic and social impact of dementia has been considered as a public health priority by the World Health Organization (Frankish and Horton 2017). The number of Americans suffering from AD will grow to almost 14 million by the year 2050 (Hebert et al. 2013). This will lead to 1 in 3 seniors dying with AD or another dementia, yet there is no cure or treatment that slows disease progression or symptom severity. With life expectancy increasing, and thus a population shifting to a more aged demographic, it is estimated that by 2050 there will be 15 million AD patients

in the United States with the cost of their care exceeding 1 trillion dollars annually (Alzheimer's 2018; Hebert et al. 2001; Hebert et al. 2013). Hence, the need to understand and treat this disease is paramount.

AD is commonly characterized by synapse and cell loss in discrete cortical and subcortical neuronal populations underlying memory, attention, and higher order cognition (e.g. prefrontal cortex, entorhinal cortex and hippocampus.) ultimately leading to an inability to undertake ordinary activities of daily living (e.g., hygiene, dressing, eating) and a loss of independent functioning. Post-mortem neuropathological hallmarks of the disease include extracellular Aβ plaques, intracellular NFTs composed of highly phosphorylated tau protein, brain atrophy and increased neuroinflammation (Selkoe 2001). However, changes in brain histopathology, and consequently in brain structure and function, are known to precede the signs and symptoms of the disease by many years.

AD pharmacotherapies

Current symptomatic therapies for AD include the acetylcholinesterase inhibitors (donepezil (Aricept; Eisai/Pfizer), galantamine (Razadyne; Johnson & Johnson) and rivastigmine (Exelon; Novartis)), and a low-affinity NMDA (N-methyl-D-aspartate) receptor antagonist (memantine) for moderate to severe AD. The acetylcholinesterase (AChE) inhibitors enact their effects by remediating, in part, the cholinergic deficit in AD, caused by the degeneration of the nucleus basalis. AChE inhibitors enhance cholinergic neurotransmission through inhibition of enzyme AChE, thus decreasing the breakdown of acetylcholine (Bartus et al. 1982). Nicotinic acetylcholine receptor sensitizers

(galantamine) have similar effects (Maelicke 2000). Memantine improves the signal-to-noise ratio of glutamatergic transmission and protects cortical neurons from the toxic effects of chronic overexposure to glutamate(Greenamyre et al. 1988). These treatments confer a delay in symptom progression of several months but have inconsistent effects on activities of daily living (Farlow, Miller, and Pejovic 2008) and a doubtful impact on the behavioral disturbances that are associated with AD (Grimmer and Kurz 2006). Furthermore, present medications do not delay the progression from minor cognitive impairment which does not significantly interfere with functional ability to dementia(Raschetti et al. 2007). Hence, the need for a better understanding of the heterogenouos mechanisms underlying AD pathophysiology will be necessary to develop a treatment regimen that modifies the progression of the disease.

AD diagnostic criteria

While the specific etiology of AD remains unknown, AD is characterized by certain pathologies required for a definitive diagnosis. Specifically, AD requires the presence of extracellular amyloid plaques (Terry, Gonatas, and Weiss 1964; Selkoe 2001; Glenner and Wong 1984) composed of insoluble aggregates of Aβ and intracellular NFTs composed of abnormally phosphorylated tau (Grundke-Iqbal, Iqbal, Quinlan, et al. 1986; Kosik, Joachim, and Selkoe 1986). While, a definite diagnosis for AD requires the presence these pathologies in the brain parenchyma following post-mortem analysis, a probable diagnosis can be achieved on a clinical basis. Various clinical instruments can be used to screen patients for AD, including the mini-mental state exam (and variants thereof), the memory impairment screen (Buschke et al. 1999), the Blessed test of

information (Katzman et al. 1983), and the Clinical Dementia rating scale (Jalbert, Daiello, and Lapane 2008).

Well characterized hallmarks of AD

β-amyloid plaque pathology

β-amyloid (Aβ) was identified as the major component of the plaques found in AD brains which is formed from the cleavage of the amyloid precursor protein (APP) by β- and γ-secretase, resulting in Aβ40 and Aβ42(Glenner and Wong 1984). Aβ42 is more prone to aggregation and is associated with neurotoxicity (Gouras et al. 2000; Greenfield et al. 1999). These Aβ aggregates assemble into β-sheets and can be histologically stained with Congo Red or thioflavin dyes. The discovery that AD could be inherited in an autosomal dominant fashion was a definitive even in the history of AD research (Goate et al. 1991). The mutation that was described was in the gene coding for APP, a holoprotein from which the amyloid-β peptide is excised via sequential cleavage by the β-APP cleaving enzyme (BACE;β-secretase) and γ-secretase. These observations led to the establishment of the amyloid cascade hypothesis. This was further supported by the discovery that AD could also be caused by autosomal dominant mutations in genes coding for presenilin 1 (PSEN1) and presenilin 2 (PSEN2), which are homologous proteins that can form the catalytic active site of γ-secretase.

The amyloid cascade hypothesis, which suggests that the deposition of the Aβ peptide in the brain is a central event in Alzheimer's disease pathology, has dominated research for the past twenty years (Hardy and Higgins 1992). Several therapeutics that were supposed to reduce Aβ production or aggregation, such as passive

immunotherapy with Aβ antibodies and BACE inhibitors, have been discontinued due to peripheral side effects (e.g., liver damage) or have failed to meet primary endpoints in Phase III clinical testing, (Kennedy et al. 2016; Honig et al. 2018). This has led researchers to evaluate more critically the importance of other AD hallmarks such as NFTs, inflammation, and oxidative stress, as well as common AD co-morbidities such as hypertension and diabetes, as important potential targets for disease-modifying therapeutics.

Tau and NFT pathology

NFTs are intracellular inclusions composed of aggregated tau proteins in the form of paired helical or straight filaments (Goedert *et al.*, 2006). Tau is normally a highly soluble protein found predominantly in neurons. Six different isoforms of tau are expressed in the adult human central nervous system (CNS) via alternative splicing of the *MAPT* gene, which comprises 16 exons and is found on chromosome 17q21.3. Regulated inclusion of exons 2 and 3 gives rise to tau isoforms with 0, 1, or 2 N-terminal inserts, whereas exclusion or inclusion of exon 10 leads to expression of tau isoforms with three (3R) or four (4R) microtubule-binding repeats (Goedert, Crowther, and Garner 1991; Binder, Frankfurter, and Rebhun 1985). Both 3R and 4R tau isoforms comprise tau aggregates in AD. The tau proteins comprising NFTs are aberrantly phosphorylated which may render it more prone to aggregation than unphosphorylated tau (Noble et al. 2013). Tau contains 85 potential serine (S), threonine (T), and tyrosine (Y) phosphorylation sites. Many of the phosphorylated residues on tau are found in the proline-rich domain of tau, flanking the microtubule-binding domain.

Braak and Braak proposed a neuropathological staging to differentiate initial, intermediate, and advanced AD based on the spread of neurofibrillary tangles (NFTs) beginning within the medial temporal lobe (MTL) memory circuit and spreading in a topographical manner to neocortex: Braak stage 0 corresponds to absence of NFTs, stages I–II to entorhinal-perirhinal cortex NFTs, stages III–IV to NFTs additionally in hippocampus and stages V–VI to NFTs distributed in wider neocortical areas(Braak and Braak 1991a, 1991b; Braak et al. 2011).Notably, corticopetal projection systems regulating memory and attention such as the LC and nucleus basalis display prominent NFT pathology concurrent with initial Braak stages but are not included in this neuropathological staging scheme (Zarow 2003, Arendt 2015). Despite Aβ plaques being studied often in favor of NFTs as a causative pathology in AD, the density of these plaques does not correlate closely with the progression of AD (Braak and Braak 1991a; Arriagada et al. 1992). The spatiotemporal development of tau pathology, however, associates very well with the cognitive decline of AD (Bierer et al. 1995; Morris et al. 1991). In particular, Nelson and colleagues demonstrated that the number of neocortical NFTs was highly correlated with antemortem performance on the MMSE in a large autopsy cohort (Nelson et al. 2007).

While these classic hallmarks of the disease have been studied at length, the etiologic factors that contribute to AD pathogenesis remain unclear**.** The amyloid cascade hypothesis and the clinical 'Jack curves' imply a temporally linear relationship between Aβ pathology, tau pathology and *in vivo* brain atrophy, and the onset of dementia. (Jack and Holtzman 2013; Selkoe and Hardy 2016) However, AD is a multifactorial disease with potential contributions from the dysregulation of a broad array

of cellular pathways (Mufson et al. 2012) indicating a much more complex process not only involving neurons, but also other cellular reactions from immune cells and the vasculature.

The cerebrovasculature—a vulnerable system in aging

While AD has many classical hallmarks like Aβ plaques and NFTs, vascular pathology is starting to be recognized as a hallmark of the disease, as well. The vasculature of the brain is quite different than that of the peripheral vasculature. Notably, the tightly regulated BBB, which is confined to the central vasculature, is a continuous endothelial membrane within brain microvessels that has sealed cell-to-cell contacts and is sheathed by mural vascular cells (smooth muscle cells on arteries and arterioles; pericytes on capillaries) and perivascular astrocyte end-feet (Iadecola and Dirnagl 2013). The BBB protects neurons from factors present in the systemic circulation and maintains the highly regulated CNS internal milieu via gap junctions and nutrient transporters, which is required for proper synaptic and neuronal functioning (Abbott, Ronnback, and Hansson 2006; Daneman and Prat 2015). Moreover, the tightly sealed cell-to-cell contacts of the BBB result in high transendothelial electrical resistance and low paracellular and transcellular permeability (Zlokovic 2008).

In this context, the concept of the neurovascular unit (NVU) emerged from the first Stroke Progress Review Group meeting of the National Institute of Neurological Disorders and Stroke of the NIH (July 2001) to emphasize the unique relationship between brain cells and the cerebral vasculature to control hyperaemia and maintain homeostasis in the CNS (Iadecola 2017; Muoio, Persson, and Sendeski 2014)

(**Figure1.1**). When these highly regulated features of the BBB break down through mounting vascular insults, however, this facilitates entry into the brain of neurotoxic blood-derived products, cells and pathogens and is associated with inflammatory and immune responses, which can initiate multiple neurodegenerative pathways (reviewed in Sweeney, Sagare, and Zlokovic 2018).

Cerebrovascular disease: A hallmark of AD

Cerebrovascular disease (CVD)—usually in the form of small vessel occlusive disease caused by chronic hypertension and other vascular risk factors— is a condition that commonly accompanies aging, underlies the pathophysiology of vascular cognitive impairment (VCI), and is frequently observed in the brains of people who died with MCI or AD (Serrano-Pozo et al. 2011). These mixed vascular pathologies in AD patients suggest that AD often involves a microvascular disorder that may contribute to its pathogenesis and high co-morbidity with CVD (Schneider et al. 2009). Additionally, CVD has the potential to induce an unpredictable change in cognition and presents challenges to correlating the severity of cognitive decline with the severity of neurodegenerative diseases. For instance, AD is associated with cerebral amyloid angiopathy (CAA), microvascular degeneration, hypertensive arteriopathy (tortuosity, fibrohyalinosis, and lipohyalinosis), disorders of the BBB, white matter lesions, microinfarctions, lacunes, and cerebral hemorrhages (Jellinger and Attems 2007). CVD is not just observed in frank aging or AD. Multiple forms of vascular dysfunction have been observed in other neurodegenerative disorders. For example, capillary leakages have been observed in the striatum of PD patients (Pienaar et al. 2015; Gray and

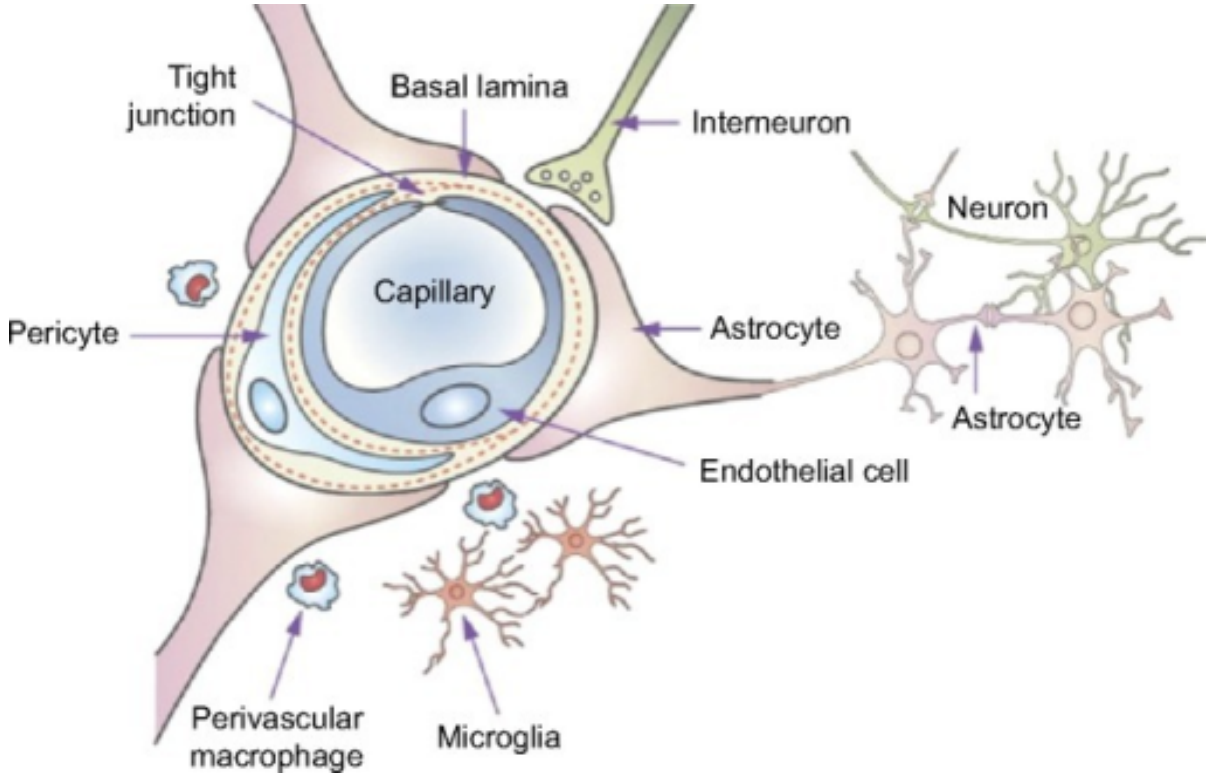

Figure 1.1 The neurovascular unit (NVU)

Schematic of the blood–brain barrier and the associated components of the neurovascular unit. *Note*: Reprinted from Adv Drug Deliv Rev, 64(7), Chen Y, Liu L. Modern methods for delivery of drugs across the blood–brain barrier. 640–665., Copyright (2012), with permission from Elsevier (Chen and Liu 2012).

Woulfe 2015), and the putamen of individuals with Huntington's disease (Drouin-Ouellet et al. 2015). Reduced mural cell coverage has been noted in brains of individuals with chronic traumatic encephalopathy and HIV-Associated dementia (Niu et al. 2014; Omalu et al. 2005). Additionally, aberrant angiogenesis has been observed in the LC and substantia nigra of individuals with PD and Lewy body dementia(Desai Bradaric et al. 2012; Wada et al. 2006).

Here we briefly review the cardinal features of these CVD lesions and outline the evidence for their involvement in the pathophysiology of AD-related dementia.

Infarcts

Cerebral infarction is focal brain necrosis due to complete and prolonged ischemia (deoxygenation) that affects all tissue elements, neurons, glia, and vessels. Lacunar infarcts are smaller infarcts in the deeper parts of the brain (e.g. basal ganglia, thalamus, white matter) and in the brain stem (Iadecola 2013). Lacunar infarcts are responsible for about 20 percent of all strokes(Williams 2001). They are caused by occlusion of deep penetrating branches of major cerebral arteries and are particularly common in hypertension and diabetes, which are associated with severe atherosclerosis of small vessels and small vessel disease(Gorelick et al. 2011; Hachinski et al. 2006).

Hemorrhagic stroke

While the majority of strokes are ischemic in nature, mortality is much higher following hemorrhagic stroke, i.e., up to 50% within the first 30 days after the insult (van Asch et al. 2010).Bleeding can be caused by traumatic brain injury (TBI) or occur spontaneously in hemorrhagic strokes, while intracerebral and subarachnoid hemorrhage account for 15% and 5% of all strokes, respectively. The hematoma increases intracranial pressure and is associated with oxidative stress, inflammation, and cell death (Pluta et al. 2009; Mracsko and Veltkamp 2014).

White matter lesions

Areas of high signal intensity on T2-weighted MRI of older individuals termed white matter hyperintensities or white matter lesions (WMLs) are of particular interest in the field of VCI. Pathological findings of WMLs include myelin pallor, tissue rarefaction associated with loss of myelin and axons, and mild gliosis (Debette and Markus 2010; Schmidt et al. 2011). These lesions are located in the deep white matter and are often seen together with vessels affected by small vessel disease (Silbert et al. 2008). Evidence suggests that at least more extensive forms of WMLs are a consequence of and indicative for small vessel disease, and thus are associated with a higher risk for stroke, dementia, and mortality (Debette and Markus 2010; Schmidt et al. 2011).

Cerebral amyloid angiopathy

CAA is characterized by the accumulation of amyloid in the leptomingeal and cerebral vessels of the central nervous system. By far the most common form of CAA is the Aβ type, defined by the accumulation of aggregated Aβ peptide in small cerebral vessels—most prominently the penetrating arterioles of the cortex (Attems et al. 2011). These deposits are located near the basement membrane or in the smooth muscle cell layer (reviewed in (Jellinger 2013). CAA can lead to vessel wall rupture and hemorrhage, microbleeds, capillary occlusion, blood flow disturbances, and to microinfarcts (Thal et al. 2009; Okamoto et al. 2012). CAA most frequently involves leptomeningeal and neocortical arteries, veins, and/or capillaries, later vessels in allocortical regions (hippocampus, entorhinal and cingulate cortex, amygdala). The hypothalamus and the cerebellum exhibit CAA as well, whereas blood vessels of the brainstem are involved later (Thal et al. 2003).

Atherosclerosis and small vessel disease

Atherosclerosis is a degenerative disorder of arteries that leads to tunica intima proliferation and accumulation of cholesterol within the vessel wall. These processes result in the generation and calcification of atherosclerotic plaques, which rupture frequently and induce local thrombosis. It can cause large brain infarcts, whereas embolism of atherogenic thrombi can lead to a broad variety of infarcts (Grinberg and Thal 2010). Small vessel disease (SVD) comprises lipohyalinosis and arteriolosclerosis. These vessel wall changes are similar to that of larger blood vessels except for calcifications not seen in small arterioles (Hachinski et al. 2006).

Cerebrovascular dysfunction in aging and AD

AD is believed to have an extensive preclinical stage since older people with a clinical diagnosis of no cognitive impairment (NCI) or MCI consistently reveal pathological signatures similar to those with frank AD (Albert et al. 2011; Markesbery et al. 2006). Moreover, the majority of MCI and AD cases also present with cerebrovascular pathology such as CAA, lipohyalinosis, microbleeds, microinfarctions, and white matter lesions (Jellinger and Attems 2007), and vascular comorbidities are significant risk factors for cognitive decline (Schneider et al. 2009).

In normal aging, CVD of any form is detectable in 75% to 90% of persons older than 90 years and frank clinical strokes affect approximately 750,000 Americans each year (Williams 2001). In one study, the US National Alzheimer Disease Coordinating Center database was used to identify 5,715 patients with an autopsy-based diagnosis of a single neurodegenerative disease (Toledo et al. 2013). Within the subgroup of 4,629 patients diagnosed as having AD who had no evidence of mixed dementia, 80% had vascular pathology including cerebrovascular disease, lacunae and multiple microinfarcts indicative of small vessel disease, hemorrhage, atherosclerosis, arteriolosclerosis and CAA (Toledo et al. 2013). Additionally, epidemiological studies have shown that AD and CVD share common risk factors such as hypertension during midlife, diabetes mellitus, smoking, apolipoprotein E (APOE) ε4 isoforms, hypercholesterolemia, homocysteinemia in addition to age (Meng et al. 2014; Barnes and Yaffe 2011; Casserly and Topol 2004; Gorelick et al. 2011). Interestingly, a recent study revealed that global CBF was lower in cognitively normal APOE4-carriers compared to APOE4 non-carriers prior to development of amyloid deposits (Michels et

al. 2016). Moreover, APOE4 subjects who developed amyloid deposition showed lower global CBF compared to those who were free of amyloid (Michels et al. 2016). Cardiovascular risk factors, e.g., atrial fibrillation and congestive heart failure, have also been linked to the pathogenesis and progression of AD and are among the most important modifiable risk factors for AD (Eriksson et al. 2010; Mielke et al. 2007; Kivipelto et al. 2006; Ahtiluoto et al. 2010; Toledo et al. 2012).

The prevalence and incidence of SVD increases with age, however, the prevalence of the lesions caused by SVD varies in the oldest old: macroscopic intracranial hemorrhages are rare, while microscopic hemorrhages that are associated with severe CAA are frequent (Tanskanen et al. 2012). In non-demented elderly subjects, lacunes and cerebral microbleeds have been associated with cognitive decline, including reduced mental speed and impaired executive functions or other neuropsychiatric symptoms (Seo et al. 2007). SVD is more common in subjects with AD and might interact with the neurodegenerative changes in AD (Esiri et al. 2014; Zekry et al. 2003). Additionally, the total length of brain capillaries is reduced in patients that died with AD (Bailey et al. 2004). These vascular reductions can diminish transport of energy substrates and nutrients across the BBB, and reduce the clearance of potential neurotoxins from the brain

Interestingly, studies have shown that the cognitive abilities of demented individuals over the age of 80 declined faster in those also suffering from CVD compared to those without comorbid CVD (Mungas et al. 2001). Furthermore, AD and CVD share risk factors including hypercholesterolemia, atherosclerosis, diabetes, hypertension, smoking, and obesity (Alzheimer's 2018). However, the direct

contributions of the vasculature, blood or its components to AD pathophysiology in remains to be elucidated. CVD and vascular lesions impair the structure and function of the NVU, which alters CBF regulation, disrupts BBB function, and reduces the brain's repair potential, supporting the notion that vascular pathology potentiates AD by reducing the threshold for cognitive impairment and accelerating the pace of dementia (Iadecola 2010). Hence, the identification of neurovascular pathologic events during the preclinical and prodromal stages of AD may provide a unified framework for understanding vascular contributions to AD and improving therapeutic target identification within a disease modifying window. To this end, our overarching hypothesis is that LC degeneration is a nexus lesion contributing to both cerebrovascular and neuronal pathology prior to the onset of cognitive impairment.

The locus coeruleus

The LC is the primary source of NE in the CNS where it modulates attentional behaviors, memory, and arousal in vulnerable, higher order cognitive regions such as prefrontal cortex (PFC) and hippocampus (Sara 2009a; Samuels and Szabadi 2008). The locus coeruleus, meaning “blue spot” in Latin, is a highly pigmented nucleus of cells in the dorsal wall of the pons, lateral to the fourth ventricle. The high concentrations of intracellular neuromelanin make the group of cells visible to the naked eye, hence the name given by its discoverer Felix Vicq d’Azyr (Counts and Mufson 2012).

The LC is remarkable in that the approximately 45,000 cells comprising this nucleus in healthy young adults, project great distances and diverge to an immense system of noradrenergic innervation in diverse brain regions. LC neurons are poorly

myelinated and have highly branched axons with extensive varicosities allowing single neurons to release NE on a broad scale throughout the brain (Levitt and Moore 1978). This structure is ideal for simultaneous global NE release in response to salient or noxious stimuli that demand focus/attention allowing for a broad spatiotemporal influence on the excitability and synaptic plasticity of cells in target fields (Bekar, He, and Nedergaard 2008; Hirata and Aston-Jones 1994). LC neurons release NE via exocytosis, not only at synapses but also from pre-synaptic varicosities. Nonsynaptic post-junctional receptors at these varicosities are mostly G-protein coupled metabotropic receptors that produce a slower modulatory response through the regulation of adenylyl cyclase and phospholipase C. Most synaptic NE is taken back into the neuron terminal via the NE transporter (NET) (Szabadi 2013). Neuronal perikarya, axons, glia, and blood vessels all express noradrenergic receptors in LC efferent fields (Kobayashi et al. 1982; Lidow and Rakic 1994; Woods et al. 1989), consistent with the role of the LC as a global mediator of arousal in the CNS. Co-transmitters in the LC include ATP, NPY, glutamate, encephalin and galanin (Counts and Mufson 2012).

Early investigations into the LC-NE system focused on vigilance and sleep–wake cycles (Hobson, McCarley, and Wyzinski 1975; Roussel et al. 1967). During quiet wakefulness, LC neurons fire at a regular slow rate (~1 Hz), whereas they show bursts of firing in response to arousing stimuli and fire at a diminished rate during drowsiness and slow-wave sleep (Aston-Jones and Bloom 1981). These neurons are completely silent during rapid eye movement (REM) sleep, when the cortical electro encephalogram has a high arousal profile (Roussel et al. 1967). Although there is

unequivocal evidence for this role in vigilance, the LC has been assigned a recognized role in many other important functions, including attention, sensory processing, synaptic plasticity, network resetting, memory formation, memory retrieval, decision making and performance facilitation (Aston-Jones and Cohen 2005). Noradrenergic signaling, together with other monoaminergic and brainstem cholinergic systems, maintains arousal via its influence on thalamocortical circuits (Fuller, Gooley, and Saper 2006), wherein NE modulates burst firing of these neurons during wakefulness to fine-tune sensory information transfer to the neocortex (McCormick 1992). In this regard, antidromically driven action potentials can be recorded from LC neurons in response to electrical stimulation of corticothalamic circuits in monkeys, while orthodromic driving of LC efferents to this circuit can be recorded following subcutaneous electrical stimulation (Aston-Jones, Foote, and Segal 1985).

The LC further modulates the collection and processing of relevant sensory information through cortical and subcortical attentional and memory circuits to optimize task performance (Berridge and Waterhouse 2003). Aston-Jones and Cohen previously proposed a theory of “adaptive gain” wherein NE integrates sensory, attentional, and memory processing by positively modulating signal gain in single neurons or populations of neurons to facilitate the processing of salient events (Aston-Jones and Cohen 2005). This increase in gain is driven by LC phasic activity in response to relevant stimuli. LC bursts and pulsatile NE efflux in target fields (e.g., PFC) increase the activity of excitatory input and decrease the activity of inhibitory input to thus increase the contrast between activated and inhibited inputs. The ensuing behavior optimizes task performance. Furthermore, this theory purports that the LC-NE system is

responsive to ongoing evaluations of task utility provided by input from PFC or related cortical structures. When utility persistently diminishes, changes in LC-NE tonic activity withdraw support for task performance, facilitating other forms of behaviors that explore alternative sources of reward, often referred to as “exploratory behavior””(Aston-Jones and Cohen, 2005). Hence, the LC essentially performs a cost– benefit analysis during task optimization to mediate attention. In addition to these well-studied roles, an often-overlooked role for LC is how its firing can influence cerebrovascular regulation and vascular tone.

The LC and the cerebrovasculature

The LC innervates the great majority of the microvasculature in the brain (Cohen, Molinatti, and Hamel 1997). In the early 1970’s, several groups noted dopamine B-hydroxylase (DBH, the synthetic enzyme for NE)-containing fibers in close association with parenchymal arterioles and capillaries in monkey and rat forebrain (**Fig. 1.2**), which persisted following superior cervical ganglionectomy (Edvinsson et al. 1973; Hartman, Zide, and Udenfriend 1972). As the adult human brain contains about 32,000 LC neurons and is estimated to contain capillaries with a total length of nearly 400 miles (Pardridge 1999; Pamphlett 2014), this means that, on average, each LC neuron acts on 20 meters of capillaries (Pamphlett 2014). Both α- and β-adrenoceptors have been detected in cerebral microvessels and both astrocytes and oligodendrocytes have been shown to have immense contacts with noradrenergic fibers (Kobayashi et al. 1982; Yokoo et al. 2000; Paspalas and Papadopoulos 1996). Thus, the LC NE projection system is a primary mediator of cerebrovascular function, regulating blood flow and

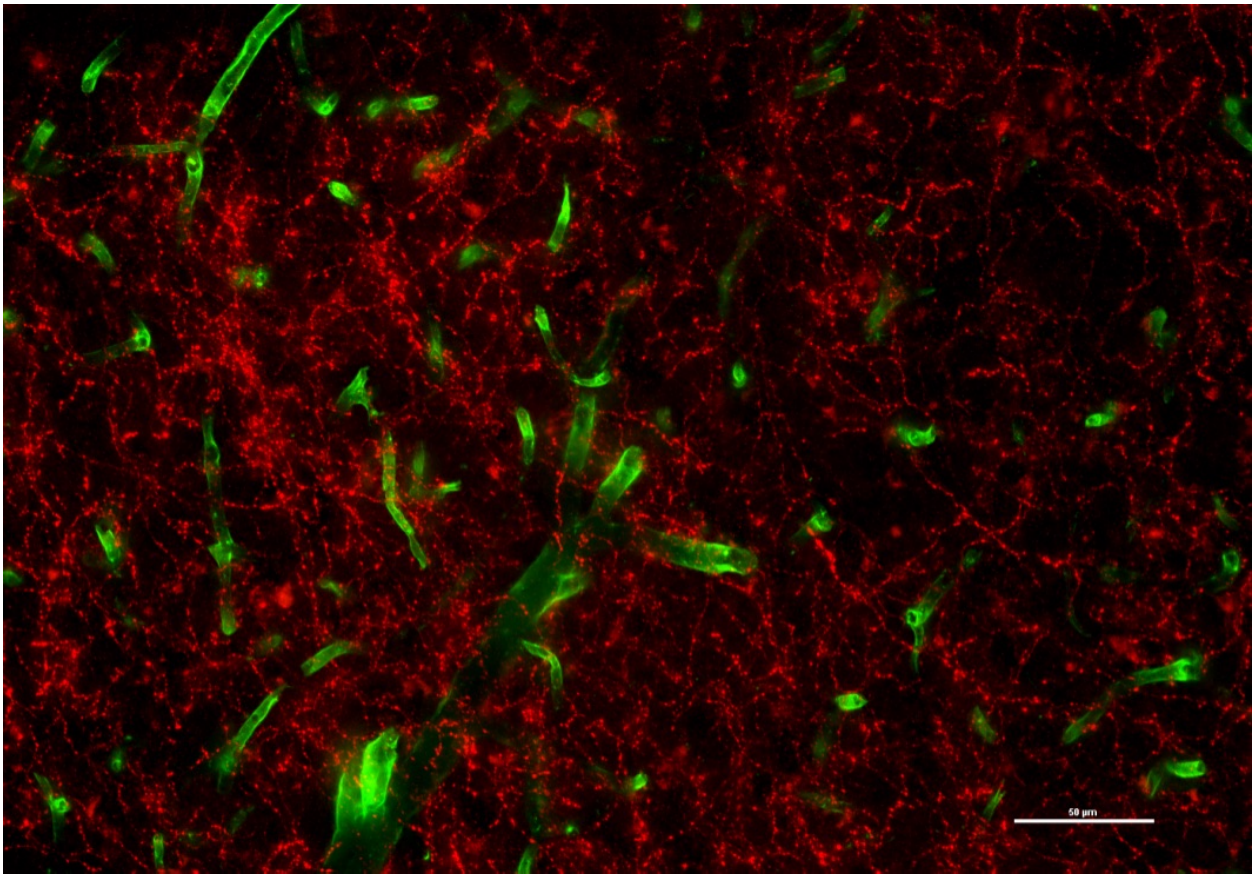

Figure 1.2. **Noradrenergic fibers densely innervate the cerebral cortex with close proximity to cerebral blood vessels.** Fluorescence Micrograph of the rat cerebral cortex showing noradrenergic fibers labeled with anti-DBH (red) and cerebral vessels labeled with ant-SMI71 (a blood brain barrier marker; green). Note the close apposition between the two markers. Scale bar =50um

vessel diameter (Raichle et al. 1975; Peppiatt et al. 2006; Bekar, Wei, and Nedergaard 2012; Kalinin et al. 2006). Bekar and colleagues have also shown that cortical NE levels, which are dependent on LC innervation, can increase neurovascular coupling in the rat cerebral cortex in order to focus oxygen to areas of high demand (Bekar, Wei, and Nedergaard 2012). With the known role of the LC in neocortical neuromodulation, the additional indication that NE signaling may influence vascular tone further implicates the LC-NE system in shaping certain features of the brains hemodynamic response to stimuli. More recently, it was reported that LC stimulation in rats increased perfusion to stimulate cortical neuronal activity (Toussay et al. 2013). In light of these data, we hypothesized that LC degeneration negatively impacts cerebrovascular function in target fields and may even exacerbate pre-existing vascular risk factors for dementia. However, to our knowledge, the extent to which this phenomenon occurs has not been examined experimentally.

The LC in neurodegenerative disorders

The LC in aging and AD

Neuron number within the LC decreases by approximately ~30% during normal aging with a notable rostro-caudal gradient of cell loss (Chan-Palay and Asan 1989; Marcyniuk, Mann, and Yates 1989). Although a nearly ubiquitous and profound loss of LC neurons (50–80%) was observed in end-stage AD cases in the early 1980s (Bondareff, Mountjoy, and Roth 1981b; Bondareff et al. 1987b; Mann et al. 1980a; Mann, Yates, and Hawkes 1983; Mann, Yates, and Marcyniuk 1984), it was largely ignored in favor of other neurotransmitter systems/nuclei, such as the glutamatergic

medial temporal lobe memory hub (Hyman, Van Hoesen, and Damasio 1987) and cholinergic nucleus basalis (NB) (Adolfsson et al. 1979; Mann et al. 1980b; Palmer et al. 1987; Zarow et al. 2003a; Mann, Yates, and Marcyniuk 1984; Zarow et al. 2003b)In fact, the extent of LC/NE degeneration precedes and surpasses nucleus basalis/acetylcholine loss in AD and is more strongly correlated with plaque and tangle accumulation (Bondareff et al. 1987a). LC degeneration also correlates better with the onset and duration of AD than degeneration of the nucleus basalis degeneration, which may be related to the observed reduction of NE levels in LC projection sites in AD (Adolfsson et al. 1979; Mann et al. 1980b; Palmer et al. 1987; Zarow et al. 2003a; Mann, Yates, and Marcyniuk 1984; Zarow et al. 2003b). LC neuron loss is even observed in AD cases lacking nucleus basalis degeneration (Wilcock et al. 1988). Furthermore, it is now apparent from clinical/pathological investigations performed by our lab and others that that significant LC cell loss can be observed in MCI and early-stage AD and correlates with cognitive function as well as clinical pathologic diagnostic criteria (Kelly et al. 2017; Arendt et al. 2015; Theofilas et al. 2017).

With respect to tau pathology, it is now recognized that NFTs accumulate in the LC early in AD and that tau pathology within the LC correlates with poorer performance on measures of cognitive function such as the Mini Mental State Exam (MMSE) (Braak and Del Tredici 2011b, 2011a; Grudzien et al. 2007). Given that Braak staging does not include brainstem pathology (see above), it is interesting to note that Braak and colleagues (Braak and Del Tredici 2012, 2011b; Braak et al. 2011) reported that AT8-positive phosphorylated tau immunostaining can be detected in the LC prior to any other structure in the brain, occasionally as early as the first few decades of life.

This latter observation could suggest that LC neurons can harbor pathological tau for surprisingly long periods before succumbing to cell death, or that these neurons are involved in age-related LC cell loss. However, transgenic mice overexpressing a mutant form of human tau prone to aberrant phosphorylation and aggregation (P301S) under control of the pan-neuronal prion promoter develop AD-like tau pathology that kills forebrain, but not LC neurons by the time the mice die at approximately 12 months (Chalermpalanupap et al. 2018; Yoshiyama et al. 2007), and primary LC cultures made from neonatal P301S mice have normal survival rates (Rorabaugh et al. 2017). Likewise, Weinshenker and colleagues recently showed that in TgF344-AD transgenic rats, which overexpress mutant human amyloid precursor protein and presenilin-1, hyperphosphorylated tau appears in the LC months prior to anywhere else in the brain (similar to humans), yet no detectable LC cell death is evident nearly a year later (Rorabaugh et al. 2017) indicating that LC NFTs may be an initiating event in AD pathogenesis.

There is also evidence for neuronal compensation within the LC in AD, including increased TH and NET expression within the LC, dendritic and axonal sprouting, increased cortical NE turnover (Hoogendijk et al. 1999; Szot et al. 2006). Together with experimental AD models showing a neuroprotective effect for NE (Heneka et al. 2006; Madrigal et al. 2007; Counts and Mufson 2010), these studies suggest that degeneration of the LC noradrenergic projection system is a cardinal feature of AD pathogenesis and likely plays a mechanistic role in the progression of the disease.

The LC in other neurodegenerative disorders

The topographical distribution of cell loss in the LC varies in AD, Parkinson's disease (PD) and depression (German et al. 1992). The type of pathology differs as well, with LC cell loss in AD and PD (Marcyniuk, Mann, and Yates 1986), gliosis in multiple sclerosis (Polak, Kalinin, and Feinstein 2011) and neuronal shrinkage in amyotrophic lateral sclerosis (Mann, Yates, and Hawkes 1983). Notably, frank LC degeneration has been observed in synucleinopathies such as PD and dementia with Lewy bodies (DLB) (Mann and Yates 1983). In PD in fact, α-synuclein pathology appears in LC neurons before infiltrating the substantia nigra pars compacta, the midbrain dopaminergic nucleus that controls motor function and degenerates in PD (Vermeiren and De Deyn 2017; Braak et al. 2003). Also, LC/NE degeneration was observed to be greater than substantia nigra/dopamine (DA) loss in PD (Zarow et al. 2003b). Additionally, LC-localized tau is observed in progressive supranuclear palsy, corticobasal degeneration, and the Pick's disease variant of frontotemporal dementia that features both Lewy bodies and tau inclusions in a subset of LC neurons (Eser et al. 2018; Irwin et al. 2016; Takauchi et al. 1995). Stage-dependent characterization of LC pathology in other neurodegenerative diseases are needed to assess the potential involvement of the noradrenergic system in disease pathogenesis.

Discussion

The LC has also been noted to degenerate before the clinical presentation of symptoms in AD pathogenesis. Furthermore, the LC NE projection system is a primary mediator of cerebrovascular function, regulating blood flow, vessel diameter, and blood volume

changes in regions of oxygen demand (Raichle et al. 1975; Peppiatt et al. 2006; Bekar, Wei, and Nedergaard 2012). Given the vast majority of AD cases presenting with concomitant CVD, understanding whether shared mechanisms are involved in AD and CVD pathogenesis may provide a unified framework for understanding vascular contributions to the progression of AD. Interestingly, at the time of Alzheimer's initial description of the disease, dementia was most often attributed to vascular insufficiency or syphilis(Engelhardt and Grinberg 2015), and Alzheimer himself was the first to associate CVD with the disease that would bear his name, noting that in Auguste Deter's brain, "the larger vascular tissues show arteriosclerotic change" (Alzheimer et al. 1995). Moreover, as the majority of cases with MCI also present with prominent cerebrovascular disease, the identification of neurovascular pathologic events that occur in the preclinical stages of AD may be essential for therapeutic target identification within a disease modifying window (Schneider et al. 2009). With their immense interactions and proximity to the vasculature of the brain, the LC may be directly susceptible to vascular toxicants, even if they were at low levels in the circulation (Pamphlett 2014). In addition, the proximity of the LC to the ventricle affords liberal access to the cerebrospinal fluid (CSF), which is an addition potential source of chemical toxicants and neuro-inflammatory molecules. Thus, when considering the evidence for the LC's role in vascular function, the loss of the noradrenergic tone with LC degeneration in AD could cause irreparable damage to the coordination of cerebral perfusion in higher-order cognitive regions. This dissertation posits that LC neuron loss and deafferentation may result in a two-hit pathogenic event that dysregulates NE's protective effects on both neuronal and vascular function, thus contributing to the

pathological and clinical expression of AD. Hence, targeting the LC using neuroprotective strategies may allow for disease modification for this disorder.

Dissertation objectives

In this dissertation project, my first goal was to examine the extent of LC degeneration prior to the onset of MCI using postmortem tissue from University of Kentucky AD Center (UKADC) subjects who were diagnosed with NCI (Braak stages 0-II), NCI with Braak stages III-V termed preclinical AD (PCAD), MCI, or mild AD, and correlate these findings with measures of cognition, AD pathology and vascular pathology recorded for these individuals. To better understand the mechanisms linking LC degeneration, neurovascular pathology, and cognition, my second goal was to lesion the LC projection system in a rat model of AD to test its effects on cognitive behaviors and markers of AD-related neuropathology and vascular dysfunction. Taken together, these goals formed the foundation of my Specific Aims to shed light on the role of LC NE projection system degeneration in neuronal and vascular pathophysiology during the transition from normal cognition to incipient disease. My Specific Aims were as follows:

Aim 1

We will test the hypothesis that LC neurons exhibit multiple neurodegenerative markers and cell loss that correlates with cerebrovascular pathology in PCAD. Addressed in **Chapter 2**, for Aim 1, I quantified the number of LC neurons that display tyrosine hydroxylase (TH) reactivity (a marker for the noradrenergic phenotype), AT8 tau pathology, DNA/RNA damage, in postmortem tissue samples from people who died with

no cognitive impairment (NCI; Braak neuropathological stages 0-II), PCAD (NCI with Braak stages III-V), mild cognitive impairment (MCI), or AD. Morphometric data was correlated with cerebrovascular, clinical, (e.g. MMSE) and pathological (e.g., Braak, NIA/Reagan) variables, and ApoE genotype.

Aim 2

We will test the hypothesis that LC deafferentation of the PFC disrupts working and spatial memory and accelerates cortical markers of CVD in a transgenic AD rat model. Addressed in **Chapter 3,** for Aim 2, I lesioned LC projection neurons innervating the prefrontal cortex (PFC) in the TgF344-19 rat model of AD using a noradrenergic - specific immunotoxin. Prior to sacrifice, lesioned and control rats were tested behaviorally for spatial and working memory with a Barnes maze task. Postmortem PFC was analyzed for cerebrovascular and AD-like pathology. Vessel remodeling, blood brain barrier dysfunction, amyloid deposition and inflammation was evaluated via immunohistochemistry and western blotting.

Impact of the proposed work

Given the renewed interest in vascular contributions to AD (Kisler et al. 2017; Snyder et al. 2015), the objective of this dissertation project is to reveal a novel role for noradrenergic signaling loss in driving cognitive impairment in AD through its effects on cerebrovascular integrity in target fields, thus providing new insights into molecular pathogenic mechanisms and therapeutic targets of disease.

LITERATURE CITED

LITERATURE CITED

Abbott, N. J., L. Ronnback, and E. Hansson. 2006. 'Astrocyte-endothelial interactions at the blood-brain barrier', *Nat Rev Neurosci*, 7: 41-53.

Adolfsson, R., C. G. Gottfries, B. E. Roos, and B. Winblad. 1979. 'Changes in the brain catecholamines in patients with dementia of Alzheimer type', *Br J Psychiatry*, 135: 216-23.

Ahtiluoto, S., T. Polvikoski, M. Peltonen, A. Solomon, J. Tuomilehto, B. Winblad, R. Sulkava, and M. Kivipelto. 2010. 'Diabetes, Alzheimer disease, and vascular dementia: a population-based neuropathologic study', *Neurology*, 75: 1195-202.

Albert, M. S., S. T. DeKosky, D. Dickson, B. Dubois, H. H. Feldman, N. C. Fox, A. Gamst, D. M. Holtzman, W. J. Jagust, R. C. Petersen, P. J. Snyder, M. C. Carrillo, B. Thies, and C. H. Phelps. 2011. 'The diagnosis of mild cognitive impairment due to Alzheimer's disease: recommendations from the National Institute on Aging-Alzheimer's Association workgroups on diagnostic guidelines for Alzheimer's disease', *Alzheimers Dement*, 7: 270-9.

Alzheimer, A., R. A. Stelzmann, H. N. Schnitzlein, and F. R. Murtagh. 1995. 'An English translation of Alzheimer's 1907 paper, "Uber eine eigenartige Erkankung der Hirnrinde"', *Clin Anat*, 8: 429-31.

Alzheimer's. 2018. '2018 Alzheimer's disease facts and figures', *Alzheimer's & Dementia: The Journal of the Alzheimer's Association*, 14: 367-429.

Arendt, T., M. K. Bruckner, M. Morawski, C. Jager, and H. J. Gertz. 2015. 'Early neurone loss in Alzheimer's disease: cortical or subcortical?', *Acta Neuropathol Commun*, 3: 10.

Arnsten, A. F., and P. S. Goldman-Rakic. 1984. 'Selective prefrontal cortical projections to the region of the locus coeruleus and raphe nuclei in the rhesus monkey', *Brain Res*, 306.

———. 1985. 'Alpha 2-adrenergic mechanisms in prefrontal cortex associated with cognitive decline in aged nonhuman primates', *Science*, 230: 1273-6.

Arriagada, P. V., J. H. Growdon, E. T. Hedley-Whyte, and B. T. Hyman. 1992. 'Neurofibrillary tangles but not senile plaques parallel duration and severity of Alzheimer's disease', *Neurology*, 42: 631-9.

Aston-Jones, G., and F. E. Bloom. 1981. 'Activity of norepinephrine-containing locus coeruleus neurons in behaving rats anticipates fluctuations in the sleep-waking cycle', *J Neurosci*, 1: 876-86.

Aston-Jones, G., and J. D. Cohen. 2005. 'An integrative theory of locus coeruleus-norepinephrine function: adaptive gain and optimal performance', *Annu Rev Neurosci*, 28.

Aston-Jones, G., S. L. Foote, and M. Segal. 1985. 'Impulse conduction properties of noradrenergic locus coeruleus axons projecting to monkey cerebrocortex', *Neuroscience*, 15: 765-77.

Attems, J., and K. A. Jellinger. 2014. 'The overlap between vascular disease and Alzheimer's disease--lessons from pathology', *BMC Med*, 12: 206.

Attems, J., K. Jellinger, D. R. Thal, and W. Van Nostrand. 2011. 'Review: sporadic cerebral amyloid angiopathy', *Neuropathol Appl Neurobiol*, 37: 75-93.

Bailey, T. L., C. B. Rivara, A. B. Rocher, and P. R. Hof. 2004. 'The nature and effects of cortical microvascular pathology in aging and Alzheimer's disease', *Neurol Res*, 26: 573-8.

Barnes, D. E., and K. Yaffe. 2011. 'The projected effect of risk factor reduction on Alzheimer's disease prevalence', *Lancet Neurol*, 10: 819-28.

Bartus, R. T., R. L. Dean, 3rd, B. Beer, and A. S. Lippa. 1982. 'The cholinergic hypothesis of geriatric memory dysfunction', *Science*, 217: 408-14.

Bekar, L. K., W. He, and M. Nedergaard. 2008. 'Locus coeruleus alpha-adrenergic-mediated activation of cortical astrocytes in vivo', *Cereb Cortex*, 18: 2789-95.

Bekar, L. K., H. S. Wei, and M. Nedergaard. 2012. 'The locus coeruleus-norepinephrine network optimizes coupling of cerebral blood volume with oxygen demand', *J Cereb Blood Flow Metab*, 32: 2135-45.

Berridge, C. W., and B. D. Waterhouse. 2003. 'The locus coeruleus-noradrenergic system: modulation of behavioral state and state-dependent cognitive processes', *Brain Res Brain Res Rev*, 42.

Bierer, L. M., P. R. Hof, D. P. Purohit, L. Carlin, J. Schmeidler, K. L. Davis, and D. P. Perl. 1995. 'Neocortical neurofibrillary tangles correlate with dementia severity in Alzheimer's disease', *Arch Neurol*, 52: 81-8.

Binder, L. I., A. Frankfurter, and L. I. Rebhun. 1985. 'The distribution of tau in the mammalian central nervous system', *J Cell Biol*, 101: 1371-8.

Bondareff, W., C. Q. Mountjoy, and M. Roth. 1981a. 'Selective loss of neurones of origin of adrenergic projection to cerebral cortex (nucleus locus coeruleus) in senile dementia', *Lancet*, 1.

———. 1981b. 'Selective loss of neurones of origin of adrenergic projection to cerebral cortex (nucleus locus coeruleus) in senile dementia', *Lancet*, 1: 783-4.

Bondareff, W., C. Q. Mountjoy, M. Roth, M. N. Rossor, L. L. Iversen, G. P. Reynolds, and D. L. Hauser. 1987a. 'Neuronal degeneration in locus ceruleus and cortical correlates of Alzheimer disease', *Alzheimer Dis Assoc Disord*, 1: 256-62.

———. 1987b. 'Neuronal degeneration in locus ceruleus and cortical correlates of Alzheimer disease', *Alzheimer Dis Assoc Disord*, 1.

Braak, H., and E. Braak. 1991a. 'Neuropathological stageing of Alzheimer-related changes', *Acta Neuropathol*, 82: 239-59.

———. 1991b. 'Neuropathological stageing of Alzheimer-related changes', *Acta Neuropathol*, 82.

Braak, H., and K. Del Tredici. 2011a. 'Alzheimer's pathogenesis: is there neuron-to-neuron propagation?', *Acta Neuropathol*, 121: 589-95.

———. 2011b. 'The pathological process underlying Alzheimer's disease in individuals under thirty', *Acta Neuropathol*, 121: 171-81.

———. 2012. 'Where, when, and in what form does sporadic Alzheimer's disease begin?', *Curr Opin Neurol*, 25: 708-14.

Braak, H., K. Del Tredici, U. Rub, R. A. de Vos, E. N. Jansen Steur, and E. Braak. 2003. 'Staging of brain pathology related to sporadic Parkinson's disease', *Neurobiol Aging*, 24: 197-211.

Braak, H., D. R. Thal, E. Ghebremedhin, and K. Del Tredici. 2011. 'Stages of the pathologic process in Alzheimer disease: age categories from 1 to 100 years', *J Neuropathol Exp Neurol*, 70: 960-9.

Buschke, H., G. Kuslansky, M. Katz, W. F. Stewart, M. J. Sliwinski, H. M. Eckholdt, and R. B. Lipton. 1999. 'Screening for dementia with the memory impairment screen', *Neurology*, 52: 231-8.

Casserly, I. P., and E. J. Topol. 2004. 'Convergence of atherosclerosis and alzheimer's disease: Cholesterol, inflammation, and misfolded proteins', *Discov Med*, 4: 149-56.

Chalermpalanupap, T., J. P. Schroeder, J. M. Rorabaugh, L. C. Liles, J. J. Lah, A. I. Levey, and D. Weinshenker. 2018. 'Locus Coeruleus Ablation Exacerbates Cognitive Deficits, Neuropathology, and Lethality in P301S Tau Transgenic Mice', *J Neurosci*, 38: 74-92.

Chan-Palay, V., and E. Asan. 1989. 'Quantitation of catecholamine neurons in the locus coeruleus in human brains of normal young and older adults and in depression', *J Comp Neurol*, 287: 357-72.

Chen, Y., and L. Liu. 2012. 'Modern methods for delivery of drugs across the blood-brain barrier', *Adv Drug Deliv Rev*, 64: 640-65.

Chen, Y., D. A. Wolk, J. S. Reddin, M. Korczykowski, P. M. Martinez, E. S. Musiek, A. B. Newberg, P. Julin, S. E. Arnold, J. H. Greenberg, and J. A. Detre. 2011. 'Voxel-level comparison of arterial spin-labeled perfusion MRI and FDG-PET in Alzheimer disease', *Neurology*, 77: 1977-85.

Chen, Z., and C. Zhong. 2013. 'Decoding Alzheimer's disease from perturbed cerebral glucose metabolism: implications for diagnostic and therapeutic strategies', *Prog Neurobiol*, 108: 21-43.

Cohen, Z., G. Molinatti, and E. Hamel. 1997. 'Astroglial and vascular interactions of noradrenaline terminals in the rat cerebral cortex', *J Cereb Blood Flow Metab*, 17: 894-904.

Counts, S. E., and E. J. Mufson. 2010. 'Noradrenaline activation of neurotrophic pathways protects against neuronal amyloid toxicity', *J Neurochem*, 113: 649-60.

———. 2012. 'Locus coeruleus.' in J. K. Mai and G. Paxinos (eds.), *The human nervous system* (Academic: London).

Daneman, R., and A. Prat. 2015. 'The blood-brain barrier', *Cold Spring Harb Perspect Biol*, 7: a020412.

Debette, S., and H. S. Markus. 2010. 'The clinical importance of white matter hyperintensities on brain magnetic resonance imaging: systematic review and meta-analysis', *BMJ*, 341: c3666.

Desai Bradaric, B., A. Patel, J. A. Schneider, P. M. Carvey, and B. Hendey. 2012. 'Evidence for angiogenesis in Parkinson's disease, incidental Lewy body disease, and progressive supranuclear palsy', *J Neural Transm (Vienna)*, 119: 59-71.

Drouin-Ouellet, J., S. J. Sawiak, G. Cisbani, M. Lagace, W. L. Kuan, M. Saint-Pierre, R. J. Dury, W. Alata, I. St-Amour, S. L. Mason, F. Calon, S. Lacroix, P. A. Gowland, S. T. Francis, R. A. Barker, and F. Cicchetti. 2015. 'Cerebrovascular and blood-brain barrier impairments in Huntington's disease: Potential implications for its pathophysiology', *Ann Neurol*, 78: 160-77.

Edvinsson, L., M. Lindvall, K. C. Nielsen, and C. Owman. 1973. 'Are brain vessels innervated also by central (non-sympathetic) adrenergic neurones?', *Brain Res*, 63: 496-9.

Engelhardt, E., and L. T. Grinberg. 2015. 'Alois Alzheimer and vascular brain disease: Arteriosclerotic atrophy of the brain', *Dement Neuropsychol*, 9: 81-84.

Erickson, M. A., and W. A. Banks. 2013. 'Blood-brain barrier dysfunction as a cause and consequence of Alzheimer's disease', *J Cereb Blood Flow Metab*, 33: 1500-13.

Eriksson, U. K., A. M. Bennet, M. Gatz, P. W. Dickman, and N. L. Pedersen. 2010. 'Nonstroke cardiovascular disease and risk of Alzheimer disease and dementia', *Alzheimer Dis Assoc Disord*, 24: 213-9.

Eser, R. A., A. J. Ehrenberg, C. Petersen, S. Dunlop, M. B. Mejia, C. K. Suemoto, C. M. Walsh, H. Rajana, J. Oh, P. Theofilas, W. W. Seeley, B. L. Miller, T. C. Neylan, H. Heinsen, and L. T. Grinberg. 2018. 'Selective Vulnerability of Brainstem Nuclei in Distinct Tauopathies: A Postmortem Study', *J Neuropathol Exp Neurol*, 77: 149-61.

Esiri, M. M., C. Joachim, C. Sloan, S. Christie, G. Agacinski, L. R. Bridges, G. K. Wilcock, and A. D. Smith. 2014. 'Cerebral subcortical small vessel disease in subjects with pathologically confirmed Alzheimer disease: a clinicopathologic study in the Oxford Project to Investigate Memory and Ageing (OPTIMA)', *Alzheimer Dis Assoc Disord*, 28: 30-5.

Farlow, M. R., M. L. Miller, and V. Pejovic. 2008. 'Treatment options in Alzheimer's disease: maximizing benefit, managing expectations', *Dement Geriatr Cogn Disord*, 25: 408-22.

Frankish, H., and R. Horton. 2017. 'Prevention and management of dementia: a priority for public health', *Lancet*, 390: 2614-15.

Fuller, P. M., J. J. Gooley, and C. B. Saper. 2006. 'Neurobiology of the sleep-wake cycle: sleep architecture, circadian regulation, and regulatory feedback', *J Biol Rhythms*, 21: 482-93.

German, D. C., K. F. Manaye, C. L. White, D. J. Woodward, D. D. McIntire, W. K. Smith, R. N. Kalaria, and D. M. Mann. 1992. 'Disease-specific patterns of locus coeruleus cell loss', *Ann Neurol*, 32.

Glenner, G. G., and C. W. Wong. 1984. 'Alzheimer's disease: initial report of the purification and characterization of a novel cerebrovascular amyloid protein', *Biochem Biophys Res Commun*, 120: 885-90.

Goate, A., M. C. Chartier-Harlin, M. Mullan, J. Brown, F. Crawford, L. Fidani, L. Giuffra, A. Haynes, N. Irving, L. James, and et al. 1991. 'Segregation of a missense mutation in the amyloid precursor protein gene with familial Alzheimer's disease', *Nature*, 349: 704-6.

Goedert, M., R. A. Crowther, and C. C. Garner. 1991. 'Molecular characterization of microtubule-associated proteins tau and MAP2', *Trends Neurosci*, 14: 193-9.

Gorelick, P. B., A. Scuteri, S. E. Black, C. Decarli, S. M. Greenberg, C. Iadecola, L. J. Launer, S. Laurent, O. L. Lopez, D. Nyenhuis, R. C. Petersen, J. A. Schneider, C. Tzourio, D. K. Arnett, D. A. Bennett, H. C. Chui, R. T. Higashida, R. Lindquist, P. M. Nilsson, G. C. Roman, F. W. Sellke, S. Seshadri, Council on Epidemiology American Heart Association Stroke Council, Council on Cardiovascular Nursing

Council on Cardiovascular Radiology Prevention, Intervention, Surgery Council on Cardiovascular, and Anesthesia. 2011. 'Vascular contributions to cognitive impairment and dementia: a statement for healthcare professionals from the american heart association/american stroke association', *Stroke*, 42: 2672-713.

Gouras, G. K., J. Tsai, J. Naslund, B. Vincent, M. Edgar, F. Checler, J. P. Greenfield, V. Haroutunian, J. D. Buxbaum, H. Xu, P. Greengard, and N. R. Relkin. 2000. 'Intraneuronal Abeta42 accumulation in human brain', *Am J Pathol*, 156: 15-20.

Gray, M. T., and J. M. Woulfe. 2015. 'Striatal blood-brain barrier permeability in Parkinson's disease', *J Cereb Blood Flow Metab*, 35: 747-50.

Greenamyre, J. T., W. F. Maragos, R. L. Albin, J. B. Penney, and A. B. Young. 1988. 'Glutamate transmission and toxicity in Alzheimer's disease', *Prog Neuropsychopharmacol Biol Psychiatry*, 12: 421-30.

Greenfield, J. P., J. Tsai, G. K. Gouras, B. Hai, G. Thinakaran, F. Checler, S. S. Sisodia, P. Greengard, and H. Xu. 1999. 'Endoplasmic reticulum and trans-Golgi network generate distinct populations of Alzheimer beta-amyloid peptides', *Proc Natl Acad Sci U S A*, 96: 742-7.

Grimmer, T., and A. Kurz. 2006. 'Effects of cholinesterase inhibitors on behavioural disturbances in Alzheimer's disease: a systematic review', *Drugs Aging*, 23: 957-67.

Grinberg, L. T., and D. R. Thal. 2010. 'Vascular pathology in the aged human brain', *Acta Neuropathol*, 119: 277-90.

Grudzien, A., P. Shaw, S. Weintraub, E. Bigio, D. C. Mash, and M. M. Mesulam. 2007. 'Locus coeruleus neurofibrillary degeneration in aging, mild cognitive impairment and early Alzheimer's disease', *Neurobiol Aging*, 28: 327-35.

Hachinski, V., C. Iadecola, R. C. Petersen, M. M. Breteler, D. L. Nyenhuis, S. E. Black, W. J. Powers, C. DeCarli, J. G. Merino, R. N. Kalaria, H. V. Vinters, D. M. Holtzman, G. A. Rosenberg, A. Wallin, M. Dichgans, J. R. Marler, and G. G. Leblanc. 2006. 'National Institute of Neurological Disorders and Stroke-Canadian Stroke Network vascular cognitive impairment harmonization standards', *Stroke*, 37: 2220-41.

Hardy, J. A., and G. A. Higgins. 1992. 'Alzheimer's disease: the amyloid cascade hypothesis', *Science*, 256: 184-5.

Hartman, B. K., D. Zide, and S. Udenfriend. 1972. 'The use of dopamine -hydroxylase as a marker for the central noradrenergic nervous system in rat brain', *Proc Natl Acad Sci U S A*, 69: 2722-6.

Hebert, L. E., L. A. Beckett, P. A. Scherr, and D. A. Evans. 2001. 'Annual incidence of Alzheimer disease in the United States projected to the years 2000 through 2050', *Alzheimer Dis Assoc Disord*, 15: 169-73.

Hebert, L. E., J. Weuve, P. A. Scherr, and D. A. Evans. 2013. 'Alzheimer disease in the United States (2010-2050) estimated using the 2010 census', *Neurology*, 80: 1778-83.

Heneka, M. T., M. Ramanathan, A. H. Jacobs, L. Dumitrescu-Ozimek, A. Bilkei-Gorzo, T. Debeir, M. Sastre, N. Galldiks, A. Zimmer, M. Hoehn, W. D. Heiss, T. Klockgether, and M. Staufenbiel. 2006. 'Locus ceruleus degeneration promotes Alzheimer pathogenesis in amyloid precursor protein 23 transgenic mice', *J Neurosci*, 26: 1343-54.

Hippius, H., and G. Neundorfer. 2003. 'The discovery of Alzheimer's disease', *Dialogues Clin Neurosci*, 5: 101-8.

Hirata, H., and G. Aston-Jones. 1994. 'A novel long-latency response of locus coeruleus neurons to noxious stimuli: mediation by peripheral C-fibers', *J Neurophysiol*, 71: 1752-61.

Hobson, J. A., R. W. McCarley, and P. W. Wyzinski. 1975. 'Sleep cycle oscillation: reciprocal discharge by two brainstem neuronal groups', *Science*, 189: 55-8.

Honig, L. S., B. Vellas, M. Woodward, M. Boada, R. Bullock, M. Borrie, K. Hager, N. Andreasen, E. Scarpini, H. Liu-Seifert, M. Case, R. A. Dean, A. Hake, K. Sundell, V. Poole Hoffmann, C. Carlson, R. Khanna, M. Mintun, R. DeMattos, K. J. Selzler, and E. Siemers. 2018. 'Trial of Solanezumab for Mild Dementia Due to Alzheimer's Disease', *N Engl J Med*, 378: 321-30.

Hoogendijk, W. J., M. G. Feenstra, M. H. Botterblom, J. Gilhuis, I. E. Sommer, W. Kamphorst, P. Eikelenboom, and D. F. Swaab. 1999. 'Increased activity of surviving locus ceruleus neurons in Alzheimer's disease', *Ann Neurol*, 45: 82-91.

Hyman, B. T., G. W. Van Hoesen, and A. R. Damasio. 1987. 'Alzheimer's disease: glutamate depletion in the hippocampal perforant pathway zone', *Ann Neurol*, 22: 37-40.

Iadecola, C. 2010. 'The overlap between neurodegenerative and vascular factors in the pathogenesis of dementia', *Acta Neuropathol*, 120: 287-96.

———. 2013. 'The pathobiology of vascular dementia', *Neuron*, 80: 844-66.

———. 2017. 'The Neurovascular Unit Coming of Age: A Journey through Neurovascular Coupling in Health and Disease', *Neuron*, 96: 17-42.

Iadecola, C., and U. Dirnagl. 2013. 'The microcircualtion--fantastic voyage: introduction', *Stroke*, 44: S83.

Irwin, D. J., J. Brettschneider, C. T. McMillan, F. Cooper, C. Olm, S. E. Arnold, V. M. Van Deerlin, W. W. Seeley, B. L. Miller, E. B. Lee, V. M. Lee, M. Grossman, and J. Q. Trojanowski. 2016. 'Deep clinical and neuropathological phenotyping of Pick disease', *Ann Neurol*, 79: 272-87.

Iturria-Medina, Y., R. C. Sotero, P. J. Toussaint, J. M. Mateos-Perez, A. C. Evans, and Initiative Alzheimer's Disease Neuroimaging. 2016. 'Early role of vascular dysregulation on late-onset Alzheimer's disease based on multifactorial data-driven analysis', *Nat Commun*, 7: 11934.

Jack, C. R., Jr., and D. M. Holtzman. 2013. 'Biomarker modeling of Alzheimer's disease', *Neuron*, 80: 1347-58.

Jalbert, J. J., L. A. Daiello, and K. L. Lapane. 2008. 'Dementia of the Alzheimer type', *Epidemiol Rev*, 30: 15-34.

Jellinger, K. A. 2002. 'Alzheimer disease and cerebrovascular pathology: an update', *J Neural Transm (Vienna)*, 109: 813-36.

———. 2013. 'Pathology and pathogenesis of vascular cognitive impairment-a critical update', *Front Aging Neurosci*, 5: 17.

Jellinger, K. A., and J. Attems. 2007. 'Neuropathological evaluation of mixed dementia', *J Neurol Sci*, 257: 80-7.

Kalinin, S., D. L. Feinstein, H. L. Xu, G. Huesa, D. A. Pelligrino, and E. Galea. 2006. 'Degeneration of noradrenergic fibres from the locus coeruleus causes tight-junction disorganisation in the rat brain', *Eur J Neurosci*, 24: 3393-400.

Katzman, R., T. Brown, P. Fuld, A. Peck, R. Schechter, and H. Schimmel. 1983. 'Validation of a short Orientation-Memory-Concentration Test of cognitive impairment', *Am J Psychiatry*, 140: 734-9.

Kelly, S. C., B. He, S. E. Perez, S. D. Ginsberg, E. J. Mufson, and S. E. Counts. 2017. 'Locus coeruleus cellular and molecular pathology during the progression of Alzheimer's disease', *Acta Neuropathol Commun*, 5: 8.

Kennedy, M. E., A. W. Stamford, X. Chen, K. Cox, J. N. Cumming, M. F. Dockendorf, M. Egan, L. Ereshefsky, R. A. Hodgson, L. A. Hyde, S. Jhee, H. J. Kleijn, R. Kuvelkar, W. Li, B. A. Mattson, H. Mei, J. Palcza, J. D. Scott, M. Tanen, M. D. Troyer, J. L. Tseng, J. A. Stone, E. M. Parker, and M. S. Forman. 2016. 'The BACE1 inhibitor verubecestat (MK-8931) reduces CNS beta-amyloid in animal models and in Alzheimer's disease patients', *Sci Transl Med*, 8: 363ra150.

Kisler, K., A. R. Nelson, A. Montagne, and B. V. Zlokovic. 2017. 'Cerebral blood flow regulation and neurovascular dysfunction in Alzheimer disease', *Nat Rev Neurosci*, 18: 419-34.

Kivipelto, M., T. Ngandu, T. Laatikainen, B. Winblad, H. Soininen, and J. Tuomilehto. 2006. 'Risk score for the prediction of dementia risk in 20 years among middle aged people: a longitudinal, population-based study', *Lancet Neurol*, 5: 735-41.

Kobayashi, H., L. Frattola, C. Ferrarese, P. Spano, and M. Trabucchi. 1982. 'Characterization of beta-adrenergic receptors on human cerebral microvessels', *Neurology*, 32: 1384-7.

Levitt, P., and R. Y. Moore. 1978. 'Noradrenaline neuron innervation of the neocortex in the rat', *Brain Res*, 139: 219-31.

Lidow, M. S., and P. Rakic. 1994. 'Unique profiles of the alpha 1-, alpha 2-, and beta-adrenergic receptors in the developing cortical plate and transient embryonic zones of the rhesus monkey', *J Neurosci*, 14: 4064-78.

Madrigal, J. L., S. Kalinin, J. C. Richardson, and D. L. Feinstein. 2007. 'Neuroprotective actions of noradrenaline: effects on glutathione synthesis and activation of peroxisome proliferator activated receptor delta', *J Neurochem*, 103: 2092-101.

Maelicke, A. 2000. 'Allosteric modulation of nicotinic receptors as a treatment strategy for Alzheimer's disease', *Dement Geriatr Cogn Disord*, 11 Suppl 1: 11-8.

Mann, D. M., J. Lincoln, P. O. Yates, J. E. Stamp, and S. Toper. 1980a. 'Changes in the monoamine containing neurones of the human CNS in senile dementia', *Br J Psychiatry*, 136.

———. 1980b. 'Changes in the monoamine containing neurones of the human CNS in senile dementia', *Br J Psychiatry*, 136: 533-41.

Mann, D. M., and P. O. Yates. 1983. 'Pathological basis for neurotransmitter changes in Parkinson's disease', *Neuropathol Appl Neurobiol*, 9: 3-19.

Mann, D. M., P. O. Yates, and J. Hawkes. 1983. 'The pathology of the human locus ceruleus', *Clin Neuropathol*, 2: 1-7.

Mann, D. M., P. O. Yates, and B. Marcyniuk. 1984. 'A comparison of changes in the nucleus basalis and locus caeruleus in Alzheimer's disease', *J Neurol Neurosurg Psychiatry*, 47: 201-3.

Marcyniuk, B., D. M. Mann, and P. O. Yates. 1989. 'The topography of nerve cell loss from the locus caeruleus in elderly persons', *Neurobiol Aging*, 10: 5-9.

Markesbery, W. R., F. A. Schmitt, R. J. Kryscio, D. G. Davis, C. D. Smith, and D. R. Wekstein. 2006. 'Neuropathologic substrate of mild cognitive impairment', *Arch Neurol*, 63: 38-46.

McCormick, D. A. 1992. 'Neurotransmitter actions in the thalamus and cerebral cortex', *J Clin Neurophysiol*, 9: 212-23.

Meng, X. F., J. T. Yu, H. F. Wang, M. S. Tan, C. Wang, C. C. Tan, and L. Tan. 2014. 'Midlife vascular risk factors and the risk of Alzheimer's disease: a systematic review and meta-analysis', *J Alzheimers Dis*, 42: 1295-310.

Mergenthaler, P., U. Lindauer, G. A. Dienel, and A. Meisel. 2013. 'Sugar for the brain: the role of glucose in physiological and pathological brain function', *Trends Neurosci*, 36: 587-97.

Michels, L., G. Warnock, A. Buck, G. Macauda, S. E. Leh, A. M. Kaelin, F. Riese, R. Meyer, R. O'Gorman, C. Hock, S. Kollias, and A. F. Gietl. 2016. 'Arterial spin labeling imaging reveals widespread and Abeta-independent reductions in cerebral blood flow in elderly apolipoprotein epsilon-4 carriers', *J Cereb Blood Flow Metab*, 36: 581-95.

Mielke, M. M., P. B. Rosenberg, J. Tschanz, L. Cook, C. Corcoran, K. M. Hayden, M. Norton, P. V. Rabins, R. C. Green, K. A. Welsh-Bohmer, J. C. Breitner, R. Munger, and C. G. Lyketsos. 2007. 'Vascular factors predict rate of progression in Alzheimer disease', *Neurology*, 69: 1850-8.

Morris, J. C., D. W. McKeel, Jr., M. Storandt, E. H. Rubin, J. L. Price, E. A. Grant, M. J. Ball, and L. Berg. 1991. 'Very mild Alzheimer's disease: informant-based clinical, psychometric, and pathologic distinction from normal aging', *Neurology*, 41: 469-78.

Mosconi, L., R. D. Andrews, and D. C. Matthews. 2013. 'Comparing brain amyloid deposition, glucose metabolism, and atrophy in mild cognitive impairment with and without a family history of dementia', *J Alzheimers Dis*, 35: 509-24.

Mracsko, E., and R. Veltkamp. 2014. 'Neuroinflammation after intracerebral hemorrhage', *Front Cell Neurosci*, 8: 388.

Mufson, E. J., L. I. Binder, S. E. Counts, S. T. DeKosky, L. Toledo-Morrell, S. D. Ginsberg, M. D. Ikonomovic, S. E. Perez, and S. W. Scheff. 2012. 'Mild cognitive impairment: pathology and mechanisms', *Acta Neuropathol*, 123.

Mungas, D., B. R. Reed, W. G. Ellis, and W. J. Jagust. 2001. 'The effects of age on rate of progression of Alzheimer disease and dementia with associated cerebrovascular disease', *Arch Neurol*, 58: 1243-7.

Muoio, V., P. B. Persson, and M. M. Sendeski. 2014. 'The neurovascular unit - concept review', *Acta Physiol (Oxf)*, 210: 790-8.

Nelson, P. T., G. A. Jicha, F. A. Schmitt, H. Liu, D. G. Davis, M. S. Mendiondo, E. L. Abner, and W. R. Markesbery. 2007. 'Clinicopathologic correlations in a large Alzheimer disease center autopsy cohort: neuritic plaques and neurofibrillary tangles "do count" when staging disease severity', *J Neuropathol Exp Neurol*, 66: 1136-46.

Niu, F., H. Yao, W. Zhang, R. L. Sutliff, and S. Buch. 2014. 'Tat 101-mediated enhancement of brain pericyte migration involves platelet-derived growth factor subunit B homodimer: implications for human immunodeficiency virus-associated neurocognitive disorders', *J Neurosci*, 34: 11812-25.

Noble, W., D. P. Hanger, C. C. Miller, and S. Lovestone. 2013. 'The importance of tau phosphorylation for neurodegenerative diseases', *Front Neurol*, 4: 83.

Okamoto, Y., T. Yamamoto, R. N. Kalaria, H. Senzaki, T. Maki, Y. Hase, A. Kitamura, K. Washida, M. Yamada, H. Ito, H. Tomimoto, R. Takahashi, and M. Ihara. 2012. 'Cerebral hypoperfusion accelerates cerebral amyloid angiopathy and promotes cortical microinfarcts', *Acta Neuropathol*, 123: 381-94.

Omalu, B. I., S. T. DeKosky, R. L. Minster, M. I. Kamboh, R. L. Hamilton, and C. H. Wecht. 2005. 'Chronic traumatic encephalopathy in a National Football League player', *Neurosurgery*, 57: 128-34; discussion 28-34.

Palmer, A. M., G. K. Wilcock, M. M. Esiri, P. T. Francis, and D. M. Bowen. 1987. 'Monoaminergic innervation of the frontal and temporal lobes in Alzheimer's disease', *Brain Res*, 401: 231-8.

Pamphlett, R. 2014. 'Uptake of environmental toxicants by the locus ceruleus: a potential trigger for neurodegenerative, demyelinating and psychiatric disorders', *Med Hypotheses*, 82: 97-104.

Pardridge, W. M. 1999. 'Blood-brain barrier biology and methodology', *J Neurovirol*, 5: 556-69.

Paspalas, C. D., and G. C. Papadopoulos. 1996. 'Ultrastructural relationships between noradrenergic nerve fibers and non-neuronal elements in the rat cerebral cortex', *Glia*, 17: 133-46.

Peppiatt, C. M., C. Howarth, P. Mobbs, and D. Attwell. 2006. 'Bidirectional control of CNS capillary diameter by pericytes', *Nature*, 443: 700-4.

Pienaar, I. S., C. H. Lee, J. L. Elson, L. McGuinness, S. M. Gentleman, R. N. Kalaria, and D. T. Dexter. 2015. 'Deep-brain stimulation associates with improved microvascular integrity in the subthalamic nucleus in Parkinson's disease', *Neurobiol Dis*, 74: 392-405.

Polak, P. E., S. Kalinin, and D. L. Feinstein. 2011. 'Locus coeruleus damage and noradrenaline reductions in multiple sclerosis and experimental autoimmune encephalomyelitis', *Brain*, 134: 665-77.

Pluta, R. M., J. Hansen-Schwartz, J. Dreier, P. Vajkoczy, R. L. Macdonald, S. Nishizawa, H. Kasuya, G. Wellman, E. Keller, A. Zauner, N. Dorsch, J. Clark, S. Ono, T. Kiris, P. Leroux, and J. H. Zhang. 2009. 'Cerebral vasospasm following

subarachnoid hemorrhage: time for a new world of thought', *Neurol Res*, 31: 151-8.

Raichle, M. E., B. K. Hartman, J. O. Eichling, and L. G. Sharpe. 1975. 'Central noradrenergic regulation of cerebral blood flow and vascular permeability', *Proc Natl Acad Sci U S A*, 72: 3726-30.

Raschetti, R., E. Albanese, N. Vanacore, and M. Maggini. 2007. 'Cholinesterase inhibitors in mild cognitive impairment: a systematic review of randomised trials', *PLoS Med*, 4: e338.

Rorabaugh, J. M., T. Chalermpalanupap, C. A. Botz-Zapp, V. M. Fu, N. A. Lembeck, R. M. Cohen, and D. Weinshenker. 2017. 'Chemogenetic locus coeruleus activation restores reversal learning in a rat model of Alzheimer's disease', *Brain*, 140: 3023-38.

Roussel, B., A. Buguet, P. Bobillier, and M. Jouvet. 1967. '[Locus ceruleus, paradoxal sleep, and cerebral noradrenaline]', *C R Seances Soc Biol Fil*, 161: 2537-41.

Samuels, E. R., and E. Szabadi. 2008. 'Functional neuroanatomy of the noradrenergic locus coeruleus: its roles in the regulation of arousal and autonomic function part I: principles of functional organisation', *Curr Neuropharmacol*, 6: 235-53.

Sara, S. J. 2009a. 'The locus coeruleus and noradrenergic modulation of cognition', *Nat Rev Neurosci*, 10: 211-23.

———. 2009b. 'The locus coeruleus and noradrenergic modulation of cognition', *Nat Rev Neurosci*, 10.

Schmidt, R., H. Schmidt, J. Haybaeck, M. Loitfelder, S. Weis, M. Cavalieri, S. Seiler, C. Enzinger, S. Ropele, T. Erkinjuntti, L. Pantoni, P. Scheltens, F. Fazekas, and K. Jellinger. 2011. 'Heterogeneity in age-related white matter changes', *Acta Neuropathol*, 122: 171-85.

Schneider, J. A., Z. Arvanitakis, W. Bang, and D. A. Bennett. 2007. 'Mixed brain pathologies account for most dementia cases in community-dwelling older persons', *Neurology*, 69: 2197-204.

Schneider, J. A., Z. Arvanitakis, S. E. Leurgans, and D. A. Bennett. 2009. 'The neuropathology of probable Alzheimer disease and mild cognitive impairment', *Ann Neurol*, 66: 200-8.

Selkoe, D. J. 2001. 'Alzheimer's disease: genes, proteins, and therapy', *Physiol Rev*, 81: 741-66.

Selkoe, D. J., and J. Hardy. 2016. 'The amyloid hypothesis of Alzheimer's disease at 25 years', *EMBO Mol Med*, 8: 595-608.

Seo, S. W., B. Hwa Lee, E. J. Kim, J. Chin, Y. Sun Cho, U. Yoon, and D. L. Na. 2007. 'Clinical significance of microbleeds in subcortical vascular dementia', *Stroke*, 38: 1949-51.

Serrano-Pozo, A., M. L. Mielke, T. Gomez-Isla, R. A. Betensky, J. H. Growdon, M. P. Frosch, and B. T. Hyman. 2011. 'Reactive glia not only associates with plaques but also parallels tangles in Alzheimer's disease', *Am J Pathol*, 179: 1373-84.

Silbert, L. C., C. Nelson, D. B. Howieson, M. M. Moore, and J. A. Kaye. 2008. 'Impact of white matter hyperintensity volume progression on rate of cognitive and motor decline', *Neurology*, 71: 108-13.

Snyder, H. M., R. A. Corriveau, S. Craft, J. E. Faber, S. M. Greenberg, D. Knopman, B. T. Lamb, T. J. Montine, M. Nedergaard, C. B. Schaffer, J. A. Schneider, C. Wellington, D. M. Wilcock, G. J. Zipfel, B. Zlokovic, L. J. Bain, F. Bosetti, Z. S. Galis, W. Koroshetz, and M. C. Carrillo. 2015. 'Vascular contributions to cognitive impairment and dementia including Alzheimer's disease', *Alzheimers Dement*, 11: 710-7.

Sweeney, M. D., A. P. Sagare, and B. V. Zlokovic. 2018. 'Blood-brain barrier breakdown in Alzheimer disease and other neurodegenerative disorders', *Nat Rev Neurol*, 14: 133-50.

Szabadi, E. 2013. 'Functional neuroanatomy of the central noradrenergic system', *J Psychopharmacol*, 27: 659-93.

Szot, P., S. S. White, J. L. Greenup, J. B. Leverenz, E. R. Peskind, and M. A. Raskind. 2006. 'Compensatory changes in the noradrenergic nervous system in the locus ceruleus and hippocampus of postmortem subjects with Alzheimer's disease and dementia with Lewy bodies', *J Neurosci*, 26: 467-78.

Takauchi, S., S. Yamauchi, Y. Morimura, K. Ohara, Y. Morita, S. Hayashi, and K. Miyoshi. 1995. 'Coexistence of Pick bodies and atypical Lewy bodies in the locus ceruleus neurons of Pick's disease', *Acta Neuropathol*, 90: 93-100.

Tanskanen, M., M. Makela, L. Myllykangas, S. Rastas, R. Sulkava, and A. Paetau. 2012. 'Intracerebral hemorrhage in the oldest old: a population-based study (vantaa 85+)', *Front Neurol*, 3: 103.

Terry, R. D., N. K. Gonatas, and M. Weiss. 1964. 'Ultrastructural Studies in Alzheimer's Presenile Dementia', *Am J Pathol*, 44: 269-97.

Thal, D. R., E. Capetillo-Zarate, S. Larionov, M. Staufenbiel, S. Zurbruegg, and N. Beckmann. 2009. 'Capillary cerebral amyloid angiopathy is associated with vessel occlusion and cerebral blood flow disturbances', *Neurobiol Aging*, 30: 1936-48.

Thal, D. R., E. Ghebremedhin, M. Orantes, and O. D. Wiestler. 2003. 'Vascular pathology in Alzheimer disease: correlation of cerebral amyloid angiopathy and arteriosclerosis/lipohyalinosis with cognitive decline', *J Neuropathol Exp Neurol*, 62: 1287-301.

Theofilas, P., A. J. Ehrenberg, S. Dunlop, A. T. Di Lorenzo Alho, A. Nguy, R. E. P. Leite, R. D. Rodriguez, M. B. Mejia, C. K. Suemoto, R. E. L. Ferretti-Rebustini, L. Polichiso, C. F. Nascimento, W. W. Seeley, R. Nitrini, C. A. Pasqualucci, W. Jacob Filho, U. Rueb, J. Neuhaus, H. Heinsen, and L. T. Grinberg. 2017. 'Locus coeruleus volume and cell population changes during Alzheimer's disease progression: A stereological study in human postmortem brains with potential implication for early-stage biomarker discovery', *Alzheimers Dement*, 13: 236-46.

Toledo, J. B., S. E. Arnold, K. Raible, J. Brettschneider, S. X. Xie, M. Grossman, S. E. Monsell, W. A. Kukull, and J. Q. Trojanowski. 2013. 'Contribution of cerebrovascular disease in autopsy confirmed neurodegenerative disease cases in the National Alzheimer's Coordinating Centre', *Brain*, 136: 2697-706.

Toledo, J. B., E. Toledo, M. W. Weiner, C. R. Jack, Jr., W. Jagust, V. M. Lee, L. M. Shaw, J. Q. Trojanowski, and Initiative Alzheimer's Disease Neuroimaging. 2012. 'Cardiovascular risk factors, cortisol, and amyloid-beta deposition in Alzheimer's Disease Neuroimaging Initiative', *Alzheimers Dement*, 8: 483-9.

Toussay, X., K. Basu, B. Lacoste, and E. Hamel. 2013. 'Locus coeruleus stimulation recruits a broad cortical neuronal network and increases cortical perfusion', *J Neurosci*, 33: 3390-401.

van Asch, C. J., M. J. Luitse, G. J. Rinkel, I. van der Tweel, A. Algra, and C. J. Klijn. 2010. 'Incidence, case fatality, and functional outcome of intracerebral haemorrhage over time, according to age, sex, and ethnic origin: a systematic review and meta-analysis', *Lancet Neurol*, 9: 167-76.

Vermeiren, Y., and P. P. De Deyn. 2017. 'Targeting the norepinephrinergic system in Parkinson's disease and related disorders: The locus coeruleus story', *Neurochem Int*, 102: 22-32.

Wada, K., H. Arai, M. Takanashi, J. Fukae, H. Oizumi, T. Yasuda, Y. Mizuno, and H. Mochizuki. 2006. 'Expression levels of vascular endothelial growth factor and its receptors in Parkinson's disease', *Neuroreport*, 17: 705-9.

Wilcock, G. K., M. M. Esiri, D. M. Bowen, and A. O. Hughes. 1988. 'The differential involvement of subcortical nuclei in senile dementia of Alzheimer's type', *J Neurol Neurosurg Psychiatry*, 51: 842-9.

Williams, G. R. 2001. 'Incidence and characteristics of total stroke in the United States', *BMC Neurol*, 1: 2.

Woods, M. D., R. I. Freshney, S. G. Ball, and P. F. Vaughan. 1989. 'Regulation of cyclic AMP formation in cultures of human foetal astrocytes by beta 2-adrenergic and adenosine receptors', *J Neurochem*, 53: 864-9.

Yokoo, H., H. Kobayashi, S. Minami, S. Shiraishi, R. Yamamoto, T. Yanagita, K. Tsuchiya, M. Mohri, and A. Wada. 2000. 'alpha(1)-Adrenergic receptor subtypes in rat cerebral microvessels', *Brain Res*, 878: 183-7.

Yoshiyama, Y., M. Higuchi, B. Zhang, S. M. Huang, N. Iwata, T. C. Saido, J. Maeda, T. Suhara, J. Q. Trojanowski, and V. M. Lee. 2007. 'Synapse loss and microglial activation precede tangles in a P301S tauopathy mouse model', *Neuron*, 53: 337-51.

Zarow, C., S. A. Lyness, J. A. Mortimer, and H. C. Chui. 2003a. 'Neuronal loss is greater in the locus coeruleus than nucleus basalis and substantia nigra in Alzheimer and Parkinson diseases', *Arch Neurol*, 60.

———. 2003b. 'Neuronal loss is greater in the locus coeruleus than nucleus basalis and substantia nigra in Alzheimer and Parkinson diseases', *Arch Neurol*, 60: 337-41.

Zekry, D., C. Duyckaerts, J. Belmin, C. Geoffre, R. Moulias, and J. J. Hauw. 2003. 'Cerebral amyloid angiopathy in the elderly: vessel walls changes and relationship with dementia', *Acta Neuropathol*, 106: 367-73.

Zenaro, E., G. Piacentino, and G. Constantin. 2017. 'The blood-brain barrier in Alzheimer's disease', *Neurobiol Dis*, 107: 41-56.

Zlokovic, B. V. 2008. 'The blood-brain barrier in health and chronic neurodegenerative disorders', *Neuron*, 57: 178-201.

Chapter 2: Locus Coeruleus Neuronal and Vascular Pathology during the Progression of Alzheimer's Disease

Introduction

Alzheimer's disease (AD) is the most common dementing disorder and is the sixth leading cause of death in the United States. Currently, 1 in 9 older adults (>65 years) in the US currently suffer from this debilitating disease. With life expectancy increasing, and thus a population shifting to a more aged demographic, it is estimated that by 2050 there will be 15 million AD patients in the United States with the cost of their care exceeding 1 trillion dollars annually (Alzheimer's 2018). While many postmortem neuropathological hallmarks of the disease have been characterized (e.g., neurofibrillary tangles [NFTs], amyloid plaques), the etiologic factors contributing to AD pathogenesis remain unclear. However, there is now emerging rationale for linking cerebrovascular disease (CVD) and vascular dysfunction to cognitive impairment (Arvanitakis et al. 2016; Nelson et al. 2016; Montagne et al. 2016). CVD—usually in the form of small vessel occlusive disease caused by chronic hypertension and other vascular risk factors—is a condition that frequently accompanies aging in general and AD in particular (Serrano-Pozo et al. 2011). In fact, the comorbidity of AD and CVD has been estimated at upwards of 70 percent (Erickson and Banks 2013; Attems and Jellinger 2014; Eriksson et al. 2010). These mixed pathologies present in AD patients suggest that AD often involves a microvascular disorder that may contribute to its pathogenesis and lower the threshold for cognitive decline (Schneider et al. 2009). For instance, AD is associated with cerebral amyloid angiopathy (CAA), microvascular

degeneration (tortuosity, fibrohyalinosis, and lipohyalinosis), disorders of the blood-brain barrier (BBB), white matter lesions, microinfarctions, lacunes, and cerebral hemorrhages (Jellinger and Attems 2007). Furthermore, AD and CVD share risk factors including hypercholesterolemia, atherosclerosis, diabetes, hypertension, smoking, and obesity (Alzheimer's 2018). However, the extent to which CVD impacts the onset of AD is unknown.

AD is believed to have an extensive preclinical stage since neuropathological examinations of older people with a clinical diagnosis of no cognitive impairment (NCI) or mild cognitive impairment (MCI)—a putative prodromal stage of AD—consistently reveal similar pathological signatures to those with frank AD (Albert et al. 2011; Markesbery et al. 2006; Kelly et al. 2017). Moreover, as the majority of cases with MCI also present with prominent CVD (Schneider et al. 2009), understanding whether shared mechanisms are involved in AD and CVD pathogenesis may provide cellular and molecular insights into vascular contributions to the progression of AD.
Thus, identifying these putative neurovascular events during the preclinical, pre-MCI stages of AD will be essential for therapeutic target identification within a disease-modifying window.

In this regard, noradrenergic neurons of the LC projection system, which provide the primary source of NE to the forebrain, mediate memory and attention (Berridge and Waterhouse 2003; Sara 2009) and degenerate in advanced AD (Berridge and Waterhouse 2003; Chan-Palay and Asan 1989; Davies and Maloney 1976; Mann et al. 1980; Mufson, Bothwell, and Kordower 1989; Whitehouse et al. 1981). However, there is evidence for the involvement of this system earlier in the disease process. For

instance, NFT deposition in the LC has been noted in aged control and cognitively impaired subjects and LC NFTs correlate with global cognition (Grudzien et al. 2007), in line with reduced NE levels in the hippocampus and cortex in AD (Adolfsson et al. 1979; Mann et al. 1980; Palmer et al. 1987). Moreover, it has been suggested that the LC is an initial site of NFT formation in young adults and during aging, thus serving as a potential site or origin for NFT propagation during disease progression (Braak and Del Tredici 2011; Grudzien et al. 2007). Furthermore, the LC NE projection system is a mediator of cerebrovascular function, regulating blood flow, vessel diameter, and blood volume changes in regions of oxygen demand (Raichle et al. 1975; Peppiatt et al. 2006; Bekar, Wei, and Nedergaard 2012). Thus, LC dysfunction and degeneration could influence the vascular pathology often seen in AD.

Reductions in LC neuron number are associated with increased cortical amyloid plaque and NFT loads (Bondareff, Mountjoy, and Roth 1981; Simic et al. 2016), and correlate better with onset and duration of AD than cholinergic nucleus basalis (NB) degeneration (Forstl et al. 1994; Mann, Yates, and Marcyniuk 1984; Zarow et al. 2003). More recently, morphometric studies have shown that the volume and number of total neurons in the LC undergo a step-wise reduction with successive Braak stage (Theofilas et al. 2016), and there is a significant loss of neuromelanin-containing LC neurons in individuals meeting the clinical pathologic criteria for MCI [e.g., clinical dementia rating (CDR) = 0.5 with low to intermediate AD pathology] (Arendt et al. 2015).

Previous work in our lab has characterized the extent of LC loss in people who died with no cognitive impairment (NCI), amnestic MCI (aMCI; a prodromal AD stage characterized by deficits in episodic memory), and AD (Kelly et al. 2017). In this study,

we reported that tyrosine hydroxylase (TH)-positive noradrenergic LC neurons are vulnerable during the onset of dementia as evidenced by their loss in aMCI and AD and that this loss correlates with multiple measures of cognitive deterioration and neuropathological accumulation. Briefly, brainstems from de-identified subjects who died with an antemortem clinical diagnosis of NCI (n = 11), aMCI (n = 10) or mild/moderate AD (n = 8) representing both genders were obtained from participants in the Rush Religious Orders Study (RROS), a longitudinal clinical pathologic study of aging and AD in elderly Catholic clergy (Bennett et al. 2002; Mufson et al. 1999). TH immunohistochemistry was used to estimate changes in the number of noradrenergic LC neurons across the clinical diagnostic groups (**Figure 2.1**). Qualitatively, we observed a step-wise decrement in TH-positive neurons within the LC from NCI to aMCI to mild/moderate AD (**Figure 2.1A**) and unbiased stereological cell counts validated these observations (**Figure 2.1 B**).

Moreover, TH-positive LC neuron number was significantly associated with individual Global Cognitive Score (GCS), the composite z-score of 17 neuropsychological tests administered prior to death, as well as with the final composite scores referable to episodic memory, semantic memory, working memory, perceptual speed, and visuospatial ability (**Figure 2.2 A-F**). With respect to neuropathological diagnostic criteria, reductions in TH-positive LC neuron numbers were negatively correlated with increasing measures of neuropathology as characterized by Braak, NIA-Reagan and CERAD staging (**Figure 2.2 G-I**).

The RROS study (Kelly et al. 2017) demonstrated that LC neuron loss is already at 30% by the time of cognitive impairment, and thus indicated to us a need to

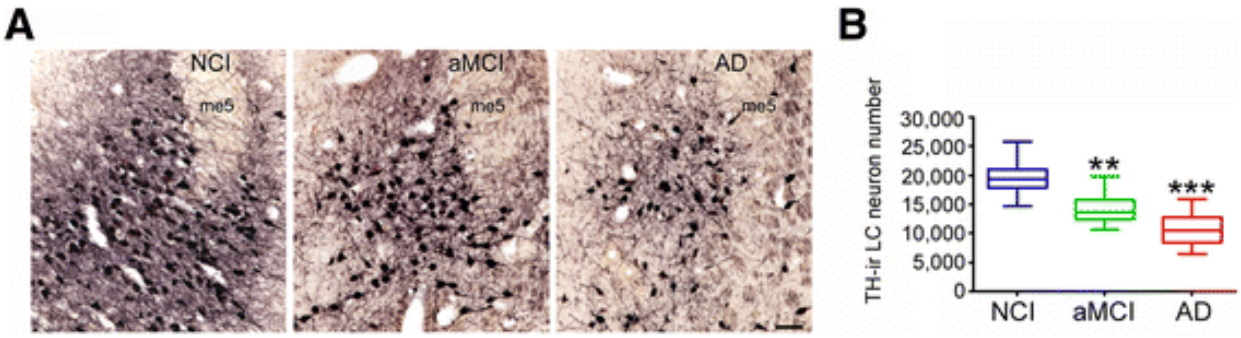

Figure 2.1 LC cell loss in aMCI

A. Representative TH+ neuron and fiber staining in dorsal pontine tissue harvested from NCI, aMCI, and mild/moderate AD subjects. **B.** Unbiased stereological cell counts revealed a significant ~30% decrease in the number of LC neurons in aMCI compared to NCI cases. There was a ~50% loss of LC neurons in the AD group compared to NCI. **, $p < 0.01$, ***, $p < 0.001$ compared to NCI, via one-way ANOVA with Bonferroni *post hoc* testing. There was also a significant ~25% difference in neuronal cell counts between the aMCI and AD groups ($p < 0.05$). me5 = mesencephalic tract of 5. Scale Bar = 100 μm.

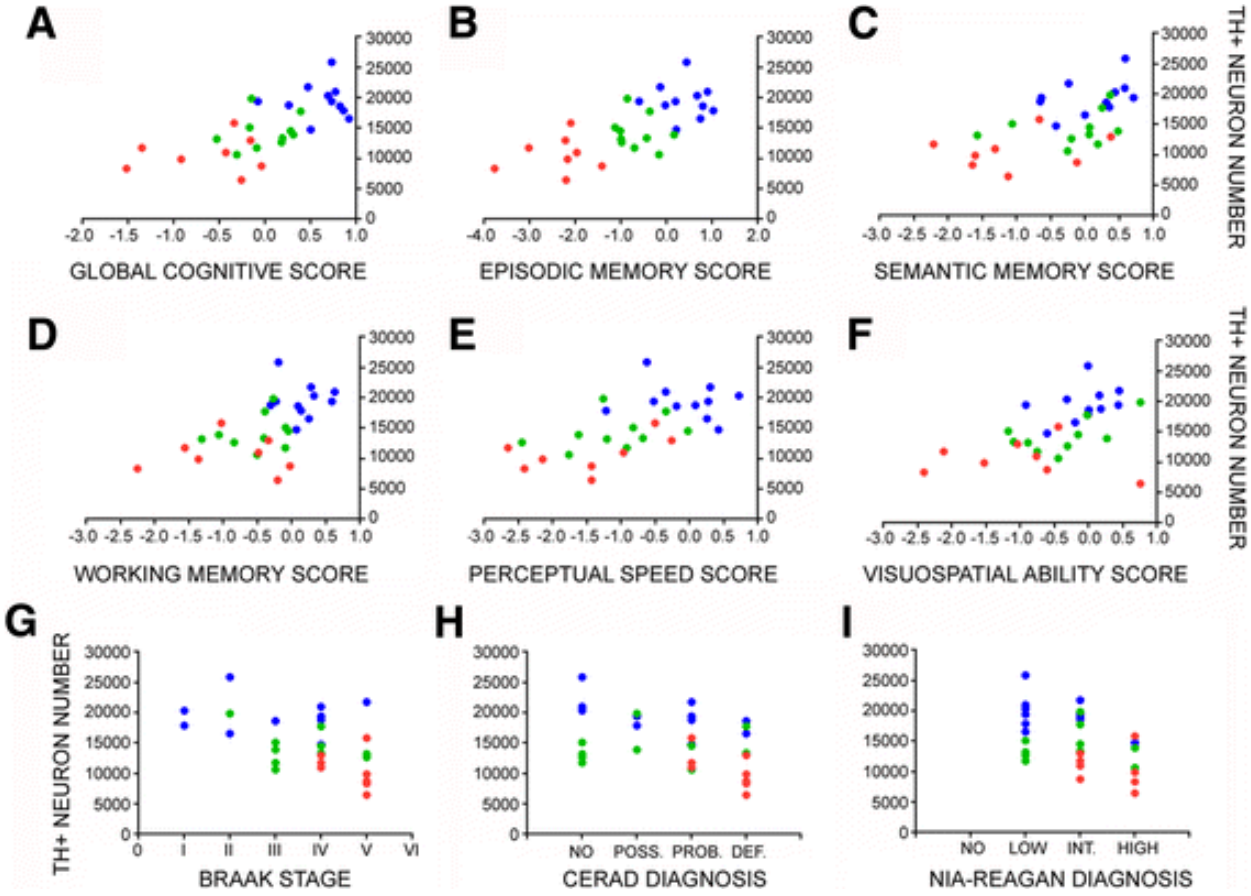

Figure 2.2 TH-ir LC neuron number correlates with multiple measures of antemortem cognition and postmortem neuropathology during the progression of AD.

Scatterplots show significant relationships between reductions in LC neurons and **A** the GCS for each individual ($r = 0.7$, $p < 0.0001$), as well as poorer performance on composite scores of **B** episodic memory ($r = 0.71$, $p < 0.0001$), **C** semantic memory ($r = 0.598$, $p = 0.0008$), **D** working memory ($r = 0.6$, $p = 0.0006$), **E** perceptual speed ($r = 0.66$, $p < 0.0001$), and **F** visuospatial ability ($r = 0.53$, $p = 0.003$). There were also significant negative correlations between TH+ neuron number and increasing neuropathology as defined by **G** Braak ($r = -0.46$, $p = 0.01$), **H** CERAD ($r =$

Figure 2.2 (cont'd)

−0.41, $p = 0.03$), and **I** NIA-Reagan ($r = -0.45$, $p = 0.01$) diagnostic criteria. All associations were tested using Spearman rank correlation analysis. Abbreviations: TH+ (TH-positive), POSS. (possible), PROB. (probable), DEF. (definite), INT. (intermediate). Symbols: NCI (*blue-filled circle*), aMCI (*green-filled circle*), AD (*red-filled circle*).

understand and characterize LC neurons prior to the transition from NCI to prodromal AD. This, in addition to the evidence that that LC dysfunction may lead to accompanying vascular pathology in AD, led us to the following study. To gain a better understanding of the pattern of LC degeneration in different disease states we enumerated and characterized LC neurons from tissue acquired from the University of Kentucky Alzheimer's Disease Center (UKADC). These cases not only included MCI and AD cases but cognitively normal individuals with low Braak scores (0-II; NCI) or higher Braak scores (III/IV) which have been deemed a preclinical AD (PCAD) group, in addition to a greater number of clinical and pathological measures related to vascular health. With these diagnostic groups we hoped to characterize potential neurovascular consequences of LC degeneration in the context of PCAD.

Methods

UKADC subjects

Formalin-fixed, paraffin-embedded pontine tissue blocks were obtained from participants in the Healthy Brain Aging Volunteers (HBAV) cohort (**Table 2.1**), which is administered by the National Institute of Aging (NIA)-funded UKADC (Schmitt et al. 2012; Neltner et al. 2016). Antemortem clinical evaluations for each subject follow the "Alzheimer's Disease Centers' Uniform Data Set," as required by NACC (Weintraub et al. 2009; Beekly et al. 2007). A major goal of the UKADC is to understand normal aging and the transition to dementia by using clinical-pathological correlation analysis. In this present study, we selected tissue blocks from 4 distinct groups that we designated as follows: The first group ("NCI") was clinically NCI with minimal neurodegeneration

Table 2.1 Inclusion/exclusion criteria for participation in the UKADC Healthy Aging Volunteers cohort:

INCLUSION CRITERIA	EXCLUSION CRITERIA
Minimum age 70 (or 65 for African Americans)	History of substance abuse (including alcohol)
Cognitively and neurologically normal	Major head injury
Family history of AD or dementia is preferred	Major psychiatric or neurological illness
Agree to brain donation at death	Medical illnesses that are non-stable, impairing, and/or have an effect on the CNS
Live within a 2 hour drive of Lexington, KY	Chronic infectious disease (e.g., HIV)
Must have a designated informant for structured interviews (e.g., CDR)	Strokes
Willing to undergo annual cognitive testing, physical and neurological exam	History of encephalitis, meningitis or epilepsy

(Braak Stage 0-II), without significant cerebrovascular disease and minimal or no amyloid deposition. The second group ("PCAD") was also clinically NCI (i.e., cognitively normal) but displays considerable AD-like pathology, including diffuse plaques, neuritic plaques and NFTs (Braak Stage III/IV) which would be sufficient to meet NIA-Reagan Institute Intermediate or High Likelihood criteria for AD (see caveat below). In addition, we selected tissue samples from subjects who died with a clinical diagnosis of MCI characterized by impairments in memory function in the absence of dementia, or with mild (Mini Mental State Exam [MMSE] scores =18-25)/moderate (MMSE = 10-18) AD.

Caveat of PCAD status: Potential confounds arising from PCAD group heterogeneity was debated at NIA workshops on the neuropathologic assessment (Hyman et al. 2012; Jicha et al. 2012) and the preclinical definition of AD (Sperling et al. 2011). The NIA panels "acknowledge that some of these individuals will never manifest clinical symptoms in their lifetime" or "should they have lived longer" (Sperling et al. 2011). However, the NIA consensus is that PCAD is best defined as those individuals with sufficient AD pathology to meet NIA-Reagan Institute Intermediate or High Likelihood criteria (Braak stage III or higher and moderate or frequent neuritic plaque scores) who had normal cognitive function as shown by antemortem psychometric test scores within the normal range after adjustment for age and education (Hyman et al. 2012; Sperling et al. 2011). This condition is viewed as representative of the PCAD stage when the disease process is most likely to be diagnosed with high sensitivity and specificity and potentially tractable to therapy.

Exclusion criteria for postmortem tissue selection:

For each case, we were supplied with a summary clinical (based on the most recent data prior to death) and neuropathological assessment, as well as subject demographics. This information was classified as, “Exempt, Category 4” from IRB review since the tissue was sampled postmortem and could not be connected to the identity of the subject. We used this data to formulate the following exclusion criteria for case selection, in order to sample cases from each of the 4 diagnostic groups with minimal potential confounding variables:

1. Clinical and/or neuropathologic evidence for comorbid neurologic disease such as vascular dementia (e.g., large strokes, lacunes), parkinsonism, Lewy body dementia, hippocampal sclerosis.
2. Tissue block was missing a significant extent of the LC based on the operational fiduciary landmarks established for semi-quantitative analysis (see below)

Power analysis, sample size, and statistics

Based on our data values from our previous studies (Kelly et al. 2017) and $\alpha = 0.05$, a sample size of 6/group was determined have 80% power to detect an effect size of 1.25 standard deviations between NCI and MCI. Using our rigorous exclusion criteria for case selection, we identified the following number of cases for each diagnostic group: NCI (n=8), PCAD (n=7), MCI (n=7), and mild/moderate AD (n=7; total n = 29). Interestingly, based on the results of this dissertation, much larger sample sets (n= >20/group) would be necessary to show differences between PCAD and NCI in any subsequent study due to the heterogeneity in LC neuron number between the two

groups (see Kelly et al. 2017). Demographic variables and neuron number were compared across groups by one-way analysis of variance (ANOVA) with Bonferroni *post hoc* testing or Fisher's exact test. Associations between LC neuron number and clinical pathological variables were tested using Spearman rank correlations. The level of statistical significance was set at $p < 0.05$.

Tissue processing and histology

Paraffin-embedded tissue blocks from samples meeting the criteria described above were sectioned at 20-μm thickness on a HM 355S automatic rotary microtome (Thermo Scientific, Waltham, MA) and mounted on charged slides. Slides were dried and 79subsequently stored at 4°C. Tissue slides (20 μm) were heated, deparaffinized in two xylenes immersions and rehydrated in descending ethanol concentrations. Slides were then placed in preheated 1% Luxol Fast Blue Solution (Sigma) for two hours at 60°C. Slides were rinsed in 95% ethanol and differentiated in 0.05% Lithium carbonate and 70% ethanol. After which, slides were stained for 5 minutes in hematoxylin solution (Harris' Modified, Fisher), and differentiated in acid alcohol and ammonia water—rinsed in tap water between each solution. Slides were finally immersed in Eosin (Eosin Y Fisher) solution for 3 minutes then subsequently dehydrated in ethanol series and cover slipped with Cytoseal (Thermo).

Operational criteria for LC morphometric analyses

Due to the incomplete nature of some of the pons tissue provided by the UKADC, a protocol was established to standardize the counting field between cases. Using

Hematoxylin & Eosin (H&E) stains with Luxol fast blue stains for myelination, slides were evaluated to find the region where the decussation of cranial nerve IV (trochlear nerve) is visible in the vellum and the mesencephalic tract of V (trigeminal nerve) was dorsolateral to the LC (**Figure 2.3**). Only cells on slides caudal to that region were enumerated to ensure a standard frame of counting. Cases that could not meet these criteria e.g., incomplete tissue blocks, damaged pontine hemispheres, etc. were eliminated from analyses.

Immunohistochemistry

Tissue slides (20 μm) were heated, deparaffinized in two xylenes immersions and rehydrated in descending ethanol concentrations and distilled water. Slides were then washed in tris buffered saline (TBS; pH 7.4) for 10mins. Slides were then boiled in preheated citric acid buffer (pH 6.0) for 20 mins at 65° Celsius then allowed to cool to room temperature. Slides were washed in TBS + 0.5% Triton-X-100 (TX) for 10 minutes. Endogenous peroxidase activity was blocked via a 10-minute incubation in 10% hydrogen peroxide (H_2O_2) in methanol. Slides were washed in TBS + 0.5% TX 3 times for 10 minutes, then blocked in 10% goat serum, 2% Bovine Serum Albumin, 0.5% TX in TBS for 1 hour. Slides were dried, and a hydrophobic barrier drawn with a PAP pen. Primary antibody was aliquoted directly onto the slides and they were incubated in humidified chamber overnight at 4°C **(See table 2.2 for list of primary antibodies and Appendix Figure A.1 for results from control immunostaining experiments).** Following primary incubation, sections were incubated in biotinylated secondary antisera for 2 hours at room temperature, followed by Vector ABC detection

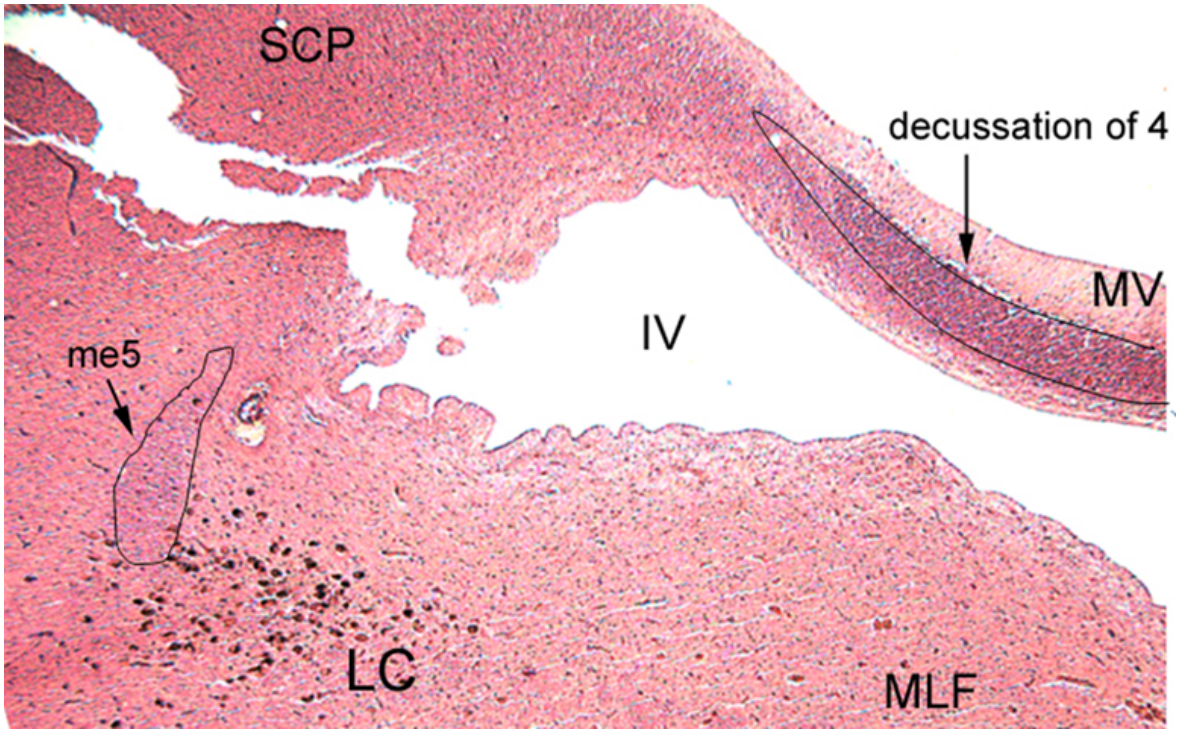

Figure 2.3 Operational definition of LC counting frame for UKADC pontine tissue

Hematoxylin and Eosin stain of UKADC pons tissue showing the start of counting frame. Landmarks we used: when the decussation of 4 (trochlear nerve) was visible in the vellum and the mesencephalic tract of 5 (trigeminal nerve) was dorsolateral to the LC. From there we counted caudally, as described above. SCP = superior cerebellar peduncle – conveys spinocerebellar tract to cerebellum for proprioception, MLF = medial longitudinal fasciculus – conveys cranial nerves 3, 4, 6, and 8

Table 2.2 Primary antibodies used to immunostain UKADC pontine tissue

Target	**Brand (Cat No.)**	**Dilution**
Tyrosine Hydroxylase (LC neuron marker)	Abcam (ab112)	1:500
DNA/RNA Oxidative Damage oh8dG, oh8G	QED bioscience (12501)	1:150
AT8 (Tau pathology marker)	Thermo (MN1020)	1:1000

kit using horseradish peroxidase (Vector Laboratories, Burlingame, CA). Antibody labeling was visualized by exposure to Vector SG chromogen (Vector Laboratories, Burlingame, CA) or 0.5mg/ml 3,3' diaminobenzidine with nickel II sulfate enhancement and 0.03% H2O2 in TBS.

LC cell enumeration

Neuromelanin and TH cell count estimations

Semi-quantitative analysis was performed using a Nikon Eclipse 80i microscope (Nikon), StereoInvestigator software (Microbrightfield Bioscience, Williston, VT) and a Retiga 4000R camera (Qimaging, Surrey, BC Canada). Briefly, an investigator blinded to experimental conditions drew a contour around each hemisphere of the LC. Using the StereoInvestigator meander scan function, total enumeration of both neuromelanin containing and TH+ cells was completed on every twelfth section ranging from 10-14 slides per case. Raw cell counts were by multiplied by the sampling fraction (12) to extrapolate the population estimate.

AT8 cell count estimations

Semi-quantitative analysis was performed using a Nikon Eclipse 80i microscope (Nikon), StereoInvestigator software (Microbrightfield Bioscience, Williston, VT) and Retiga 4000R camera (Qimaging, Surrey, BC Canada). Briefly, an investigator blinded to experimental conditions drew a contour around each hemisphere of the LC. Using the StereoInvestigator meander scan function, total enumeration of AT8+ cells was completed on every 24th section. Raw AT8+ cell counts were divided by total cell

counts to determine ratio of AT8+ LC cells to correct for observed cell loss across groups as raw counts showed no statistical difference across groups (**Appendix Figure A.2**).

DNA/RNA damage cell count estimations

Semi-quantitative analysis was performed using a Nikon Eclipse 80i microscope (Nikon), StereoInvestigator software (Microbrightfield Bioscience, Williston, VT) and a Retiga 4000R camera (Qimaging, Surrey, BC Canada). Briefly, an investigator blinded to experimental conditions drew a contour around each hemisphere of the LC. Using the StereoInvestigator meander scan function, total enumeration of cells positive for DNA/RNA damage was completed on 3 non-consecutive sections from each case. Raw immunoreactivity (IR)+ cell counts were divided by total cell counts to determine ratio of LC cells displaying DNA/RNA damage markers.

Histopathological analysis

Semiquantitative assessment of the vascular pathologies in the pons was performed on a 1:12 series of H&E-stained slides. These data were collected blinded to all clinical information and previous pathological diagnoses and were scored according to semiquantitative scoring methods that were previously described (Neltner et al. 2016). The first 6 vessels perpendicular to the field of view of each case were scored and then averaged for one pontine score. The severity was graded on a 4-point scale, ranging from 0 to 3+. The degree of involvement—or occlusion of the vessels—was graded in quartiles (0, 1%–25%, 26%–50%, 51%–75%, and 76%–100%).

Results

Case demographics

Table 2.3 summarizes the clinical, neuropathological, and demographic characteristics of the 29 cases examined. Statistical analysis revealed no significant differences in age, sex, education level, post-mortem interval (PMI) or APOE4 status across the groups examined. Although, not statistically significant, the higher percentage of APOE4 carriers diagnosed with MCI or AD might accurately reflect the relative risk for the disease conferred by this genotype. The diagnosis of dementia or AD met recommendations by the joint working group of the National Institute of Neurologic and Communicative Disorders and Stroke/AD and Related Disorders Association (NINCDS/ADRDA) (McKhann et al. 1984). The MCI subjects exhibited impairment in episodic memory on neuropsychological testing but did not meet the criteria for AD or dementia. These criteria for MCI are consistent with those used by others in the field (Petersen et al. 2001).

The AD subjects performed significantly worse on the MMSE compared to the NCI cases ($p = 0.0001$). Braak scores were also significantly different across the clinical groups. The NCI cases displayed significantly lower Braak scores than the AD group ($p < 0.0001$). NCI cases were classified as Braak stages 0 (25%) I/II (75%), III/IV (0%), or V/VI (0%). The PCAD cases were 0 (0%) I/II (0%), III/IV (100%), or V/VI (0%). The MCI cases met the criteria for Braak stages 0 (0%) I/II (43%), III/IV (57%), and V/VI (0%), and the AD cohort was classified as Braak stages 0 (0%) I/II (14%) III/IV (43%) or V/VI (43%). The NIA-Reagan diagnosis for likelihood of AD differentiated NCI and MCI from AD subjects ($p = 0.104$). CERAD scores were trending higher in AD compared to

Table 2.3 Subject clinical, demographic and neuropathological characteristics

Clinical Diagnosis	NCI	PCAD	MCI	AD	P-value	Pair-wise comparison	Statistics
	(*N* = 8)	(*N* = 7)	(*N* = 7)	(*N* = 7)			
Age (years) at death:							
Mean ± SD	85.75± 8.155	90.14± 6.176	87.14 ± 3.761	81.71 ± 10.19	0.2313	--	ANOVA with Bonferroni
(Range)	(72-94)	(84-101)	(84-95)	(68–93)			
Number (%) of males:	5 (62.5)	3(42.9)	3(42.9)	5(71.4)	0.6193	--	Fisher's exact
Years of education:						--	
Mean ± SD	16 ± 2.563	16.14 ± 0.8997	17.14 ± 1.069	16 ±2.582	0.6504		ANOVA with Bonferroni
(Range)	(12-20)	(15-18)	(16-18)	(12-20)			
Post Mortem Interval (PMI)						--	
Mean ± SD	3.8 ± 2.6	3.7 ± 2.1	3.4 ± 1.4	4.4 ± 2.0	0.88		
(Range)	1.8-10	1.3-10.8	1.2-6	2.7-8.5			ANOVA with Bonferroni
Infarcts							
Mean ± SD	0.125 ±0.353	0.5714 ±0.7868	3.429 ±3.552	0.7143 ±0.9512	p<0.05	NCI, PCAD<MCI	ANOVA with Bonferroni
(Range)	(0-1)	(0-2)	(0-9)	(0-2)			
Number (%) with Hypertension	5(62.5%)	4(57.1%)	4(57.1%)	4(57.1%)	0.9961		ANOVA with Bonferroni
Number (%) with ApoE ε4 allele:	1(14%)	0(0%)	3(42.9%)	4(57.1%)	0.0563	NCI, PCAD< (trending) MCI, AD	Fisher's exact

Table 2.3 (cont'd)

MMSE:							
Mean ± SD	29.13 ±0.8345	28.86 ±1.464	26±1.915	19.43±5.192		AD<NCI, PCAD, MCI	
(Range)	(28-30)	(26-30)	(23-28)	(11-25)			
Distribution of Braak scores:					<0.0001	NCI< PCAD, MCI, AD	ANOVA with Bonferroni
0	2	0	0	0			
I/II	6	0	3	1			
III/IV	0	7	4	3			
V/VI	0	0	0	4			
Clinical Diagnosis	**NCI**	**PCAD**	**MCI**	**AD**	**P-value**	**Pair-wise comparison**	**Statistics**
	(*N* = 8)	**(*N* = 7)**	**(*N* = 7)**	**(*N* = 7)**			
NIA Reagan diagnosis (likelihood of AD):					0.1046		ANOVA with Bonferroni
No AD	2	2	2	1			
Low	5	0	3	1			
Intermediate	1	5	2	2			
High	0	0	0	3			
CERAD diagnosis:					0.088	NCI< AD	ANOVA with Bonferroni
No AD	4	2	2	0			
Possible	1	0	2	0			
Probable	2	3	3	5			
Definite	1	2	0	2			

NCI and MCI (p =0.088), yet were not significantly different. Subjects with MCI had a significantly higher number of infarcts compared to NCI and PCAD individuals (p=0.01012, p=0.0372 respectively). This could possibly represent MCI as a prodromal state for both vascular cognitive impairment or mixed dementia. No differences were noted between groups in number of subjects with hypertension.

TH+ LC neuron number is decreased in MCI and AD and PCAD cases display a differential topography of degeneration compared to NCI

TH immunohistochemistry was used to estimate changes in the number of noradrenergic LC neurons across the clinical diagnostic groups. Qualitatively, we observed a decrement in TH-positive neurons within the LC from NCI to PCAD to MCI to mild/moderate AD in a step-wise manner between groups (**Figure 2.4 D**). Semiquantitative enumeration of LC cells validated these observations (**Figure 2.4 A**). The estimated number of TH-positive LC neurons in the **NCI** group was 17712 ± 4782 (range = 12432-24516), whereas neuron number was progressively decreased in the **PCAD** (13959± 6024; range = 6240-21522), **MCI** (9859± 4384; range = 2940-15152) and **AD** groups (1620± 5213; range = 1620-15900). Statistical comparisons revealed a significant ~40% decrease in the number of LC neurons in MCI compared to NCI cases. (p=0.0178) (**Figure 2.4 A**). An additional ~10-15% decrease in LC neuron number was quantified in AD compared to NCI resulting in a ~50-55% loss of LC neurons in the AD group compared to NCI (p=0.0178) (**Figure 2.4 A**). Total LC neuron number was similar between males and females in each diagnostic group (**Appendix Figure A.3**).

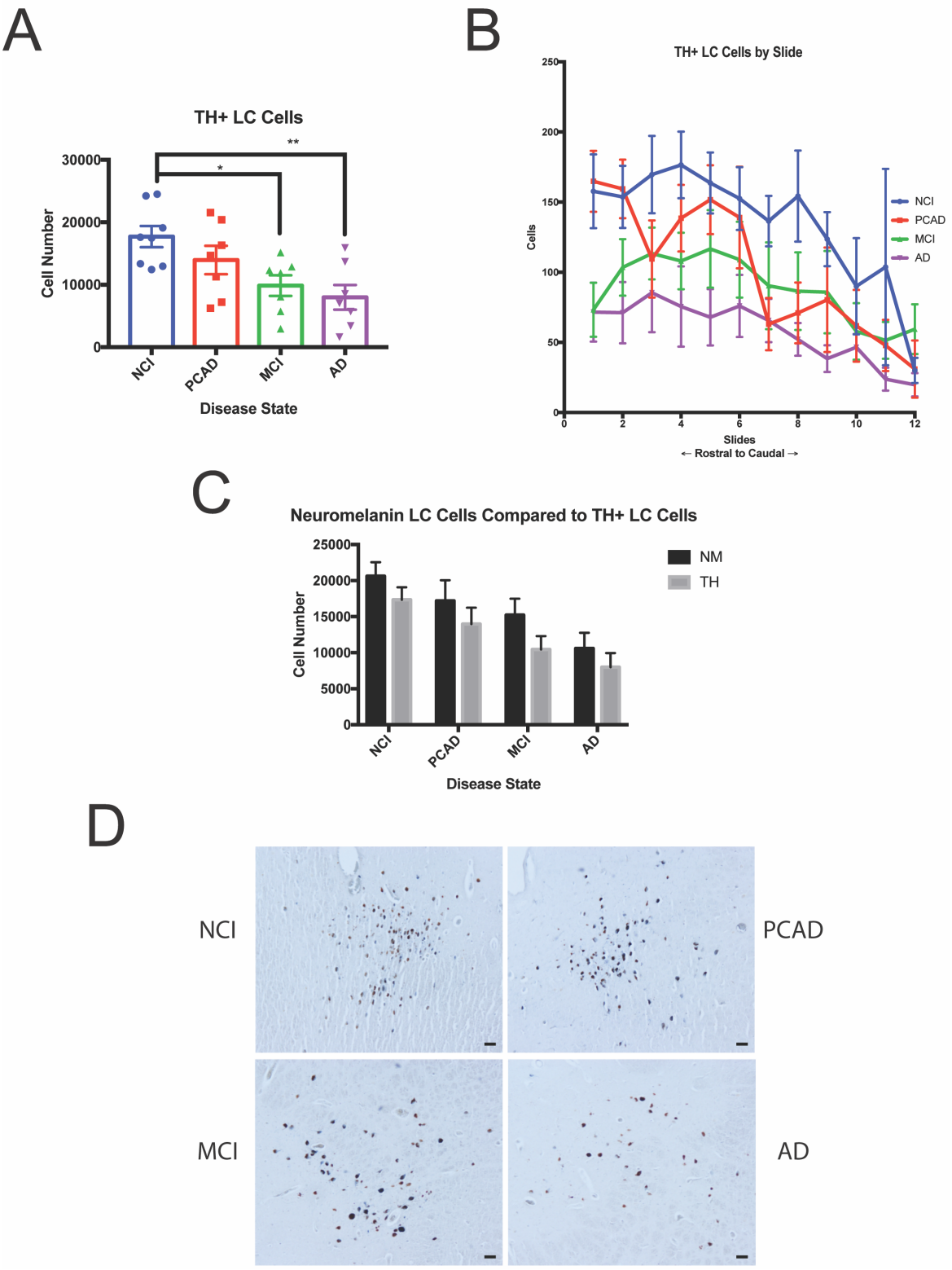

Figure 2.4 TH + LC Cell number is decreased in MCI and AD and PCAD cases display a differential topography of degeneration compared to controls

Figure 2.4 (cont'd)

A. Semi-quantitative cell counts revealed a significant ~40% decrease in the number of LC neurons in MCI compared to NCI cases ($p<0.05$) and a ~50% loss of LC neurons in the AD group compared to NCI ($p < 0.01$) via one-way ANOVA with Bonferroni *post hoc* testing. There were no significant differences between the PCAD case and NCI cases. Error bars represent SEM **B.** Further investigation into the topography of cell loss throughout the LC revealed significantly different linear regressions ($p<0.001$) between all cases. PCAD cases revealed a highly variable medial cell number per slide, with cell numbers close to AD cases in the caudal portion of the pons. Analysis of individual slide positions revealed NCI and PCAD differed significantly at relative slide #3, 4, 7-11 ($p<0.05$). Error bars represent SD.**C.** Comparisons of neuromelanin LC cell numbers to TH+ LC cell counts revealed no significant difference in noradrenergic phenotype during disease progression **D**. Representative TH immunostained images showing step-wise cell loss by disease state in the LC. Scale bars represent 50μm

While the number of TH-positive cells in the LC of PCAD individuals did not differ significantly between MCI or NCI groups, the pattern or topography of the degeneration of PCAD LC did differ dramatically from NCI (**Figure 2.4 B**). All pathological groups followed a linear rostral-caudal pattern of LC cells per slides. However, evaluation of these patterns via regression analysis indicated significantly different pattern of rostral to caudal LC number between NCI and PCAD ($p=0.0059$), wherein the topography of cell loss in PCAD more closely mirrored MCI and AD in the more caudal portions of the LC. Furthermore, comparing NCI with PCAD showed that the NCI groups had more cells within the majority of sections (7 out of 12 significantly different; $p<0.05$). Further, there was no statistical difference in the number of TH+ cells compared to neuromelanin containing LC cells (**Figure 2.4 C)** indicating a consistent TH phenotype across disease states.

TH+ LC cell number correlates with clinical cognitive measures

Estimated TH+ LC neuronal counts were correlated with demographic data, antemortem cognitive test performance, and postmortem neuropathologic variables. Neuron number was not associated with age, gender or ApoE status. However, lower LC neuron numbers and MMSE scores displayed a significant positive association ($r = 0.5379$, $p = 0.0026$) (**Figure 2.5 A)**. With respect to neuropathological diagnostic criteria, reductions in TH-positive LC neuron numbers were not correlated with increasing measures of neuropathology as characterized by Braak ($r = .283$, $p = 0.21$), NIA-Reagan ($r = -.10$, $p = 0.60$), and CERAD ($r = -.024$, $p = 0. 9$) staging (**Figure 2.5 B-D**).

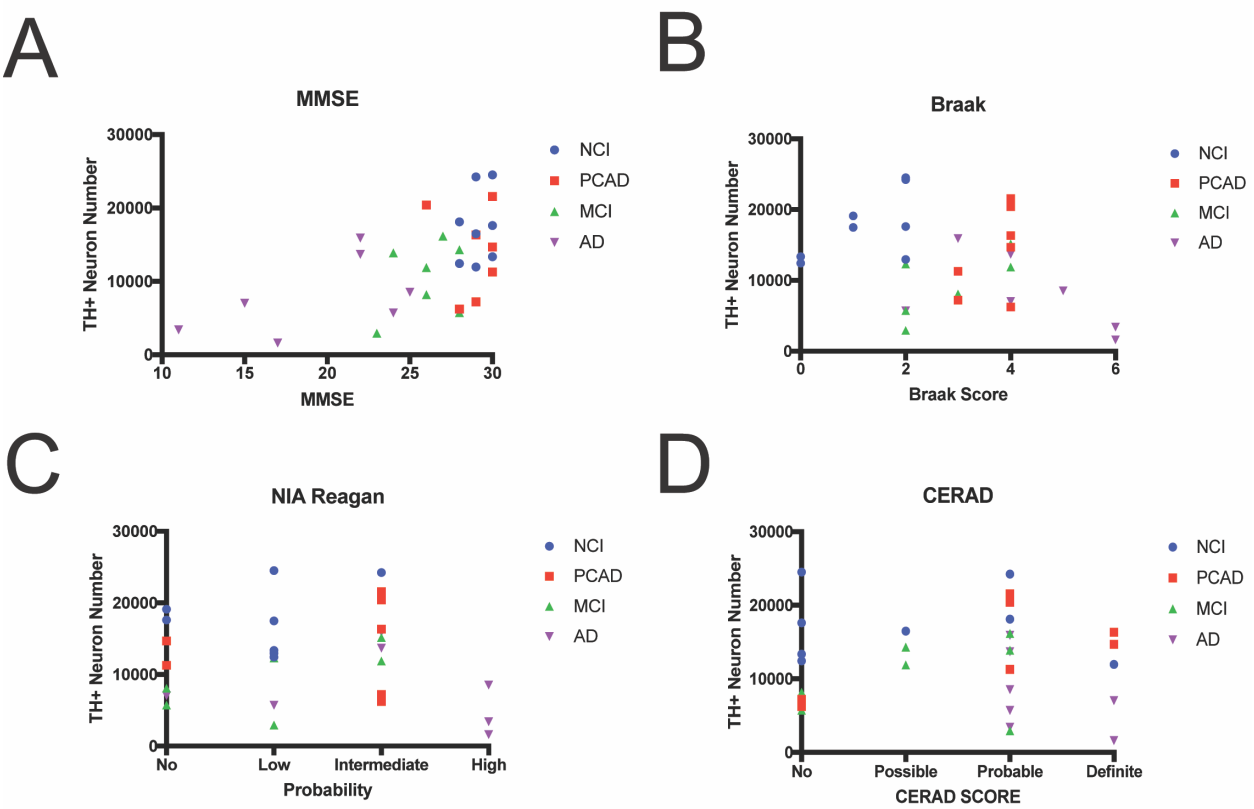

Figure 2.5 TH-positive LC neuron number correlates with MMSE but not neuropathology during the progression of AD.

A. Spearman rank correlation analyses revealed a positive association between LC TH positive cells and MMSE score ($r = 0.5379$, $p = 0.0026$) but not **B** Braak ($r = .283$, $p = 0.21$), **C** NIA Reagan ($r = -.10$, $p = 0.60$), or **D** CERAD scores ($r = -0.24$, $p = 0.9$)

Pontine arteriosclerosis severity is increased in MCI and AD

There is a widely recognized link between hypertension and arteriolosclerosis in the brain and other organs (Kanbay et al. 2011; Venkatachalam et al. 2010; Dozono et al. 1991). Using pathological scoring methods previously described by the UKADC for global arteriosclerosis measures in these cases (Neltner et al. 2014), we sought to identify when or if vascular changes in the pons surrounding the LC could be identified (**Figure 2.6 C)**. The LC sits on one of the largest capillary beds in the CNS and has high metabolic demands requiring constant blood flow (Bekar, Wei, and Nedergaard 2012; Szabadi 2013; Pamphlett 2014), thus disruptions in or dysfunction in the vasculature could lead to hypoperfusion or hypoxic conditions (Cipolla 2009). Ratings of arterioles surrounding the LC in the pons revealed higher arteriosclerosis severity in MCI ($p=0.0053$) and AD ($p<0.0001$) compared to NCI in H&E stained pontine tissue (**Figure 2.6 A)**. There was also a significant difference between PCAD and AD severity ($p=0.0003$) and a trending difference in observed arteriosclerosis between PCAD and MCI ($p=.08$). Correlation analyses revealed an association of higher arteriosclerosis score to lower TH-positive cell number that was trending toward significance ($p=0.11$ $r=-0.3$) **Figure 2.6 B**).

Ratio of AT8 positive LC cells increases across pathological groups

AT8 tau is a prominent pre-tangle modification in AD that appears as pathological tau first begins to deposit in affected neurons, implying it may act at the early stages of tau-mediated pathogenesis (Bancher et al. 1993; Kanaan et al. 2011). Additionally, Braak staging does not consider the brainstem in its pathological assessment (Braak and

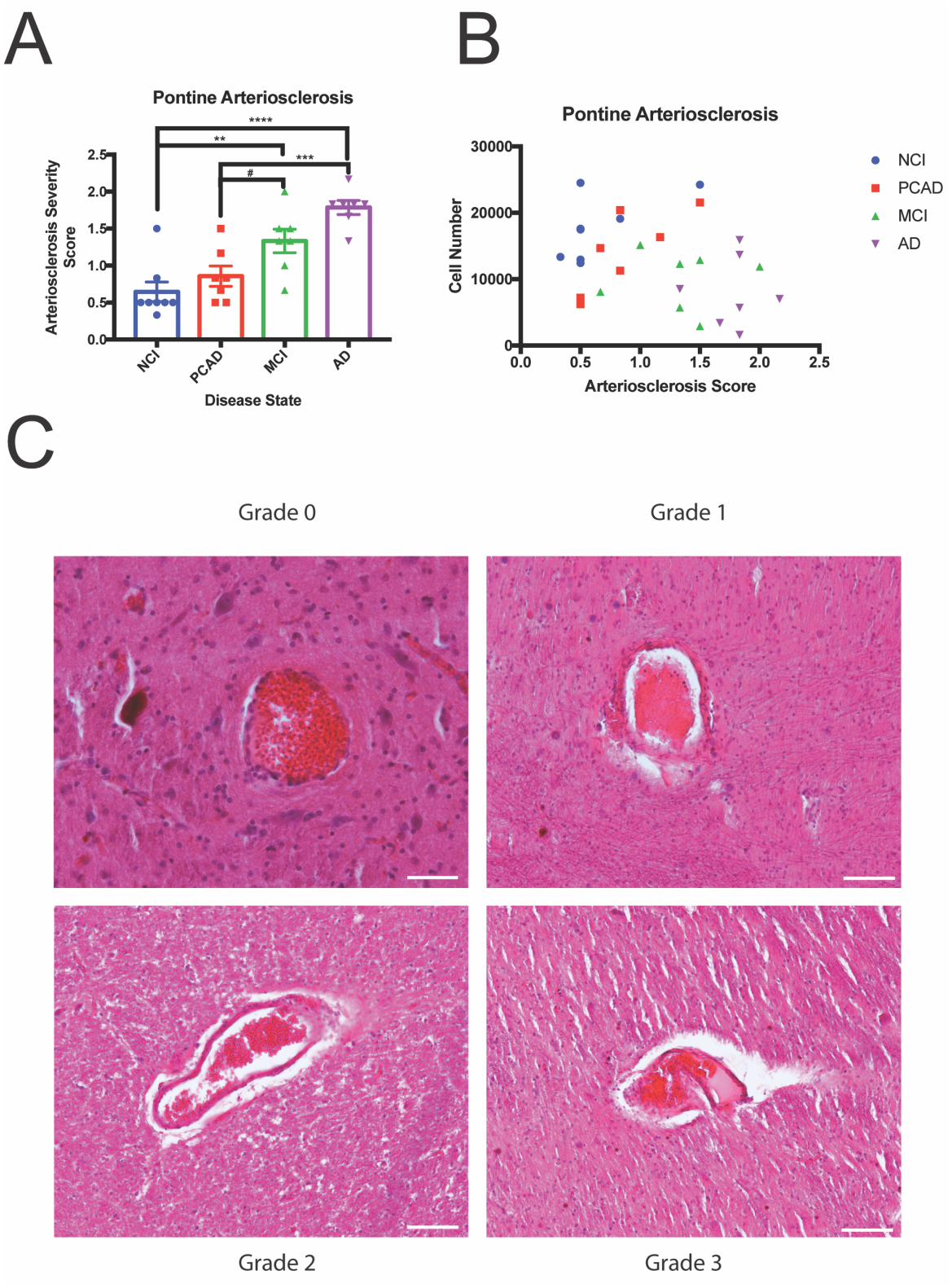

Figure 2.6 Pontine arteriosclerosis is increased in MCI and AD

Figure 2.6 (cont'd)

Arteriosclerosis of pontine vessels surround the LC was measured as previously described (Neltner et al. 2014). **A.** A significant increase in pontine severity was noted between MCI ($p=0.0053$) and AD ($p<0.0001$) compared to NCI. There was also a significant difference between PCAD and AD severity ($p=0.0003$) and a trending difference in observed arteriosclerosis between PCAD and MCI ($p=.08$). Error bars represent SEM **B.** Correlation analyses revealed an association of higher arteriosclerosis score to lower TH-positive cell number that was trending toward significance ($p=0.11$ $r= -0.3$) **C.** Representative images of vessels graded corresponding to severity. Scale bars: Grade 0= 50μm, Grade 1-3= 100μm. Error bars=SEM.

Braak 1991) and recent reports have implicated LC NFTs as a possible primary propagation point for tau pathology (Braak and Del Tredici 2012). Thus, semiquantitative analysis of AT8 immunostained LC cells was completed to enumerate the ratio of AT8-positive to total LC cells (**Figure 2.7 D**). This analysis revealed a significant increase in AT8 ratio in PCAD individuals compared to NCI (p=0.0005; **Figure 2.7 A**). AT8 ratios also were increased between all successive groups except PCAD and MCI (p=.4279). This is unsurprising given the average corresponding Braak scores for these groups, even though the brainstem is not included in Braak staging. (see **Table 2.3)**. Further, AT8 burden positively correlated with Braak scores (r= 0.4613, p=0.012) and negatively associated with LC number (r=-0.6716 p<0.0001).

Percentage of LC cells displaying DNA/ RNA damage increases across pathological groups.

Pontine tissue was immunostained with an antibody that recognizes several markers of DNA/RNA damage (8-hydroxy-2'-deoxyguanosine (oh8dG), 8-hydroxyguanine (oh8G), and 8-hydroxyguanosine (oh8G)). Analysis of the ratio of LC cells harboring damage revealed high reactivity ratios across all groups(**Figure2.8)**. Significantly higher damage ratios were observed in MCI (p=0.0198) and AD (p=) compared to NCI (**Figure 2.8)**, as well as in PCAD when compared to MCI(p=0.0017) and AD(p<0.0001). With this stark difference between cognitively normal individuals and impaired individuals, we ran correlation analyses and revealed that the damage ratio was significantly correlated with LC cell number (r=-.4614, p=0.0117) and MMSE score (r=-.6821, p<0.0001)

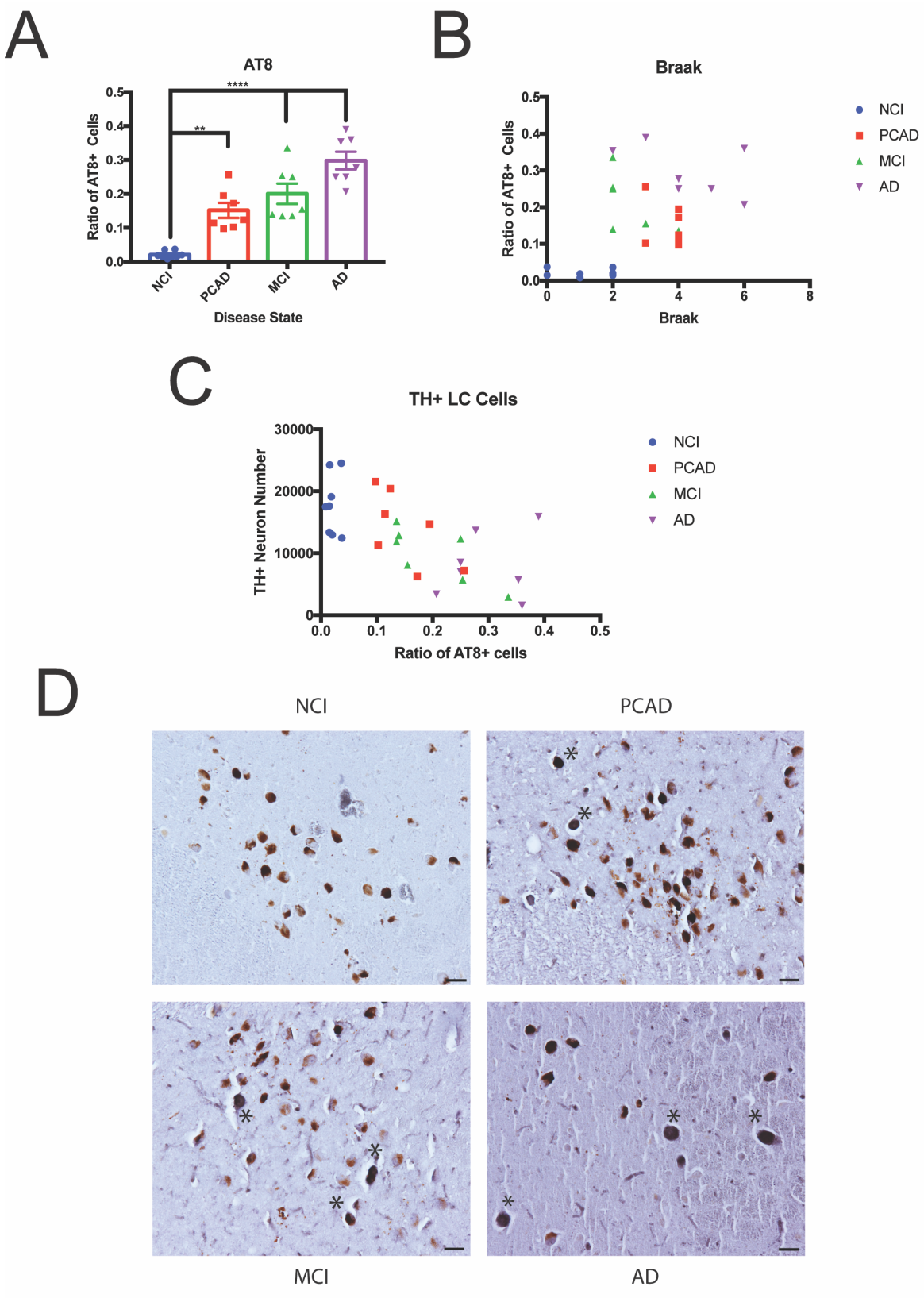

Figure 2.7 LC AT8 tau burden is increased in PCAD, MCI and AD

Figure 2.7 (cont'd)

A. Semi-quantitative cell counts revealed a significant ~3-fold increase in the AT8 ratio of LC neurons in PCAD compared to NCI cases ($p<0.01$) and a subsequent 4-5-fold increase in AT8 ratio in MCI and AD cases ($p < 0.0001$) compared to NCI via one-way ANOVA with Bonferroni *post hoc* testing. Error bars represent SEM. Spearman-rank correlational analysis revealed **B.** LC AT8 tau burden is positively correlated with Braak score ($r= 0.4613$, $p=0.012$) and **C.** negatively associated with LC number ($r=-0.6716$ $p<0.0001$). **D.** Representative images showing AT8 tau positive LC cells. Note the DAB-Ni labeling of AT8 compared to neuromelanin+ LC neurons. Asterisks indicate some of the NFTs present. Scale bars indicate 50μm. Error bars=SEM.

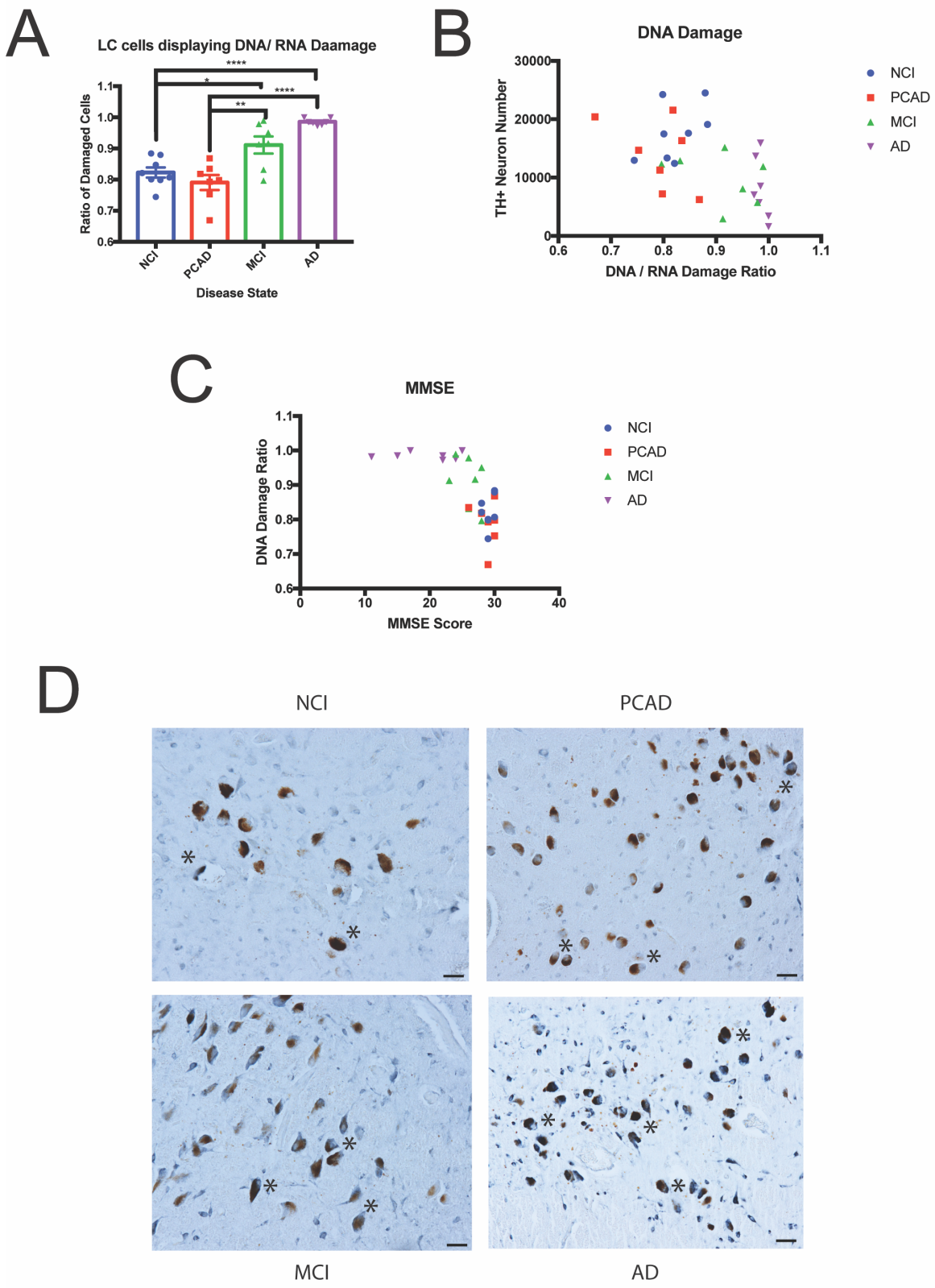

Figure 2.8 DNA/RNA oxidative damage in the LC is increased in MCI and AD and correlated with neuron number and MMSE

Figure 2.8 (cont'd)

A. Semi-quantitative cell counts revealed a significant increase in the DNA/RNA damage ratio of LC neurons in MCI ($p=0.0198$) and AD ($p<0.0001$) cases compared to NCI cases via one-way ANOVA with Bonferroni *post hoc* testing. Significant increases in damage ration were also ($p=0.0017$) and AD($p<0.0001$) compared to PCAD via one-way ANOVA with Bonferroni *post hoc* testing. Error bars represent SEM. Spearman-rank correlational analysis revealed **B.** DNA/RNA damage is negatively correlated with LC number ($r= -.4614$, $p=0.0117$) and **C.** negatively associated with MMSE ($r=-0.6716$ $p<0.0001$). **D.** Representative images showing LC cells labeled for oxidative damage. Scale bars indicate 50μm. Note the SG labeling of DNA/RNA damage (asterisks) compared to neuromelanin+ LC neurons and the relative intensity of reactivity between groups. Error bars=SEM.

Discussion

We demonstrate in this report that TH-positive, noradrenergic LC neurons are vulnerable during the onset of dementia as evidenced by their significant loss during the transition from NCI to MCI and AD and the association of this loss with multiple measures of cognitive deterioration and neuropathological accumulation. Furthermore, whereas differences in LC neuron loss were not significant in PCAD subjects compared to NCI, we observed differences in the topography of LC cell loss between NCI individuals and PCAD as well as PCAD and MCI. Thus, this group may represent LC degeneration in which regions of the LC that are necessary for normal cognition are still relatively conserved, although a positive association between LC neuron number and lower MMSE scores were observed across the diagnostic groups. The caudal LC third showed less differences in cell number across pathological groups, suggesting a gradient of vulnerability within the nucleus as previously reported (Theofilas et al. 2017). The discrepancy in the observed loss of LC neurons between our two studies utilizing the RROS and the UKADC (~30% compared to ~40%) could be related to cohort group classifications (i.e., the addition of the PCAD classification; MCI vs specifically aMCI) or possibly to the quantification methods (i.e. stereology vs. total enumeration).

Two reports from other groups have shown that LC neurodegeneration coincides with both mounting Braak stage pathology (Theofilas et al. 2017)and cognitive impairment (Arnsten and Goldman-Rakic 1984).Theofilas and colleagues reported that LC volume decreases ~8.4% with each successive Braak stage, resulting in a significant ~25% loss of LC volume between control cases neuropathologically diagnosed postmortem as Braak stage III compared to stage 0(Theofilas et al.

2017).This volume loss mirrored a similar rate of change in total pigmented and non-pigmented LC neuron numbers, as measured by unbiased stereology (Theofilas et al. 2017). While a slight difference in LC cell number was observed in our cohort of PCAD individuals compared to NCI, these differences were not significant, and we calculated that a higher-powered study would be needed to further elucidate differences between PCAD and NCI cases in the UKADC cohort.

Theofilas and colleagues also noted that the topography of LC volume and cell loss appears to follow a rostro-caudal gradient similar to that reported in frank AD cases (Theofilas et al. 2017; German et al. 1992). Here we report similar rostro-caudal gradient loss that highlighted the differences between PCAD and NCI LC topography. We also report that the loss of TH-positive LC cells, presumably noradrenergic LC neurons also correlates with Braak stage in the RROS but not in our UKADC cohort. In addition, we found that TH-positive neuron loss correlated with increasing neuropathologic burden based on NIA-Reagan and CERAD diagnostic criteria in the RROS but not in UKADC subjects. As reductions in LC neuron number have been associated with increased cortical amyloid plaque and NFT loads in cases of frank AD (Bondareff et al. 1987; Simic et al. 2016), the RROS observations in early stage cases indicate a strong relationship between LC projection system degeneration and the pathologic sequela of AD. The lack of association between LC neuron number and neuropathological criteria in the UKADC cases could be due to the inclusion of the PCAD group, which added considerable heterogeneity, to the lower sample size, or possibly to differences in postmortem diagnostic staging between the two centers. However, both the UKADC and the RROS studies showed a positive correlation

between TH positive LC number and cognition as represented by the MMSE or GCS, which are consistent with other reports (Wilson et al. 2013).

Arendt and colleagues previously used unbiased stereology to demonstrate a significant ~13% loss of neuromelanin-positive LC neurons in subjects classified as MCI/prodromal AD (CDR 0.5 who also displayed “low” to “intermediate” amyloid-Braak-CERAD (ABC) diagnostic scores (Hyman et al. 2012)) compared to those classified as controls (CDR 0 and “not” ABC score) (Arendt et al. 2015). Subjects classified as mild/moderate AD exhibited ~30–45% LC cell loss compared to controls. This study revealed that LC cell loss, which is prominent in cases of frank AD (Bondareff, Mountjoy, and Roth 1981; Chan-Palay and Asan 1989; Davies and Maloney 1976; Mann et al. 1980; Mufson, Bothwell, and Kordower 1989; Whitehouse et al. 1981), appears to occur early in the clinical progression of AD, concurrent with cell loss in the nucleus basalis and entorhinal cortex(Arendt et al. 2015).Notably, our estimate of total TH-positive LC cell number in NCI (17712 ± 4782) was similar to other studies (Ohm, Busch, and Bohl 1997; German et al. 1988; Tomonaga 1983) and, more specifically, to Arendt and colleagues’ unbiased estimate of total neuromelanin-positive neurons (17, 487 ± 2,736) for this group.

A novel aspect of our study looked at arteriosclerosis specifically in the pons and noted increased arteriosclerosis in MCI and AD. Looking even more in depth at pontine vascular health could elucidate mechanisms of LC toxicant burden (Pamphlett 2014), and metabolic deficits (Kelly et al. 2017). The noted early arteriole dysfunction observed at MCI in addition to infarct leveled being increased in this disease state could be indicative of a relationship between vascular health and cognitive status. This is

supported by evidence that polymorphisms in the certain genes (*APOE*4, *CR1*, *BIN1*, and *PICALM*) contribute both to an earlier time of onset of AD and to the development of coronary artery disease (Echt et al. 1991; Boiocchi et al. 2009; Schaefer et al. 1994). Furthermore, the trending relationship between LC cell number and arteriosclerosis severity indicates that survival of LC cells could be in part related to the vascular health of surrounding LC vessels. As the LC sits on one of the biggest capillary beds in the CNS, toxicants could enter LC neurons aided by the extensive exposure these neurons have to the vasculature, as well as by stressors that upregulate LC activity (Pamphlett 2014; Kelly et al. 2017; Kalinin et al. 2006). However, we could not make definitive observations about the relationship between LC cell loss and deafferentation and vascular pathology in these cases, setting the stage for our *in vivo* LC lesion studies in Chapter 3.

Our present UKADC study further expanded on the RROS and previous studies to investigate AT8 tau pathology in the LC. As hyperphosphorylated tau accrual in the LC is one of the first detectable signs of Alzheimer's disease neuropathology in the brain, appearing decades prior to cognitive impairment (Braak and Del Tredici 2012) we showed increases in AT8 immunoreactivity step-wise across disease groups. While our TH-positive LC counts did not correlate with Braak staging, AT8 immunoreactivity in the LC did. This is interesting as Braak staging does not consider the brainstem in its pathological assessment (Braak and Braak 1991) and thus LC NFT burden may be a better indicator of disease severity than global NFT burden (Braak and Del Tredici 2012).

Finally, we looked at markers of LC DNA/RNA damage in the UKADC cohort and measured a profound increase in the ratio of LC neurons bearing oxidative damage in MCI and AD individuals. Previously, we reported both molecular dysregulation of mitochondrial function and neuritic/structural plasticity coinciding with the loss of LC neurons prior to the transition from NCI to prodromal AD (Kelly et al. 2017). Specifically, levels of Nrf1(nuclear respiratory factor 1) and Cytc1 (cytochrome c1) were both significantly downregulated in LC neurons in aMCI and AD relative to NCI (Kelly et al. 2017). Nrf1 is a transcription factor that directs the expression of several functional classes of genes involved in mitochondrial function, including those regulating redox homeostasis, mitochondrial biogenesis, calcium homeostasis, and cytochrome oxidase activity(Dhar, Liang, and Wong-Riley 2009) and Cyt1 is the heme-containing component in the cytochrome b-c1 complex III of the respiratory chain, accepting electrons from Rieske protein and transferring it to cytochrome c, which couples to cytochrome oxidase(Trumpower 1981). It has also been shown that insulin resistance impairs glucose metabolism and mitochondrial function, thus increasing production of reactive oxygen species (Abolhassani et al. 2017). Additionally, in MCI, mitochondrial dysfunction and oxidative damage may induce synaptic dysfunction due to energy failures in neurons thus resulting in impaired cognitive function (Leon et al. 2016). Therefore, the previously observed mitochondrial dysfunction in MCI could lead to the presently described increases in DNA and RNA damage in the LC, and subsequent cognitive impairment.

Perhaps the most striking feature of the LC is the immensity and divergence of its noradrenergic forebrain efferents (Foote 1997; Counts and Mufson 2012), extensive

complex dendritic arborization pattern, and the long distance these perikarya project to reach their forebrain innervation sites (Arendt et al. 1995; Arendt et al. 1997; Morrison, Molliver, and Grzanna 1979). In this regard, LC neurons are similar to other selectively vulnerable long forebrain projection neuron systems (e.g., cholinergic basal forebrain neurons, substantia nigra pars compacta neurons, and dorsal raphe neurons, among others (Arendt 2000; Berridge and Waterhouse 2003; Mattson and Magnus 2006; Mesulam 1999; Sara 2009) that are heavily reliant on energy metabolism and cytoskeletal integrity to modulate synaptic input. These long projection systems are likely more prone to cellular stress given their position in the brain's organization. Further, since both the cholinergic basal forebrain and the LC have immense vascular interactions (Sato, Sato, and Uchida 2004; Bekar, Wei, and Nedergaard 2012; Cohen, Molinatti, and Hamel 1997), the extent to which dysregulation of these pathways influence vascular dysfunction and the onset of cognitive decline warrants further comparative assessments. As NE has potent anti-inflammatory properties and promotes Aβ clearance in animal models of AD(Chalermpalanupap et al. 2013; Kalinin et al. 2012), it is not surprising that lesioning the LC or reducing NE levels exacerbates AD-like pathology, neuroinflammation, and/or cognitive impairment in amyloid-based transgenic mouse models (Chalermpalanupap et al. 2013; Heneka et al. 2002; Heneka et al. 2006; Jardanhazi-Kurutz et al. 2010). Hence, targeting the LC using neuroprotective strategies may allow for disease modification in AD (Chamberlain and Robbins 2013). Chapter 3 explores this possibility further from the perspective of a dual role for LC degeneration for AD-like and vascular pathology.

APPENDIX

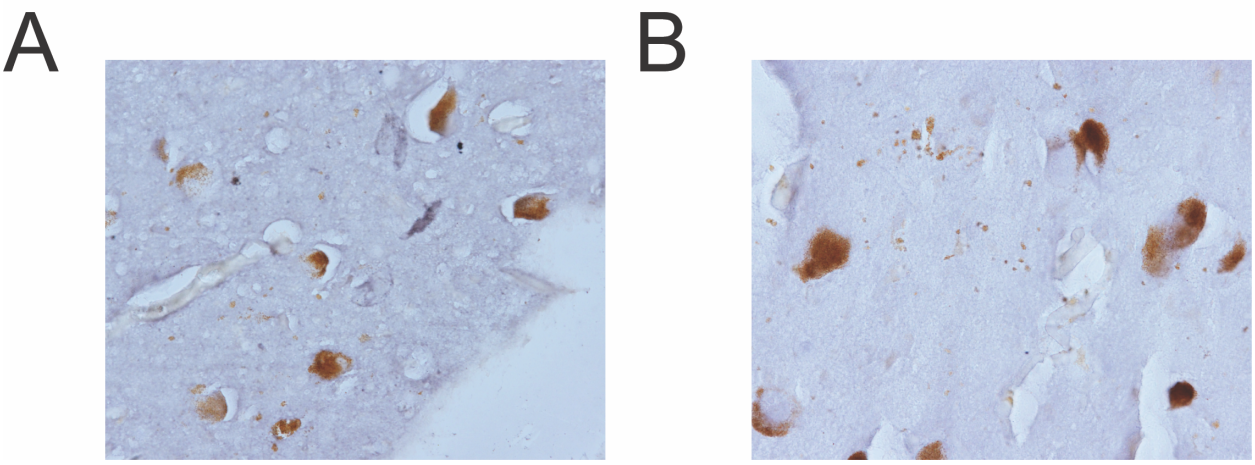

Figure A.1 Primary Delete IHC

IHC control staining was done without primary antibody to validate antibody specificity. Both mouse (**A**) and rabbit (**B**) secondary antibodies showed minimal background reactivity.

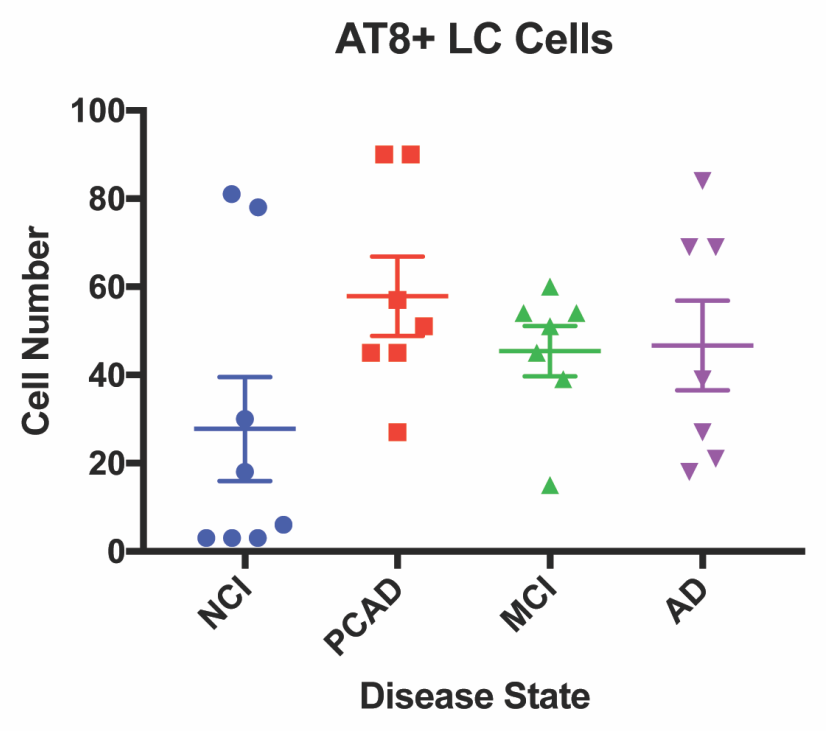

Figure A.2 Raw AT8 Cell Counts

Total enumeration of AT8+ LC cells revealed no differences between groups.

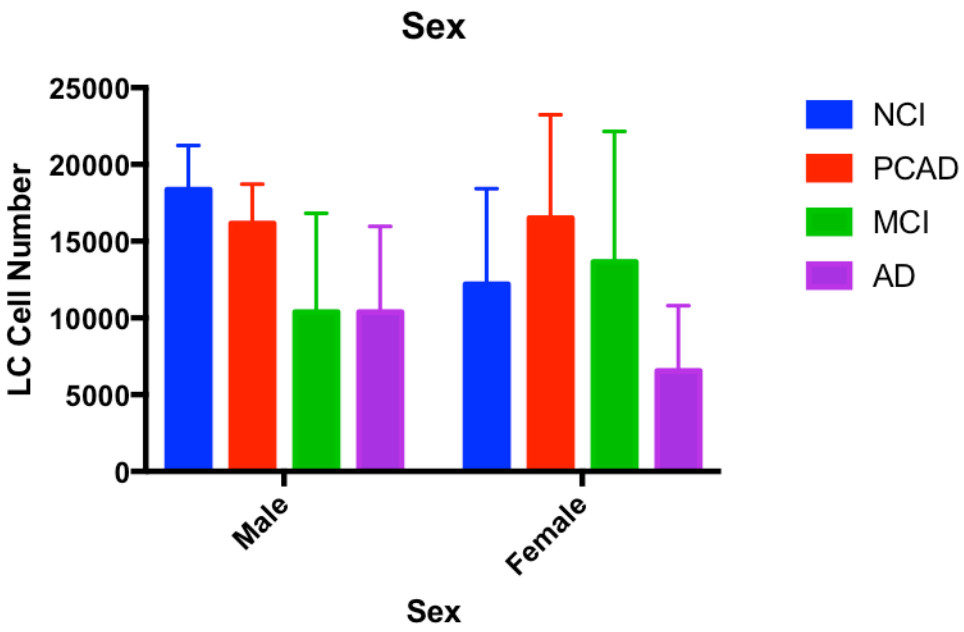

Figure A.3 LC TH+ Cell Number is Consistent Between Sexes

No statistical differences in LC cell counts observed between sexes via two-way ANOVA. Error bars = standard deviation.

LITERATURE CITED

LITERATURE CITED

Abolhassani, N., J. Leon, Z. Sheng, S. Oka, H. Hamasaki, T. Iwaki, and Y. Nakabeppu. 2017. 'Molecular pathophysiology of impaired glucose metabolism, mitochondrial dysfunction, and oxidative DNA damage in Alzheimer's disease brain', *Mech Ageing Dev*, 161: 95-104.

Adolfsson, R., C. G. Gottfries, B. E. Roos, and B. Winblad. 1979. 'Changes in the brain catecholamines in patients with dementia of Alzheimer type', *Br J Psychiatry*, 135: 216-23.

Albert, M. S., S. T. DeKosky, D. Dickson, B. Dubois, H. H. Feldman, N. C. Fox, A. Gamst, D. M. Holtzman, W. J. Jagust, R. C. Petersen, P. J. Snyder, M. C. Carrillo, B. Thies, and C. H. Phelps. 2011. 'The diagnosis of mild cognitive impairment due to Alzheimer's disease: recommendations from the National Institute on Aging-Alzheimer's Association workgroups on diagnostic guidelines for Alzheimer's disease', *Alzheimers Dement*, 7: 270-9.

Alzheimer's. 2018. '2018 Alzheimer's disease facts and figures', *Alzheimer's & Dementia: The Journal of the Alzheimer's Association*, 14: 367-429.

Arendt, T. 2000. 'Alzheimer's disease as a loss of differentiation control in a subset of neurons that retain immature features in the adult brain', *Neurobiol Aging*, 21.

Arendt, T., M. K. Bruckner, V. Bigl, and L. Marcova. 1995. 'Dendritic reorganisation in the basal forebrain under degenerative conditions and its defects in Alzheimer's disease. III. The basal forebrain compared with other subcortical areas', *J Comp Neurol*, 351.

Arendt, T., M. K. Bruckner, M. Morawski, C. Jager, and H. J. Gertz. 2015. 'Early neurone loss in Alzheimer's disease: cortical or subcortical?', *Acta Neuropathol Commun*, 3: 10.

Arendt, T., C. Schindler, M. K. Bruckner, K. Eschrich, V. Bigl, D. Zedlick, and L. Marcova. 1997. 'Plastic neuronal remodeling is impaired in patients with Alzheimer's disease carrying apolipoprotein epsilon 4 allele', *J Neurosci*, 17.

Arnsten, A. F., and P. S. Goldman-Rakic. 1984. 'Selective prefrontal cortical projections to the region of the locus coeruleus and raphe nuclei in the rhesus monkey', *Brain Res*, 306.

Arvanitakis, Z., A. W. Capuano, S. E. Leurgans, D. A. Bennett, and J. A. Schneider. 2016. 'Relation of cerebral vessel disease to Alzheimer's disease dementia and cognitive function in elderly people: a cross-sectional study', *Lancet Neurol*, 15: 934-43.

Attems, J., and K. A. Jellinger. 2014. 'The overlap between vascular disease and Alzheimer's disease--lessons from pathology', *BMC Med*, 12: 206.

Bancher, C., H. Braak, P. Fischer, and K. A. Jellinger. 1993. 'Neuropathological staging of Alzheimer lesions and intellectual status in Alzheimer's and Parkinson's disease patients', *Neurosci Lett*, 162: 179-82.

Beekly, D. L., E. M. Ramos, W. W. Lee, W. D. Deitrich, M. E. Jacka, J. Wu, J. L. Hubbard, T. D. Koepsell, J. C. Morris, W. A. Kukull, and N. I. A. Alzheimer's Disease Centers. 2007. 'The National Alzheimer's Coordinating Center (NACC) database: the Uniform Data Set', *Alzheimer Dis Assoc Disord*, 21: 249-58.

Bekar, L. K., H. S. Wei, and M. Nedergaard. 2012. 'The locus coeruleus-norepinephrine network optimizes coupling of cerebral blood volume with oxygen demand', *J Cereb Blood Flow Metab*, 32: 2135-45.

Bennett, D. A., R. S. Wilson, J. A. Schneider, D. A. Evans, L. A. Beckett, N. T. Aggarwal, L. L. Barnes, J. H. Fox, and J. Bach. 2002. 'Natural history of mild cognitive impairment in older persons', *Neurology*, 59.

Berridge, C. W., and B. D. Waterhouse. 2003. 'The locus coeruleus-noradrenergic system: modulation of behavioral state and state-dependent cognitive processes', *Brain Res Brain Res Rev*, 42.

Boiocchi, C., M. Zorzetto, I. Sbarsi, A. Pirotta, S. Schirinzi, C. Falcone, and M. Cuccia. 2009. 'CR1 genotype and haplotype involvement in coronary artery disease: the pivotal role of hypertension and dyslipidemia', *Int J Mol Med*, 24: 181-7.

Bondareff, W., C. Q. Mountjoy, and M. Roth. 1981. 'Selective loss of neurones of origin of adrenergic projection to cerebral cortex (nucleus locus coeruleus) in senile dementia', *Lancet*, 1: 783-4.

Bondareff, W., C. Q. Mountjoy, M. Roth, M. N. Rossor, L. L. Iversen, G. P. Reynolds, and D. L. Hauser. 1987. 'Neuronal degeneration in locus ceruleus and cortical correlates of Alzheimer disease', *Alzheimer Dis Assoc Disord*, 1: 256-62.

Braak, H., and E. Braak. 1991. 'Neuropathological stageing of Alzheimer-related changes', *Acta Neuropathol*, 82.

Braak, H., and K. Del Tredici. 2011. 'The pathological process underlying Alzheimer's disease in individuals under thirty', *Acta Neuropathol*, 121: 171-81.

———. 2012. 'Where, when, and in what form does sporadic Alzheimer's disease begin?', *Curr Opin Neurol*, 25: 708-14.

Chalermpalanupap, T., B. Kinkead, W. T. Hu, M. P. Kummer, T. Hammerschmidt, M. T. Heneka, D. Weinshenker, and A. I. Levey. 2013. 'Targeting norepinephrine in mild cognitive impairment and Alzheimer's disease', *Alzheimers Res Ther*, 5: 21.

Chamberlain, S. R., and T. W. Robbins. 2013. 'Noradrenergic modulation of cognition: therapeutic implications', *J Psychopharmacol*, 27: 694-718.

Chan-Palay, V., and E. Asan. 1989. 'Alterations in catecholamine neurons of the locus coeruleus in senile dementia of the Alzheimer type and in Parkinson's disease with and without dementia and depression', *J Comp Neurol*, 287.

Cipolla, M. J. 2009. *The Cerebral Circulation* (San Rafael (CA)).

Cohen, Z., G. Molinatti, and E. Hamel. 1997. 'Astroglial and vascular interactions of noradrenaline terminals in the rat cerebral cortex', *J Cereb Blood Flow Metab*, 17: 894-904.

Counts, S. E., and E. J. Mufson. 2012. 'Locus coeruleus.' in J. K. Mai and G. Paxinos (eds.), *The human nervous system* (Academic: London).

Davies, P., and A. J. Maloney. 1976. 'Selective loss of central cholinergic neurons in Alzheimer's disease', *Lancet*, 2.

Dhar, S. S., H. L. Liang, and M. T. Wong-Riley. 2009. 'Nuclear respiratory factor 1 co-regulates AMPA glutamate receptor subunit 2 and cytochrome c oxidase: tight coupling of glutamatergic transmission and energy metabolism in neurons', *J Neurochem*, 108: 1595-606.

Dozono, K., N. Ishii, Y. Nishihara, and A. Horie. 1991. 'An autopsy study of the incidence of lacunes in relation to age, hypertension, and arteriosclerosis', *Stroke*, 22: 993-6.

Echt, D. S., P. R. Liebson, L. B. Mitchell, R. W. Peters, D. Obias-Manno, A. H. Barker, D. Arensberg, A. Baker, L. Friedman, H. L. Greene, and et al. 1991. 'Mortality and morbidity in patients receiving encainide, flecainide, or placebo. The Cardiac Arrhythmia Suppression Trial', *N Engl J Med*, 324: 781-8.

Erickson, M. A., and W. A. Banks. 2013. 'Blood-brain barrier dysfunction as a cause and consequence of Alzheimer's disease', *J Cereb Blood Flow Metab*, 33: 1500-13.

Eriksson, U. K., A. M. Bennet, M. Gatz, P. W. Dickman, and N. L. Pedersen. 2010. 'Nonstroke cardiovascular disease and risk of Alzheimer disease and dementia', *Alzheimer Dis Assoc Disord*, 24: 213-9.

Foote, S. L. 1997. 'The primate locus coeruleus: the chemcial neuroanatomy of the nucleus, its efferent projection, and its target receptors.' in F. E. Bloom, A. Bjorklund and T. Hokfelt (eds.), *Handbook of chemical neuroanatomy* (Elsevier: Amsterdam).

Forstl, H., R. Levy, A. Burns, P. Luthert, and N. Cairns. 1994. 'Disproportionate loss of noradrenergic and cholinergic neurons as cause of depression in Alzheimer's disease--a hypothesis', *Pharmacopsychiatry*, 27.

German, D. C., K. F. Manaye, C. L. White, D. J. Woodward, D. D. McIntire, W. K. Smith, R. N. Kalaria, and D. M. Mann. 1992. 'Disease-specific patterns of locus coeruleus cell loss', *Ann Neurol*, 32.

German, D. C., B. S. Walker, K. Manaye, W. K. Smith, D. J. Woodward, and A. J. North. 1988. 'The human locus coeruleus: computer reconstruction of cellular distribution', *J Neurosci*, 8.

Grudzien, A., P. Shaw, S. Weintraub, E. Bigio, D. C. Mash, and M. M. Mesulam. 2007. 'Locus coeruleus neurofibrillary degeneration in aging, mild cognitive impairment and early Alzheimer's disease', *Neurobiol Aging*, 28: 327-35.

Heneka, M. T., E. Galea, V. Gavriluyk, L. Dumitrescu-Ozimek, J. Daeschner, M. K. O'Banion, G. Weinberg, T. Klockgether, and D. L. Feinstein. 2002. 'Noradrenergic depletion potentiates beta -amyloid-induced cortical inflammation: implications for Alzheimer's disease', *J Neurosci*, 22.

Heneka, M. T., M. Ramanathan, A. H. Jacobs, L. Dumitrescu-Ozimek, A. Bilkei-Gorzo, T. Debeir, M. Sastre, N. Galldiks, A. Zimmer, M. Hoehn, W. D. Heiss, T. Klockgether, and M. Staufenbiel. 2006. 'Locus ceruleus degeneration promotes Alzheimer pathogenesis in amyloid precursor protein 23 transgenic mice', *J Neurosci*, 26: 1343-54.

Hyman, B. T., C. H. Phelps, T. G. Beach, E. H. Bigio, N. J. Cairns, M. C. Carrillo, D. W. Dickson, C. Duyckaerts, M. P. Frosch, E. Masliah, S. S. Mirra, P. T. Nelson, J. A. Schneider, D. R. Thal, B. Thies, J. Q. Trojanowski, H. V. Vinters, and T. J. Montine. 2012. 'National Institute on Aging-Alzheimer's Association guidelines for the neuropathologic assessment of Alzheimer's disease', *Alzheimers Dement*, 8: 1-13.

Jardanhazi-Kurutz, D., M. P. Kummer, D. Terwel, K. Vogel, T. Dyrks, A. Thiele, and M. T. Heneka. 2010. 'Induced LC degeneration in APP/PS1 transgenic mice accelerates early cerebral amyloidosis and cognitive deficits', *Neurochem Int*, 57: 375-82.

Jellinger, K. A., and J. Attems. 2007. 'Neuropathological evaluation of mixed dementia', *J Neurol Sci*, 257: 80-7.

Jicha, G. A., E. L. Abner, F. A. Schmitt, R. J. Kryscio, K. P. Riley, G. E. Cooper, N. Stiles, M. S. Mendiondo, C. D. Smith, L. J. Van Eldik, and P. T. Nelson. 2012. 'Preclinical AD Workgroup staging: pathological correlates and potential challenges', *Neurobiol Aging*, 33: 622 e1-22 e16.

Kalinin, S., D. L. Feinstein, H. L. Xu, G. Huesa, D. A. Pelligrino, and E. Galea. 2006. 'Degeneration of noradrenergic fibres from the locus coeruleus causes tight-junction disorganisation in the rat brain', *Eur J Neurosci*, 24: 3393-400.

Kalinin, S., P. E. Polak, S. X. Lin, A. J. Sakharkar, S. C. Pandey, and D. L. Feinstein. 2012. 'The noradrenaline precursor L-DOPS reduces pathology in a mouse model of Alzheimer's disease', *Neurobiol Aging*, 33.

Kanaan, N. M., G. A. Morfini, N. E. LaPointe, G. F. Pigino, K. R. Patterson, Y. Song, A. Andreadis, Y. Fu, S. T. Brady, and L. I. Binder. 2011. 'Pathogenic forms of tau inhibit kinesin-dependent axonal transport through a mechanism involving activation of axonal phosphotransferases', *J Neurosci*, 31: 9858-68.

Kanbay, M., L. G. Sanchez-Lozada, M. Franco, M. Madero, Y. Solak, B. Rodriguez-Iturbe, A. Covic, and R. J. Johnson. 2011. 'Microvascular disease and its role in the brain and cardiovascular system: a potential role for uric acid as a cardiorenal toxin', *Nephrol Dial Transplant*, 26: 430-7.

Kelly, S. C., B. He, S. E. Perez, S. D. Ginsberg, E. J. Mufson, and S. E. Counts. 2017. 'Locus coeruleus cellular and molecular pathology during the progression of Alzheimer's disease', *Acta Neuropathol Commun*, 5: 8.

Leon, J., K. Sakumi, E. Castillo, Z. Sheng, S. Oka, and Y. Nakabeppu. 2016. '8-Oxoguanine accumulation in mitochondrial DNA causes mitochondrial dysfunction and impairs neuritogenesis in cultured adult mouse cortical neurons under oxidative conditions', *Sci Rep*, 6: 22086.

Mann, D. M., J. Lincoln, P. O. Yates, J. E. Stamp, and S. Toper. 1980. 'Changes in the monoamine containing neurones of the human CNS in senile dementia', *Br J Psychiatry*, 136.

Mann, D. M., P. O. Yates, and B. Marcyniuk. 1984. 'A comparison of changes in the nucleus basalis and locus caeruleus in Alzheimer's disease', *J Neurol Neurosurg Psychiatry*, 47: 201-3.

Markesbery, W. R., F. A. Schmitt, R. J. Kryscio, D. G. Davis, C. D. Smith, and D. R. Wekstein. 2006. 'Neuropathologic substrate of mild cognitive impairment', *Arch Neurol*, 63: 38-46.

Mattson, M. P., and T. Magnus. 2006. 'Ageing and neuronal vulnerability', *Nat Rev Neurosci*, 7.

McKhann, G., D. Drachman, M. Folstein, R. Katzman, D. Price, and E. M. Stadlan. 1984. 'Clinical diagnosis of Alzheimer's disease: report of the NINCDS-ADRDA Work Group under the auspices of Department of Health and Human Services Task Force on Alzheimer's Disease', *Neurology*, 34.

Mesulam, M. M. 1999. 'Neuroplasticity failure in Alzheimer's disease: bridging the gap between plaques and tangles', *Neuron*, 24.

Montagne, A., D. A. Nation, J. Pa, M. D. Sweeney, A. W. Toga, and B. V. Zlokovic. 2016. 'Brain imaging of neurovascular dysfunction in Alzheimer's disease', *Acta Neuropathol*, 131: 687-707.

Morrison, J. H., M. E. Molliver, and R. Grzanna. 1979. 'Noradrenergic innervation of cerebral cortex: widespread effects of local cortical lesions', *Science*, 205.

Mufson, E. J., M. Bothwell, and J. H. Kordower. 1989. 'Loss of nerve growth factor receptor-containing neurons in Alzheimer's disease: a quantitative analysis across subregions of the basal forebrain', *Exp Neurol*, 105.

Mufson, E. J., E. Y. Chen, E. J. Cochran, L. A. Beckett, D. A. Bennett, and J. H. Kordower. 1999. 'Entorhinal cortex beta-amyloid load in individuals with mild cognitive impairment', *Exp Neurol*, 158.

Nelson, A. R., M. D. Sweeney, A. P. Sagare, and B. V. Zlokovic. 2016. 'Neurovascular dysfunction and neurodegeneration in dementia and Alzheimer's disease', *Biochim Biophys Acta*, 1862: 887-900.

Neltner, J. H., E. L. Abner, S. Baker, F. A. Schmitt, R. J. Kryscio, G. A. Jicha, C. D. Smith, E. Hammack, W. A. Kukull, W. D. Brenowitz, L. J. Van Eldik, and P. T. Nelson. 2014. 'Arteriolosclerosis that affects multiple brain regions is linked to hippocampal sclerosis of ageing', *Brain*, 137: 255-67.

Neltner, J. H., E. L. Abner, G. A. Jicha, F. A. Schmitt, E. Patel, L. W. Poon, G. Marla, R. C. Green, A. Davey, M. A. Johnson, S. M. Jazwinski, S. Kim, D. Davis, J. L. Woodard, R. J. Kryscio, L. J. Van Eldik, and P. T. Nelson. 2016. 'Brain pathologies in extreme old age', *Neurobiol Aging*, 37: 1-11.

Ohm, T. G., C. Busch, and J. Bohl. 1997. 'Unbiased estimation of neuronal numbers in the human nucleus coeruleus during aging', *Neurobiol Aging*, 18.

Palmer, A. M., G. K. Wilcock, M. M. Esiri, P. T. Francis, and D. M. Bowen. 1987. 'Monoaminergic innervation of the frontal and temporal lobes in Alzheimer's disease', *Brain Res*, 401: 231-8.

Pamphlett, R. 2014. 'Uptake of environmental toxicants by the locus ceruleus: a potential trigger for neurodegenerative, demyelinating and psychiatric disorders', *Med Hypotheses*, 82: 97-104.

Peppiatt, C. M., C. Howarth, P. Mobbs, and D. Attwell. 2006. 'Bidirectional control of CNS capillary diameter by pericytes', *Nature*, 443: 700-4.

Petersen, R. C., R. Doody, A. Kurz, R. C. Mohs, J. C. Morris, P. V. Rabins, K. Ritchie, M. Rossor, L. Thal, and B. Winblad. 2001. 'Current concepts in mild cognitive impairment', *Arch Neurol*, 58.

Raichle, M. E., B. K. Hartman, J. O. Eichling, and L. G. Sharpe. 1975. 'Central noradrenergic regulation of cerebral blood flow and vascular permeability', *Proc Natl Acad Sci U S A*, 72: 3726-30.

Sara, S. J. 2009. 'The locus coeruleus and noradrenergic modulation of cognition', *Nat Rev Neurosci*, 10.

Sato, A., Y. Sato, and S. Uchida. 2004. 'Activation of the intracerebral cholinergic nerve fibers originating in the basal forebrain increases regional cerebral blood flow in the rat's cortex and hippocampus', *Neurosci Lett*, 361: 90-3.

Schaefer, E. J., S. Lamon-Fava, J. L. Jenner, J. R. McNamara, J. M. Ordovas, C. E. Davis, J. M. Abolafia, K. Lippel, and R. I. Levy. 1994. 'Lipoprotein(a) levels and risk of coronary heart disease in men. The lipid Research Clinics Coronary Primary Prevention Trial', *JAMA*, 271: 999-1003.

Schmitt, F. A., P. T. Nelson, E. Abner, S. Scheff, G. A. Jicha, C. Smith, G. Cooper, M. Mendiondo, D. D. Danner, L. J. Van Eldik, A. Caban-Holt, M. A. Lovell, and R. J. Kryscio. 2012. 'University of Kentucky Sanders-Brown healthy brain aging volunteers: donor characteristics, procedures and neuropathology', *Curr Alzheimer Res*, 9: 724-33.

Schneider, J. A., Z. Arvanitakis, S. E. Leurgans, and D. A. Bennett. 2009. 'The neuropathology of probable Alzheimer disease and mild cognitive impairment', *Ann Neurol*, 66: 200-8.

Serrano-Pozo, A., M. L. Mielke, T. Gomez-Isla, R. A. Betensky, J. H. Growdon, M. P. Frosch, and B. T. Hyman. 2011. 'Reactive glia not only associates with plaques but also parallels tangles in Alzheimer's disease', *Am J Pathol*, 179: 1373-84.

Simic, G., M. Babic Leko, S. Wray, C. R. Harrington, I. Delalle, N. Jovanov-Milosevic, D. Bazadona, L. Buee, R. Silva, G. Giovanni, C. M. Wischik, and P. R. Hof. 2016. 'Monoaminergic neuropathology in Alzheimer's disease', *Prog Neurobiol*.

Sperling, R. A., P. S. Aisen, L. A. Beckett, D. A. Bennett, S. Craft, A. M. Fagan, T. Iwatsubo, C. R. Jack, Jr., J. Kaye, T. J. Montine, D. C. Park, E. M. Reiman, C. C. Rowe, E. Siemers, Y. Stern, K. Yaffe, M. C. Carrillo, B. Thies, M. Morrison-Bogorad, M. V. Wagster, and C. H. Phelps. 2011. 'Toward defining the preclinical stages of Alzheimer's disease: recommendations from the National Institute on Aging-Alzheimer's Association workgroups on diagnostic guidelines for Alzheimer's disease', *Alzheimers Dement*, 7: 280-92.

Szabadi, E. 2013. 'Functional neuroanatomy of the central noradrenergic system', *J Psychopharmacol*, 27: 659-93.

Theofilas, P., A. J. Ehrenberg, S. Dunlop, A. T. Di Lorenzo Alho, A. Nguy, R. E. P. Leite, R. D. Rodriguez, M. B. Mejia, C. K. Suemoto, R. E. L. Ferretti-Rebustini, L. Polichiso, C. F. Nascimento, W. W. Seeley, R. Nitrini, C. A. Pasqualucci, W.

Jacob Filho, U. Rueb, J. Neuhaus, H. Heinsen, and L. T. Grinberg. 2017. 'Locus coeruleus volume and cell population changes during Alzheimer's disease progression: A stereological study in human postmortem brains with potential implication for early-stage biomarker discovery', *Alzheimers Dement*, 13: 236-46.

Theofilas, P., A. J. Ehrenberg, S. Dunlop, A. T. Lorenzo Alho, A. Nguy, R. E. Leite, R. D. Rodriguez, M. B. Mejia, C. K. Suemoto, R. E. Ferretti-Rebustini, L. Polichiso, C. F. Nascimento, W. W. Seeley, R. Nitrini, C. A. Pasqualucci, W. Jacob Filho, U. Rueb, J. Neuhaus, H. Heinsen, and L. T. Grinberg. 2016. 'Locus coeruleus volume and cell population changes during Alzheimer's disease progression: A stereological study in human postmortem brains with potential implication for early-stage biomarker discovery', *Alzheimers Dement*.

Tomonaga, M. 1983. 'Neuropathology of the locus ceruleus: a semi-quantitative study', *J Neurol*, 230.

Trumpower, B. L. 1981. 'Function of the iron-sulfur protein of the cytochrome b-c1 segment in electron-transfer and energy-conserving reactions of the mitochondrial respiratory chain', *Biochim Biophys Acta*, 639.

Venkatachalam, M. A., K. A. Griffin, R. Lan, H. Geng, P. Saikumar, and A. K. Bidani. 2010. 'Acute kidney injury: a springboard for progression in chronic kidney disease', *Am J Physiol Renal Physiol*, 298: F1078-94.

Weintraub, S., D. Salmon, N. Mercaldo, S. Ferris, N. R. Graff-Radford, H. Chui, J. Cummings, C. DeCarli, N. L. Foster, D. Galasko, E. Peskind, W. Dietrich, D. L. Beekly, W. A. Kukull, and J. C. Morris. 2009. 'The Alzheimer's Disease Centers' Uniform Data Set (UDS): the neuropsychologic test battery', *Alzheimer Dis Assoc Disord*, 23: 91-101.

Whitehouse, P. J., D. L. Price, A. W. Clark, J. T. Coyle, and M. R. DeLong. 1981. 'Alzheimer disease: evidence for selective loss of cholinergic neurons in the nucleus basalis', *Ann Neurol*, 10.

Wilson, R. S., S. Nag, P. A. Boyle, L. P. Hizel, L. Yu, A. S. Buchman, J. A. Schneider, and D. A. Bennett. 2013. 'Neural Reserve, Neuronal Density in the Locus Coeruleus, and Cognitive Decline', *Neurology*, 80.

Zarow, C., S. A. Lyness, J. A. Mortimer, and H. C. Chui. 2003. 'Neuronal loss is greater in the locus coeruleus than nucleus basalis and substantia nigra in Alzheimer and Parkinson diseases', *Arch Neurol*, 60: 337-41.

Chapter 3: Locus coeruleus disconnection induces forebrain vascular pathology in a transgenic rat model of Alzheimer's disease

Introduction

Alzheimer's disease (AD), which is characterized by β-amyloid (Aβ) plaques and tau neurofibrillary tangles (NFTs), is the most prevalent form of dementia representing a significant social and economic burden on a global scale (Alzheimer's 2018). Current therapies for AD provide only marginal symptomatic relief and do not slow disease progression. Therefore, understanding the mechanisms of AD initiation and progression is a critical scientific goal worldwide. Although research efforts have enhanced the understanding of certain disease mechanisms, so far efforts to modify the progression of AD have failed, possibly because the AD field lacks proper models for preclinical experiments (Karran and Hardy 2014).

In this regard, there is strong scientific rationale for linking cerebrovascular disease (CVD) to AD pathogenesis (Arvanitakis et al. 2016; Attems and Jellinger 2014; Bailey et al. 2004). CVD, usually in the form of small vessel occlusive disease caused by chronic hypertension and other vascular risk factors, is a condition that frequently accompanies aging in general and AD in particular (Grinberg and Thal 2010). These mixed pathologies in AD patients suggest that AD often involves a microvascular disorder that may contribute to its pathogenesis and high co-morbidity with CVD (Schneider et al. 2009).

It has been noted for some time that the locus coeruleus (LC), the major forebrain-projecting noradrenergic nucleus in the brain, degenerates in AD and in mild

cognitive impairment (MCI) (Theofilas et al. 2017; Haglund et al. 2016; Weinshenker 2008; Kelly et al. 2017). At the time of clinical diagnosis of MCI, significant loss of LC neurons, LC projection fibers, and forebrain norepinephrine (NE) and LC fibers is evident (Braak and Del Tredici 2012; Mather and Harley 2016; Kelly et al. 2017). Additionally, the LC has been shown to play a role in neurovascular coupling and cortical perfusion (Bekar, Wei, and Nedergaard 2012; Toussay et al. 2013). Furthermore, LC cell loss has been shown to be a better predictor of cognitive symptoms than degeneration in other brain regions affected by AD, including the entorhinal cortex, hippocampus, and nucleus basalis ((Wilson et al. 2013; Kelly et al. 2017; Arendt et al. 2015).

LC-NE projection system activity is critical for attention, arousal and specific aspects of learning and memory (Sara 2009; Aston-Jones and Cohen 2005). Greater LC neuron density protects against cognitive decline during ageing, while tangle burden in the LC is correlated with cognitive decline (Kelly et al. 2017; Counts and Mufson 2010; Grudzien et al. 2007; Wilson et al. 2013). In addition, NE has potent anti-inflammatory properties and promotes Aβ clearance (Counts and Mufson 2010; Chalermpalanupap et al. 2013; Heneka et al. 2002; Feinstein, Kalinin, and Braun 2016). Thus, it is not surprising that experimental, neurotoxic damage of LC terminals or reducing NE levels exacerbates AD-like pathology, neuroinflammation, and/or cognitive impairment in amyloid-based transgenic mouse models (Heneka et al. 2002; Feinstein et al. 2002; Heneka et al. 2006).

For the present study, we sought to construct a more relevant preclinical AD model by leveraging a recently generated TgF344-19 AD (TgF344) rat model that

expresses mutant human amyloid precursor protein (APP; *APPsw*) and presenilin 1 (*PS1ΔE9*) and displays canonical amyloid plaques as well as core components of AD that are often missing in transgenic mice, including age-dependent cognitive impairment, cerebral amyloid angiopathy (CAA), Aβ oligomers, endogenous tau pathology, gliosis and apoptotic neuronal loss in the forebrain (Cohen *et al.*, 2013). Because rats are 4–5 million years closer to humans than mice in evolution, the rat is more intelligent than the mouse and is capable of learning a wider variety of tasks that are important to cognitive research (Yang et al. 2004). The size of the animal also enhances its use as a disease model, not just because of the ability to perform a wider variety of surgical procedures, but also because of the proportional size of important substructures in organs that affects both how much of the organ is involved in an experimental lesion. This is particularly important in the central nervous system.

However, these rats, like most animal models do not exhibit age dependent loss of LC neurons like humans do. (Rorabaugh et al. 2017; Cohen et al. 2013). Based on these features, we reasoned that an LC-lesioned TgF344 rat model might be a good candidate to accurately replicate LC pathology and dysfunction in MCI or early AD, and moreover, lesioning LC innervation in the PFC would amplify both the AD and cerebrovascular pathologies and provide valuable insights into early disease mechanisms and potential locus coeruleus NE-based therapies.

Methods

Experimental overview

Cohorts of 6-month-old male and female transgenic Fischer 344-19 (TgF344) rats (n=7-10/sex/group), were bilaterally injected with dopamine beta hydroxylase- saporin (DBH-sap) or control untargeted mouse IgG saporin (IgG-sap) into the prefrontal cortex (PFC). Rats underwent behavioral testing 2 weeks and 6 weeks post op. The open field test, elevated plus test and the Barnes maze task were employed. All cohorts were sacrificed 24 hours after completing behavior. After sacrifice brains were analyzed via quantitative or semi-quantitative immunohistochemistry (IHC) for AD-like and cerebrovascular pathology, as well as western blots to analyze proteins of interest to blood brain barrier integrity (Summarized in **Figure 3.1**).

Animals

We used male and female TgF344 rats on the Fisher 344 background, overexpressing Amyloid precursor protein Swedish mutation *(APPswe)* and Δ exon 9 mutant human presenilin-1 (*PS1ΔE9*) under the mouse prion protein promoter (Cohen et al. 2013). TgF344 rats manifest age-dependent cerebral amyloidosis that precedes tauopathy, gliosis, apoptotic loss of neurons in the cerebral cortex and hippocampus, and cognitive disturbance (Cohen et al. 2013; Rorabaugh et al. 2017; Pentkowski et al. 2018). Original breeding colonies were provided by the Rat Resource Center (St. Louis, MO). Rats were bred by backcrossing hemizygous transgene positive animals to wild type Fisher 344 littermates and aged to 6 months. All animals were given food and water *ad libitum* and housed in 12h:12h reverse light-dark cycle conditions in the Van Andel

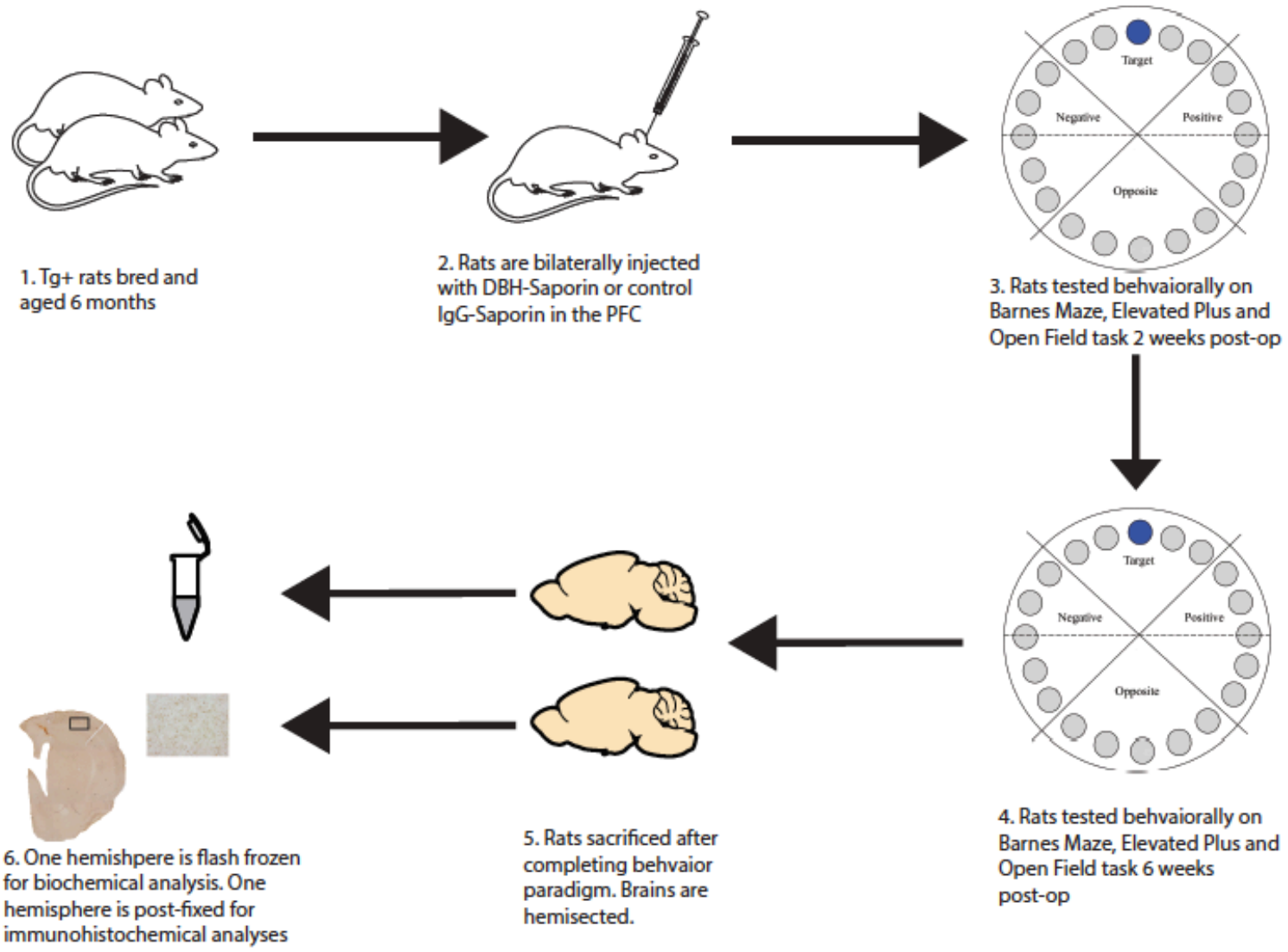

Figure 3.1 Experimental workflow

Figure 3.1 (cont'd)

TgF344-AD rats were backcrossed to wild-type (WT) littermates to create hemizygous test animals. At 6 months of age, animals underwent surgery to bilaterally lesion the noradrenergic fibers of the PFC. Two weeks after surgery staples were removed and rats were tested on the Barnes maze as well as the elevated plus maze and the open field test. Behavior was repeated 6 weeks post-surgery. Twenty-four hours after final behavior trials were completed, rats were sacrificed and perfused and brains were hemisected and either flash frozen or post-fixed.

Research Institute vivarium, which is fully Association for Assessment and Accreditation of Laboratory Animal Care (AAALAC) approved. All procedures were conducted in accordance with guidelines set by the Institutional Animal Care and Use Committee (IACUC) of Michigan State University.

Power analysis and sample sizes

A total of 27 age matched transgenic rats were employed for this study, as follows: DBH-sap, male (n =7), DBH-sap Female (n=6), IgG-sap Male (n=8), IgG-sap Female (n=6). Power analyses of preliminary experiments indicated an n of 5/group would have 90% power to indicate 1.25 standard deviations between DBH and IgG lesioned animals on behavior. Animals that did not exhibit >30% DBH signal loss compared to mean IgG-sap signal were eliminated from analyses. No sex differences were observed in the animals in behavior or pathology, so sexes were evaluated together as done previously (Rorabaugh et al. 2017; Cohen et al. 2013).

Immunotoxin

For this study, immunotoxins consisting of a monoclonal antibody to DBH or a control IgG coupled by disulfide bonds to saporin were directly injected into the PFC of test animals (Wrenn et al. 1996). Saporin is obtained from the seeds of the Soapwort plant (*Saponaria officinalis*), a plant that grows wildly in Britain and other parts of Europe. Saporin is a plant enzyme with N-glycosidase activity that depurinates a specific nucleotide in the ribosomal RNA 28S, thus irreversibly blocking protein synthesis and leading ultimately to cell death (**Figure 3.2**). DBH-sap has been shown to be selectively

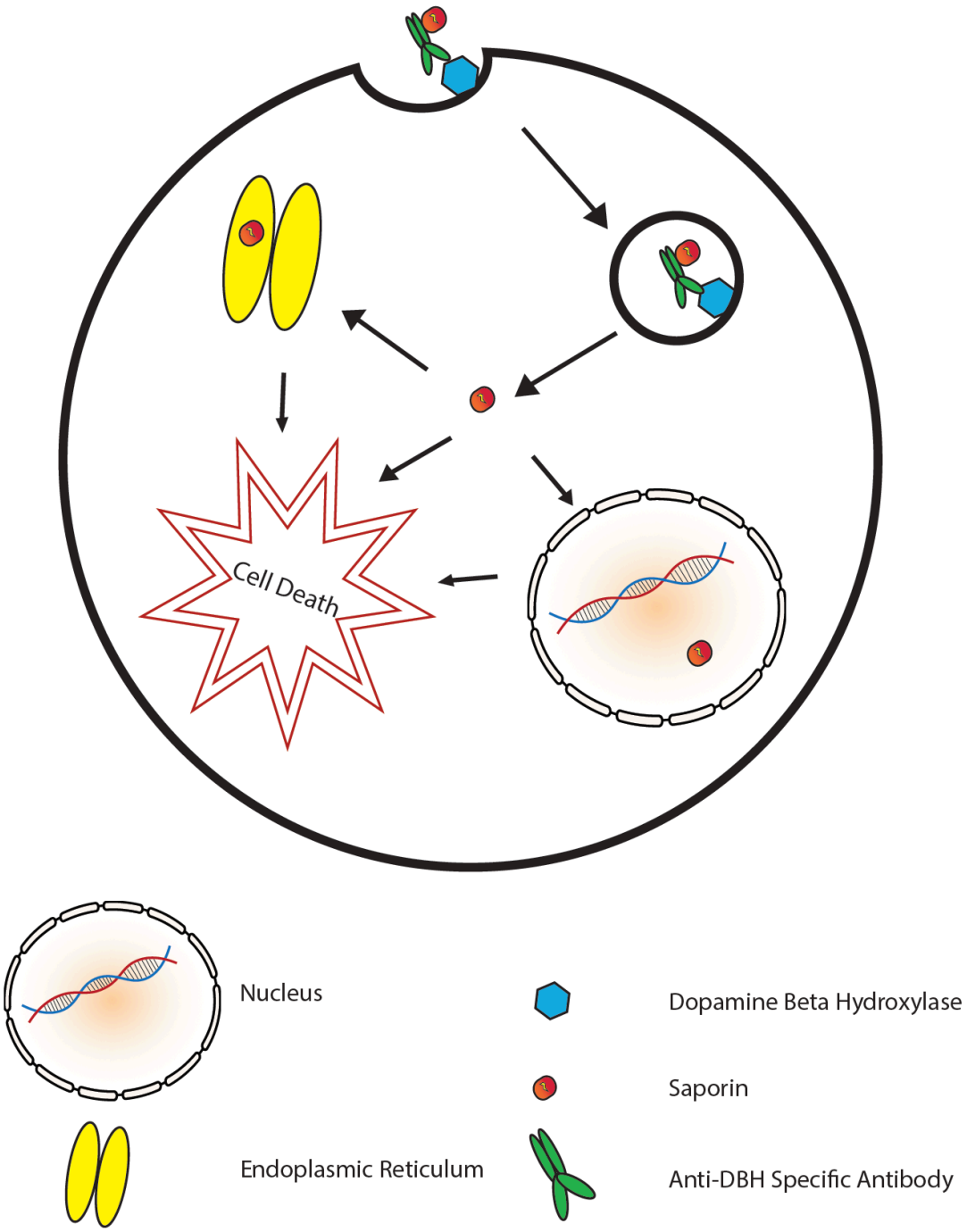

Figure 3.2 DBH-sap is a Noradrenergic Specific Immunotoxin

DBH-sap is a highly specific noradrenergic lesioning agent. It specifically targets cells that express DBH. The immunotoxin is composed of an antibody specific to DBH

Figure 3.2 (cont'd)

conjugated to a saporin. The vesicular DBH enzyme is exposed to the exterior milieu upon release of norepinephrine and thus allows these cells to endocytose the DBH-sap upon reuptake of the enzyme. Once inside the cell, the saporin is able to disrupt protein assembly by inactivating ribosomes and ultimately lead to cell death.

toxic to peripheral noradrenergic sympathetic neurons in rats after systemic injection, or to central LC neurons via intraventricular injection (Ostock et al. 2014; Patrone et al. 2018; Wrenn et al. 1996). The specificity of DBH-sap correlates well with uptake of the DBH antibody when injected intraventricularly. Unlike other lesioning methods, this molecular lesioning agent assures definitive ablation of the target neurons expressing rat DBH. The control lesion consists of an untargeted mouse IgG conjugated to a saporin (IgG-sap). This is the first study of its kind to inject the immunotoxin into a specific region in the cortex in the context of AD-like pathology.

Surgeries

All surgical procedures were performed under Equithesin anesthesia delivered via intraperitoneal injection. Rats were placed in a stereotaxic frame and two 2.5 µg (4.0 µL volume) injections of DBH-sap or control IgG-sap (ATS bio, San Diego, CA) were injected in the PFC at coordinates (relative to bregma; from dura) AP +1.2, ML ±2.0, DV -3.0. A Hamilton syringe needle (Hamilton Gas Tight syringe 80,000, 26s/2" needle; Hamilton, Reno, NV) was used for injection. The needle was lowered to the site and immunotoxin injection began immediately at a rate of 0.5 µl/minute and remained in place after the injection for an additional 5 minutes before being slowly retracted.

Behavior

Open field test

Locomotor activity was evaluated using a standard open field test. The open field apparatus (Stoelting, Wood Dale, IL) consisted of an open topped, 2x2 acrylic black box

measuring 40.6 × 40.6 × 38 cm. The box was placed at table height and all experimental sessions were recorded by a video camera placed above the apparatus and analyzed with a video-tracking software (ANY-maze, Stoelting, Wood Dale, IL). All movements were automatically recorded and time mobile and distance traveled were plotted and the data were used to measure locomotor activity. The observation boxes were cleaned using 70% ethanol before the first run of the day, between subjects, and after the last run of the day. On the day of testing, rats in their home cages were brought into the experimental room. Rats remained in the experimental room for 30 min, after which each rat was placed into the center of the observation box and recording began immediately. Movement was recorded in 5 min bins for 30 min.

Elevated plus maze

To ensure the DBH-sap lesion did not produce any off target anti-anxiolytic effects due to the LC's immense innervation in amygdala (Szabadi 2013), we tested the rats on the elevated plus maze (EPM). The EPM is a plus-shaped apparatus commonly employed to test for anxiety-like behaviors in rodents. It consists of four arms arranged in a plus shape, elevated 50 cm off the floor. Two arms are 10 cm wide platforms that extend away from the maze (open arms), whereas the other two arms are 10 cm platforms that contain walls that are 50 cm high (closed arms). Rats were put in the center of the platform facing an open arm and were allowed to explore the maze for 5 min. Time spent in open arms was analyzed as a measure of relative fear/anxiety compared to control.

Barnes maze

The Barnes maze was developed by Carol Barnes to test for spatial and working memory function in rats in order to overcome the stress induced by swimming in the Morris water maze (MWM) (Barnes 1979). In the test, animals are placed in the middle of a circular table containing holes around the edges and receive negative reinforcement, in the form of bright lights, an exposed environment, and noise, motivating them to escape to a dark cage hidden underneath one of the holes. Similar to the MWM, the Barnes maze allows for evaluation of spatial reference memory and learning but without inducing despair and anxiety that commonly are seen in the water maze in the form of floating and thigmotaxis (Sun and Alkon 2004; Holscher 1999; Schulz et al. 2007).

The Barnes Maze protocol used in this study was based off the short-protocol Barnes maze protocol previously published by Attar and colleagues (Attar et al. 2013). The advantage of the shorter training periods allowed for elucidating minor differences between animals that may have been over-trained in other protocols. The maze is a grey circular platform (122 cm diameter), elevated 90 cm from the floor, containing 20 holes (10 cm in diameter) disposed circularly at the edge of the platform (Stoelting, Wood Dale, IL). One of the holes (target hole) is connected to an escape box (10 × 10 × 15 cm). There were visual cues on the walls, located approximately 50-100 cm from the apparatus. During the behavioral sessions, the lights were turned on to increase escape motivation as well as a white noise machine turned to max volume (HomeMedics, Commerce Township, MI).

In the habituation session, the animals were slowly pulled to the escape hole in a clear cylinder then given 120 seconds to freely enter the escape hole. Afterwards, the animals were submitted to a set of 2 daily training sessions, with 2 or 3 trials (all trials explained in detail in **Table 3.1**). The inter-trials interval was the duration of cleaning the apparatus (with a 70% alcohol solution). The first training session was performed 24 hours after the habituation session. All trials lasted 120 s or until the animals reached the escape box. However, if the rats did not reach the target hole, the experimenter gently guided the animal towards it at the end of the trial using a clear cylinder. After reaching the escape box, animals remained inside for at least 60 s before being returned to its home cage. The escape box was always located in the same place during training. Animals were tested in groups of four, in order that all trials averaged 20 mins between each trial per animal. Retrieval of spatial learning was evaluated in the probe session, which was conducted after the rest day, 48 hours after the last training day. The procedure was similar to the training trials, but the escape box was removed. At the beginning of each session, the animals were placed in an opaque container at the center of the maze. The container was then pulled up, and the animal was released to explore the maze. All experimental sessions were recorded by a video camera placed above the apparatus and analyzed with a video-tracking software (ANY-maze, Stoelting, Wood Dale, IL).

Behavioral analysis was performed using the same protocols during both evaluation timepoints except during the second round of testing. Training was reduced by one trial on days 2 and 3—to two and one trial respectively—in order to avoid over-training. The Barnes behavior protocol is summarized in **Table 3.1.** The Barnes maze

Table 3.1 Summary of Barnes maze protocol

Day	Description
1	**Habituation Day**: Animals placed in clear cylinder and slowly guided to target hole over 30s. Animal remained at target hole for 120 seconds to encourage entry. If animal did not enter, animal was nudged or placed in to the escape box. Animal remained in escape box for at least 60s before being returned to home cage.
2	**Training Day 1:** Animals placed in opaque cylinder in center of maze, cylinder was removed, and animal was allowed to freely roam maze for 120s. If animal did not enter escape cage by the end of trial, animal was guided to the escape cage with clear cylinder. If animal did not enter hole, animal was nudged or placed in to escape box. Animal remained in escape box for at least 60s before being returned to home cage. Process was repeated for a total of 3 trials per animal (*2 trials total during round 2*).
3	**Training Day 2:** Animals were placed in opaque cylinder in center of maze, cylinder was removed, and animal was allowed to freely roam maze for 120s. If animal did not enter escape cage by the end of trial, animal was guided to the escape cage with clear cylinder. If animal did not enter hole, animal was nudged or placed in to escape box. Animal remained in escape box for at least 60s before being returned to home cage. Process was repeated for a total of 2 trials per animal. (*1 trial total during round 2*)
4	**Rest day:** No behavior testing completed
5	**Probe day:** Escape cage was remove from maze. Each animal was placed in opaque cylinder in center of maze, cylinder was removed, and animal was allowed to freely roam maze for 120s. After 120s of recording was completed, animal was returned to home cage.

task classically measures spatial memory over the course of a training period with multiple trials. Parameters analyzed in these experiments included time spent in target quadrant, latency to target hole entry, and incorrect revisits to holes already investigated. The two former parameters are classic measures of spatial learning and memory. The latter measure of incorrect revisits measures working memory. Working memory measures memory within a test or trial. Working memory errors (or "revisits") in these experiments were defined as searching the same hole twice within a trial when the revisit occurred after the inspection of other holes (Rosenfeld and Ferguson 2014).

Euthanasia

Twenty-four hours after completing the final behavior trials, rats were deeply anesthetized (60mg/kg, pentobarbital, i. p.) and perfused intracardially with 0.9% saline containing 10,000 USP/L heparin. Rat brains were immediately removed and hemisected in the sagittal plane at midline using a brain block. One hemisphere was post-fixed in 4% paraformaldehyde (Electron Microscopy Sciences, Hatfield, PA) in 0.1M phosphate buffer (pH 7.2) for 24-48hrs and processed for immunohistochemistry, whereas the other hemisphere was flash frozen and processed for biochemical analyses.

Immunohistochemistry

Tissue processing for IHC

Post-fixed brain hemispheres were transferred to 15% sucrose in 0.1M phosphate buffer until saturated, then 30% sucrose in 0.1M phosphate buffer until saturated. Brains

were frozen on dry ice and sectioned at a 40µm thickness on the coronal plane using a sliding microtome. Serial sections were processed for IHC using the free-floating method.

Brightfield and fluorescence IHC

Tissue sections (one 1:12 series/antibody experiment) were rinsed in Tris-buffered saline (TBS; pH 7.4) and non-fluorescent sections were quenched in 0.3% H_2O_2 for 1 hour at room temperature. Tissue was the permeabilized with TBS + 0.5% Triton X-100 (TBS-TX) and blocked in TBS/TX/10% normal goat serum for 1 hour, followed by overnight incubation in primary antisera (antibodies and dilutions listed in **Table 3.2**) in TBS+ 1% goat seurm at 4°C under constant agitation. Following primary antibody incubation, sections were rinsed with TBS-TX and incubated in biotinylated secondary antisera (Vector; 1:500 dilution) or fluorescent secondary (Alex Flour; 1:500 dilution) for 2 hours at room temperature, followed by TBS-TX. Brightfield IHC was further processed with Vector ABC detection kit for one hour at room temperature (Vector Laboratories, Burlingame, CA) and antibody labeling was visualized by exposure to 0.5mg/ml 3,3' diaminobenzidine (DAB) and 0.03% H_2O_2 in TBS or to DAB+ Nickel enhancement (2.5mg/mL nickel ammonium sulfate) and 0.03% H_2O_2 in TBS. Sections were mounted on subbed slides, dehydrated via ascending ethanol washes, cleared with xylenes, and cover-slipped with Cytoseal (ThermoFisher, Waltham, MA). Images were taken on a Nikon Eclipse 90i microscope with a Nikon DS-Ri1 camera. Figures were produced in Photoshop CC (San Jose, CA), with brightness, saturation, and

Table 3.2 Primary antibodies used to immunostain TgF344 rat tissue

Target	Brand (Cat No.)	Dilution
DBH (LC neuron marker)	Immunostar (22806)	1:4000
Albumin	ProteinTech (16475-1-AP)	1:500 (IHC) 1:10,000 (WB)
Smooth Muscle Actin (ACTA2)	ProteinTech (23081-1-AP)	1:1000
MOAB-2	Gift from Dr. Nicholas Kanaan	1:4000
GFAP	Abcam (7260)	1:10000 (IHC) 1:20000 (WB)
Iba1	Wako	1:1000

sharpness adjusted only as needed to best replicate the immunostaining as viewed directly under the microscope.

LI-COR IHC

Serial tissue sections (1:12) were rinsed in TBS-TX then blocked in 10% normal goat serum for 1 hour. Sections were then incubated in primary antisera (antibodies and dilutions listed in **Table 3.2**) overnight at 4°C under constant agitation. Following primary incubation, sections were rinsed with TBS-TX then incubated with LI-COR near-infrared secondary antibodies for 2 hours at room temperature in the dark. Antibodies used were IRDye800 conjugated goat anti-rabbit and IRDye680 conjugated goat anti-mouse (LI-COR Biosciences, 926-68020, 1:500) (LI-COR Biosciences; 926-32211, 1:500). Sections were then rinsed in TBS, mounted on subbed slides, dehydrated via ascending ethanol washes, cleared with xylenes, and cover-slipped with Cytoseal (ThermoFisher, Waltham, MA). Slides were left to dry for 48 hours in the dark at room temperature before imaging.

LI-COR tissue imaging

DBH density

Scans were obtained of the 1:12 series of tissue stained with the LI-COR near-infrared secondary antibodies and used to determine DBH signal intensity. For DBH signal intensity, boundaries were drawn around the entire PFC and outlined freehand using the LI-COR Image Studio 3.1 software to obtain an average signal strength. Tracings began at +5mm from bregma and were terminated at bregma. Reported integrated

intensity measurements of DBH expression were collected using the 800nm channel and were normalized to background levels obtained from a 100-pixel sampling area in the basal ganglia of each brain. Data were represented as the mean cortical DBH integrated intensity measurement per brain. The individual drawing the boundaries around the brain areas was blinded to the lesion of the animals.

MOAB-2 amyloid density

MOAB-2 (mouse IgG2b) is a pan-specific, high-titer antibody to Aβ residues 1-4 (Youmans et al. 2012). Scans were obtained of the 1:12 series of tissue stained with the LI-COR near-infrared secondary antibodies and used to determine amyloid signal intensity. Our DBH staining intensity data showed that DBH signal loss was also found in cortical regions beyond PFC, most likely due to the highly bifurcated morphology of corticopetal LC axons (Counts and Mufson 2012). Therefore, to measure MOAB-2 amyloid signal intensity, boundaries were drawn around either the entire cortex and outlined freehand using the LI-COR Image Studio 3.1 software to obtain an averaged signal strength normalized to area. For this study, we also sampled the entire hippocampus for comparison.

Albumin density

Scans were obtained of the 1:12 series of tissue stained with the LI-COR near-infrared secondary antibodies and used to determine albumin signal intensity. For albumin signal intensity, boundaries were drawn around the entire cortex outlined freehand using the LI-COR Image Studio 3.1 software to obtain an average signal strength.

Reported integrated intensity measurements of albumin expression were collected using the 800nm channel and were normalized to background levels obtained in the brainstem of each brain. Data were represented as the mean cortical albumin integrated intensity measurement per brain. The individual drawing the boundaries around the brain areas was blinded to the lesion of the animals.

Vessel wall to lumen measurements

Wall to lumen ratios (WLRs) of PFC parenchymal arterioles were measured based on previous methods as an index of cerebral vessel remodeling, where increased wall: lumen measurements indicate increased myogenic tone and reduced vasoreactivity (Dorrance, Rupp, and Nogueira 2006; Baumbach and Hajdu 1993). Briefly, animals were randomized, the rater was blinded, and the first 6 PFC parenchymal arterioles coursing perpendicular to the visual plane via Meander Scan function (MBF Bioscience) in the alpha-actin 2 (ACTA2) labeled tissue (see **Table 3.2**) were measured. Capillaries were defined as small vessels lined by a single layer of endothelial cells, the diameter of which was < 10 μm. Therefore, vessels with irregular profiles, or diameters less than 12 μm were excluded from counting. Since the majority of arterioles sampled were smaller than 50 μm in diameter and larger arterioles were not equally found in-plane between the two groups of rats, intergroup comparison of arteriole profile was based only on arterioles with an external diameter < 50 μm. Arterioles were easily identified by the presence of smooth muscle cells (labeled by ACTA2) disposed circumferentially. Measurements were made on a Nikon Eclipse 90i microscope with a Nikon DS-Ri1

camera using Nikon Elements AR analysis software. Ratio was calculated with the following equation:

$$WLR = \frac{1}{2} \times \frac{vessel\ outer\ diameter - vessel\ luminal\ diamter}{vessel\ luminal\ diameter}$$

Western blot analyses

The flash frozen hemisphere of the brain was frozen at -18°C for at least one hour in a cryostat chamber before being microdissected with a small tissue punch (1.5 mm diameter) while being held at a constant -12°C on a modified cold plate (Teca, Chicago, IL). Frozen dissected structures were placed in pre-chilled microcentrifuge tubes and stored at -80°C until analysis.

Samples for western blot analyses were homogenized at 4°C for 2 hours using the RIPA Lysis Buffer System (Santa Cruz, Dallas, TX). Total protein concentration was determined by the Pierce BCA Protein Assay (ThermoFisher, Waltham, MA). Western blot protocol was completed as previously described (Polinski et al. 2016). Protein lysates (20 µg/sample or 10 µg/sample) were electrophoresed in duplicate using SDS-PAGE Criterion gels (BIO-RAD, Hercules, CA) and transferred to Immobilon-FL membranes (Millipore, Bedford, MA). Membranes were incubated in primary antisera to albumin (as a measure of BBB leakage) or GFAP (as an index of astrogliosis/ inflammation) overnight (see **Table 3.2** for antibodies and dilutions). Blots were rinsed then incubated in LI-COR secondary antibodies. IRDye800 conjugated goat anti-rabbit and IRDye680 conjugated goat anti-mouse (LI-COR Biosciences, 926-68020, 1: 20,000; LI-COR Biosciences; 926-32211, 1: 20,000) were used as secondary antibodies. All

antibody dilutions were made in 2% non-fat dairy milk in TBS. Multiplexed signal intensities were imaged with both 700 and 800 nm channels in a single scan with a resolution of 169μm using the Odyssey infrared image system (LI-COR Biosciences).

Statistics

Data analysis and graph creation were performed using GraphPad Prism software (GraphPad, version 7 La Jolla, CA). All data sets were verified for normality using D'Agostino and Pearson omnibus testing. To compare DBH vs. IgG injected rats, student t-tests were used. No sex differences were observed so sexes were evaluated together for this study, as done previously (Cohen et al. 2013; Rorabaugh et al. 2017). The level of statistical significance was set at $p < 0.05$.

Results

DBH-sap lesioned animals exhibit spatial and working memory deficits 2 weeks post-op

Two weeks after surgeries, animals were evaluated on the Barnes Maze and showed deficits during the probe trial (see **Table 3.1** for protocol; Attar et al. 2013; Barnes 1979). While TgF344 animals show age related cognitive deficits, none are exhibited in the TgF344 rat at 6 months compared to wild type fisher littermates with this behavior paradigm (Cohen et al. 2013). Animals with the DBH-sap lesion spent significantly less time in the target quadrant during the probe trial (**Figure 3.3 A-B**; p=0.0132) and were significantly slower to find the target hole (**Figure 3.3 C**; p=0.0105). Both of these measures indicate a deficit in spatial memory. Interestingly, the DBH-sap animals also

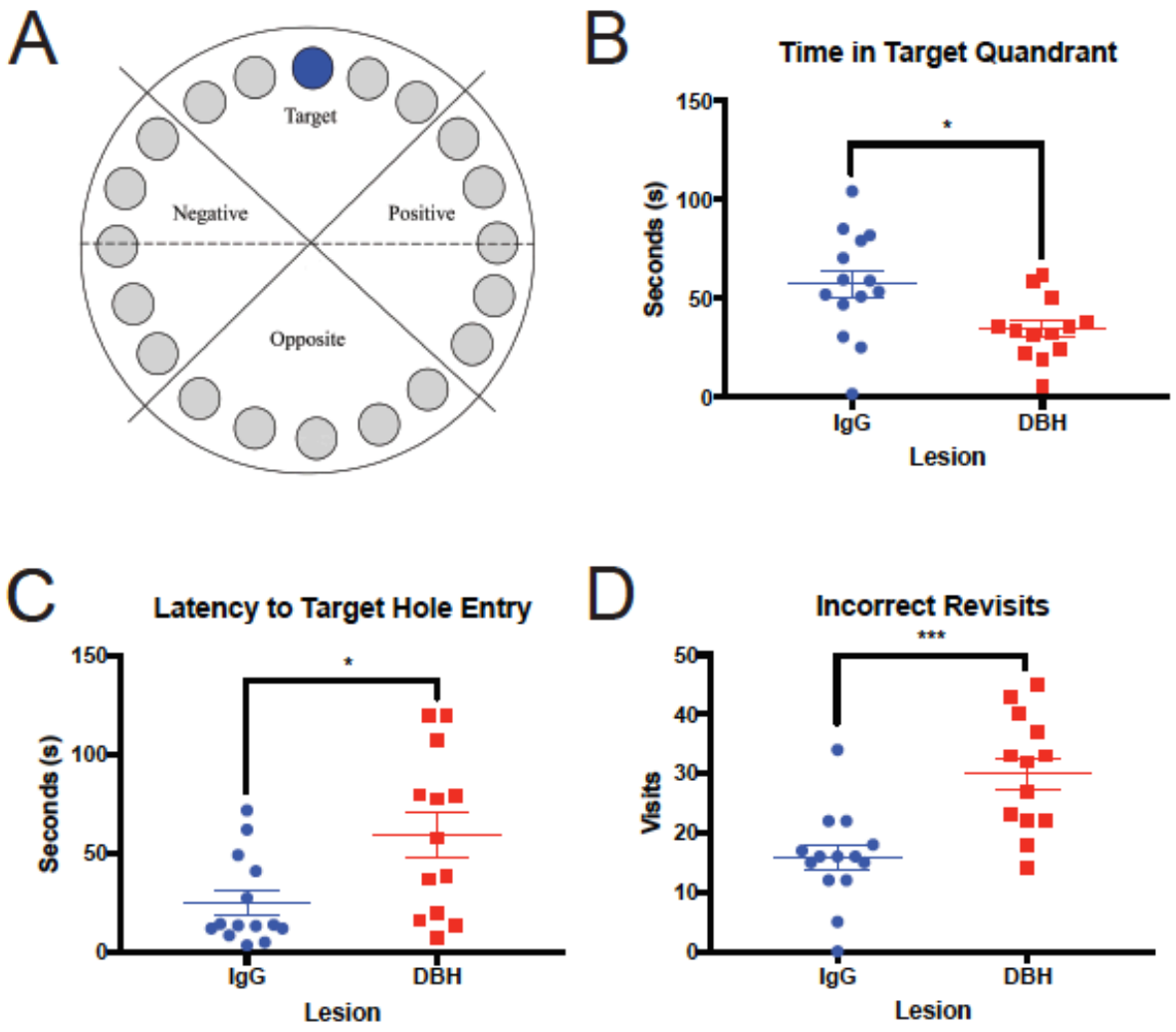

Figure 3.3 DBH-sap lesioned TgF344 rats are impaired 2 weeks post-op in measures of spatial and working memory compared to control IgG-sap animals

Animals were evaluated on the Barnes Maze at two weeks post-op**. A.** Schematic of maze. **B.** DBH-sap lesioned animals spent significantly less time in the target quadrant during the probe trial (p=0.0132; measure of spatial memory). **C.** DBH-sap animals were also significantly slower to find the target hole during probe trial (p=0.0105; measure of spatial memory). **D.** IgG-sap control animal made fewer revisits to holes already investigated (p=0.0003; measure of working memory). Error bars=SEM.

showed a greater number of revisits to holes that they had already investigated during the probe trial (**Figure 3.3 D**; p=0.0003). While a newer measure in Barnes maze task, a greater number of revisits has been shown to indicate a deficit in working memory (Kesby et al. 2015).

In addition, there were no significant differences between DBH-sap or IgG-sap lesioned animals during the open field test, which included measurements of time mobile (**Figure 3.4 A-B**; p=0.4955) and distance traveled (**Figure 3.4 C;** p=0.5386). This finding indicated that there were no locomotor effects of the lesion at 2 weeks post-op. Moreover, to ensure that there were no anti-anxiolytic effects of the lesions that might impact cognitive or motor behavior, we evaluated the animals using the elevated plus maze (Walf and Frye 2007). Due to the immense innervation the LC has on the amygdala (McCall et al. 2017; Price and Amaral 1981) and the highly bifurcated nature of the LC (Szabadi 2013) we used this test to ensure any behavior phenotypes we observed were not a result of a change in fear/anxiety. Using this test, we observed no differences in the time spent in the open arms (**Figure 3.4 D-E;** p= .7161) indicating no adverse effects of the DBH-sap lesion in fear and anxiety-related behaviors compared to control.

DBH-sap lesioned animals have continued spatial and working memory deficits 6 weeks post-op

At 6 weeks post-op, we tested to see if a worsened behavioral phenotype was observable in the DBH-sap lesioned animals compared to control IgG-sap lesioned animals. The training protocol was shortened during the second round of behavior in

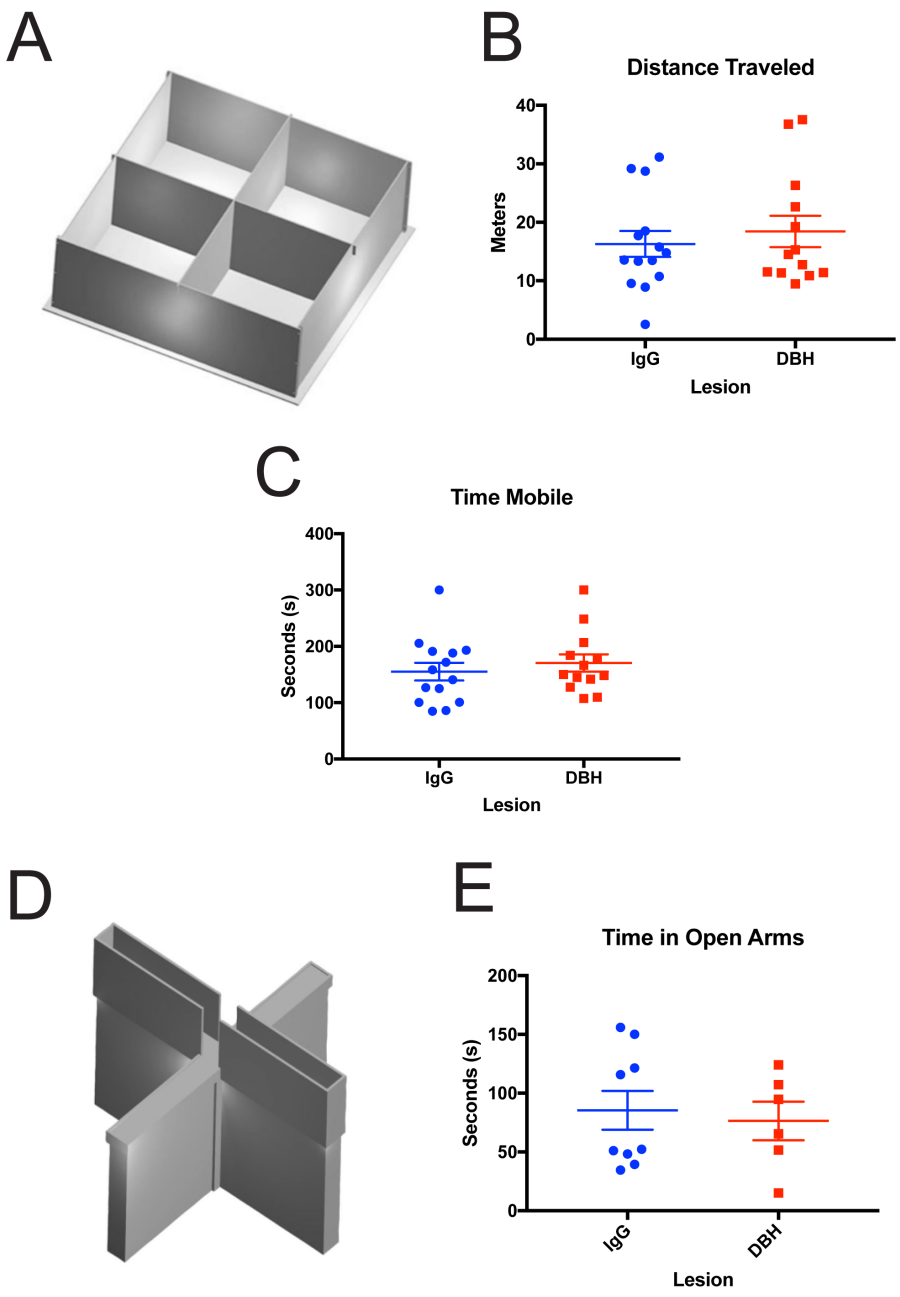

Figure 3.4 No locomotor or anxiety differences observed between control IgG-sap and DBH-sap lesioned animals 2 weeks post-op

To test for any compromising locomotor or anxiety effects of the DBH-sap lesion animals were evaluated on the open field test and elevated plus maze. **A** Schematic of the open field test box. **B** No significant differences observed between DBH sap or IgG

Figure 3.4 (cont'd)

sap lesioned animals time mobile (p=0.4955) or **C** distance traveled (p=0.5386) indicating no locomotor effects of the lesion at 2 weeks post-op. **D** Schematic of the elevated plus maze. **E** Later cohorts were evaluated using the elevated plus maze. No differences in the time spent in the open arms (p= .7161) indicating no adverse effects of the DBH-sap lesion in fear and anxiety-related behaviors compared to control. Error bars=SEM.

order to avoid a ceiling effect with overtraining (see **Table 3.1**). Animals with the DBH-sap lesion again spent significantly less time in the target quadrant during the probe trial with a more robust difference observable compared to testing at 2 weeks post-op (**Figure 3.5 A-B**; p=0.0083). The DBH-sap lesioned animals also continued to display a greater latency to find the target hole was sustained in the second round of behavior. This was in part due to a slight improvement in the ability of the IgG-sap animals to find the target hole coupled with no net change in the DBH-sap group. (**Figure 3.5 C**; p=0.0002). DBH-sap animals also continued to exhibit working memory deficits at 6 weeks post-op, making significantly more revisits to holes previously investigated than IgG-sap animals (**Figure 3.5 D**; p=0.0003) Again, animals showed no differences in locomotor activity (**Figure 3.6 A-C**) or in fear or anxiety-like behavior (**Figure 3.6 D-E**).

The DBH-sap lesion dramatically reduces noradrenergic fiber innervation in the PFC and leads to corresponding LC cell death

DBH-Sap has been previously validated as a NE-specific immunotoxin in intraventricular surgeries (Wrenn et al. 1996; Ostock et al. 2014; Patrone et al. 2018). To validate the immunotoxin's effect in a tissue specific lesion to the PFC, we used LI-COR near-infrared immunohistochemistry to compare the NE fiber immunoreactivity intensity between the DBH-sap and IgG-sap lesioned animals. Blinded quantification of the prefrontal cortex immunoreactivity showed a 50% reduction in DBH signal in DBH-sap animals ($p<0.0001$; **Figure 3.7 A-B, E**). Furthermore, evaluation of the LC showed robust loss of DBH-positive cells as to be expected based on previous reports (**Figure 3.7 C-D;** (Wrenn et al. 1996; Ostock et al. 2014; Patrone et al. 2018).

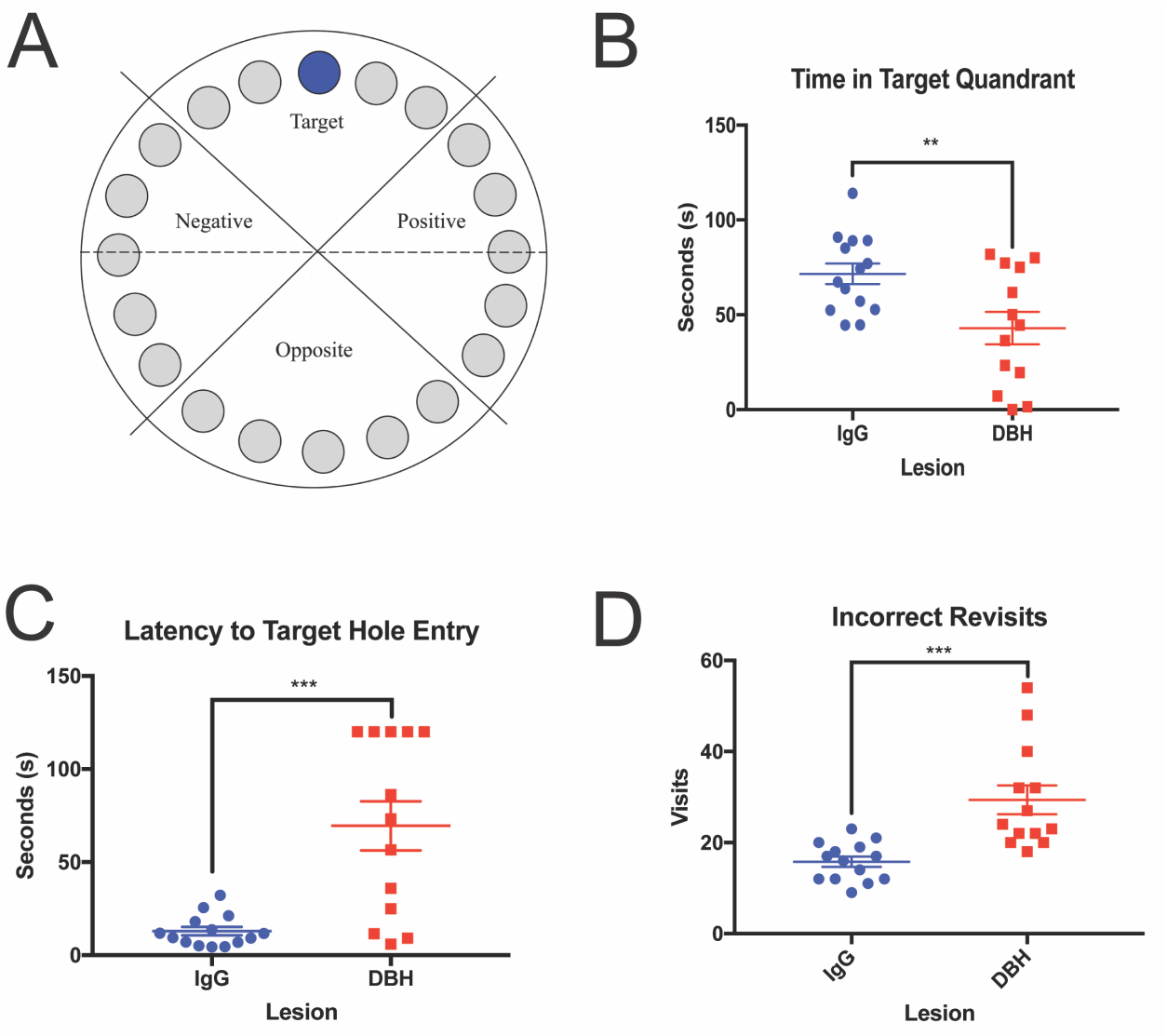

Figure 3.5 DBH-sap lesioned TgF344 rats are impaired 6 weeks post-op in measures of spatial and working memory compared to control IgG-sap animals

Animals were evaluated on the Barnes Maze at 6 weeks post-op using a shorter training paradigm (see **Table 3.1**). **A.** Schematic of maze. **B.** DBH-sap lesioned animals spent significantly less time in the target quadrant during the probe trial (p=0.0083; measure of spatial memory). **C.** DBH-sap animals were also significantly slower to find the target hole during probe trial (p=0.002; measure of spatial memory). **D.** IgG-sap control animal

Figure 3.5 (cont'd)

made fewer revisits to holes already investigated (p=0.0003; measure of working memory). Error bars=SEM.

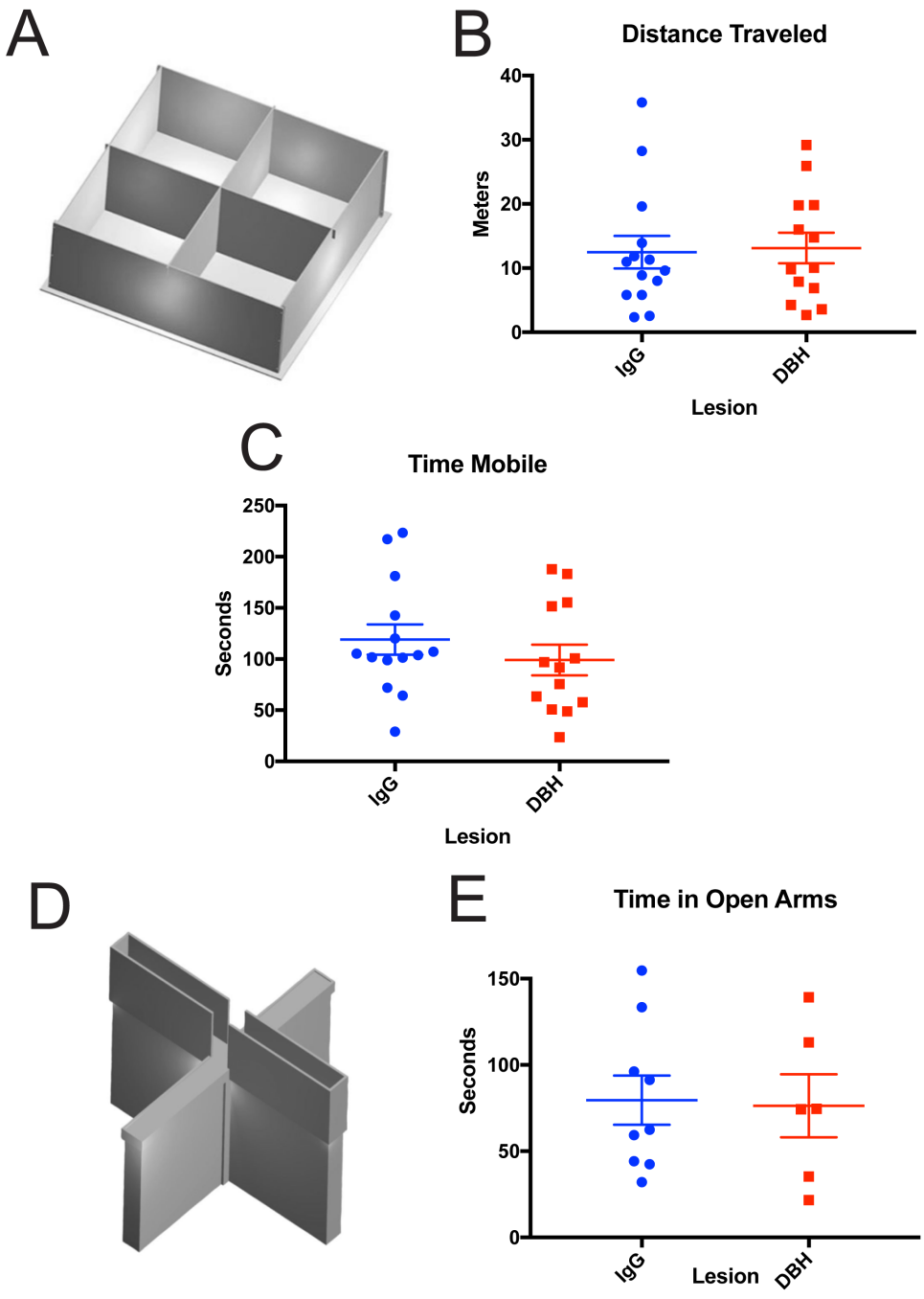

Figure 3.6 No locomotor or anxiety differences observed between IgG-sap and DBH-sap lesioned animals 6 weeks post-op

To test for any compromising locomotor or anxiety effects of the DBH-sap lesion animals were evaluated on the open field test and elevated plus maze. **A** Schematic of

Figure 3.6 (cont'd)

the open field test box. **B** No significant differences observed between DBH-sap or IgG-sap lesioned animals time mobile (p=0.3493) or **C** distance traveled (p=0.8547) indicating no locomotor effects of the lesion at 2 weeks post-op. **D** Schematic of the elevated plus maze. **E** Later cohorts were evaluated using the elevated plus maze. No differences in the time spent in the open arms (p= .7161) indicating no adverse effects of the DBH-sap lesion in fear and anxiety-related behaviors compared to control. Error bars=SEM.

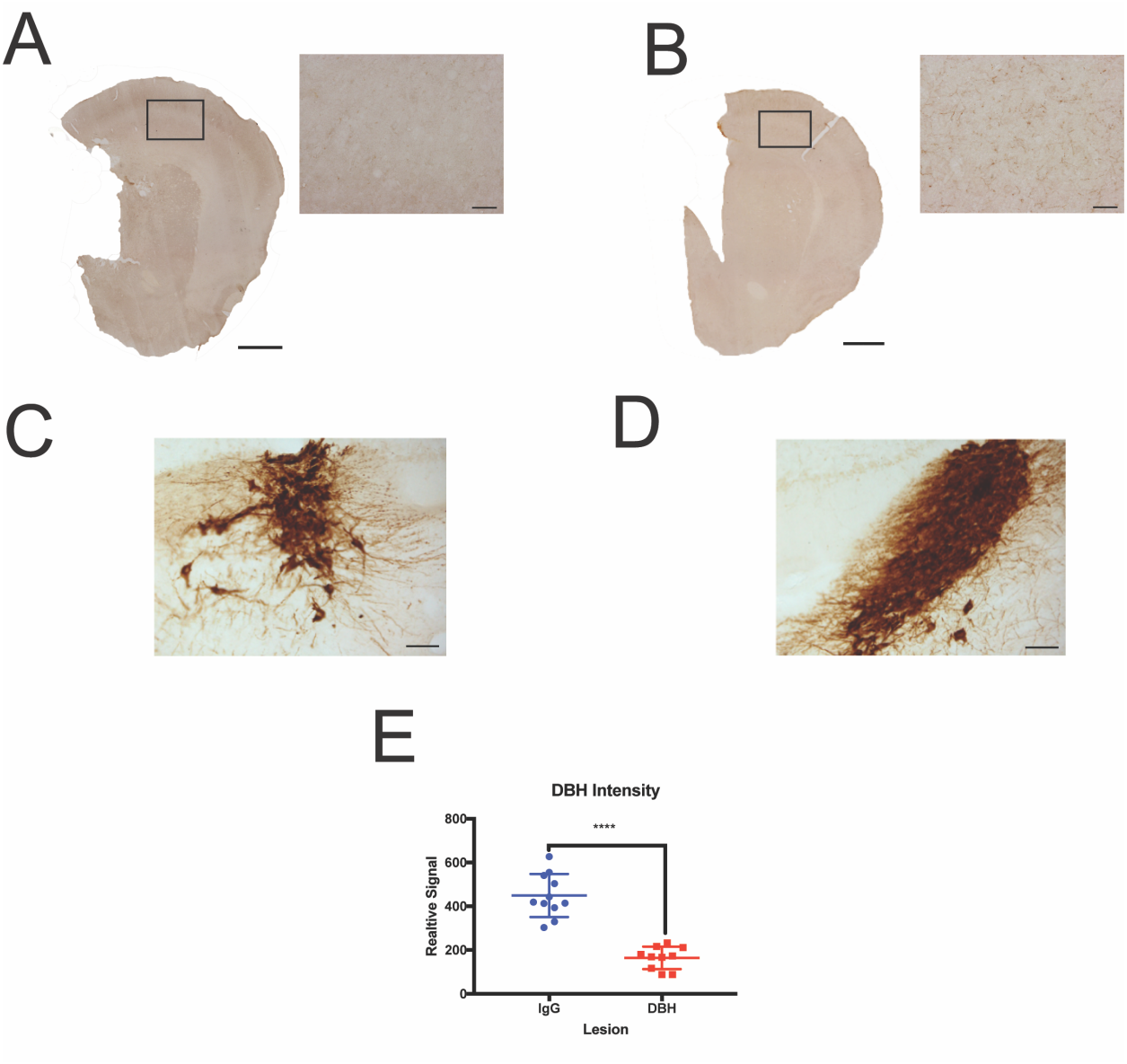

Figure 3.7 DBH reactivity is significantly decreased in TgF344 rats after DBH-sap lesion

Representative DBH immunostaining in DBH-sap lesioned cortex (**A**) and IgG-sap lesioned cortex (**B**). IgG-sap lesioned animals exhibit robust DBH positive staining in the LC (**D**) while DBH-sap LC cells are greatly reduced in number and reactivity (**C**). Signal intensity analysis of LI-COR IHC revealed profound reduction in the DBH reactivity of

Figure 3.7 (cont'd)

cortical fibers in DBH-sap lesioned animals (**E**: $p<0.0001$). **A-B** large image scale bars =1000um inset images scale bars =50um **C-D** scale bars= 50um. Error bars=SEM.

DBH-sap lesioned TgF344 rats exhibit increased amyloid and microgliosis pathology in the cortex and hippocampus

To determine whether lesioning of the PFC with DBH-sap could accelerate AD-like Aβ plaque pathology, we measured MOAB-2 immunoreactivity in the entire cortex and hippocampus of lesioned animals. MOAB-2 (mouse IgG2b) is a specific, high-titer antibody to Aβ residues 1-4 (Youmans et al. 2012). MOAB-2 does not cross react with amyloid precursor protein (APP) making it a superior marker for plaques. DBH-sap animals exhibited a 30% increased MOAB-2 amyloid burden in the cortex (**Figure 3.8 A-B**; $p<0.001$). Additionally, MOAB-2 amyloid signal intensity was also increased (10%) in the hippocampus of DBH-sap animals compared to controls (**Figure 3.8 C;** $p<0.05$) indicating that resulting pathology was not just localized to the lesioned PFC tissue. Upon examination of nickel-enhanced DAB MOAB-2 immunohistochemistry, it was evident that not only were the size of the plaques increased in DBH-sap lesioned animals, but the number of plaques were also increased (**Figure 3.8 A**). Furthermore, dual-label fluorescent IHC with the microglial marker Iba1 revealed increased microglial ramification surrounding MOAB-2 plaques (**Figure 3.8 D**). This indicated not only an increase in amyloid burden but an additional increase in microgliosis displayed by the TgF344 rat (Cohen et al. 2013).

DBH-sap lesion induces vessel remodeling as evidenced by an increased WLR

The WLR is an important parameter in vascular medicine because it indicates the health of the vascular wall as well as the degree of stenosis. The WLR has been used as a measure of hypertension or vessel remodeling in previous studies (Dorrance, Rupp, and

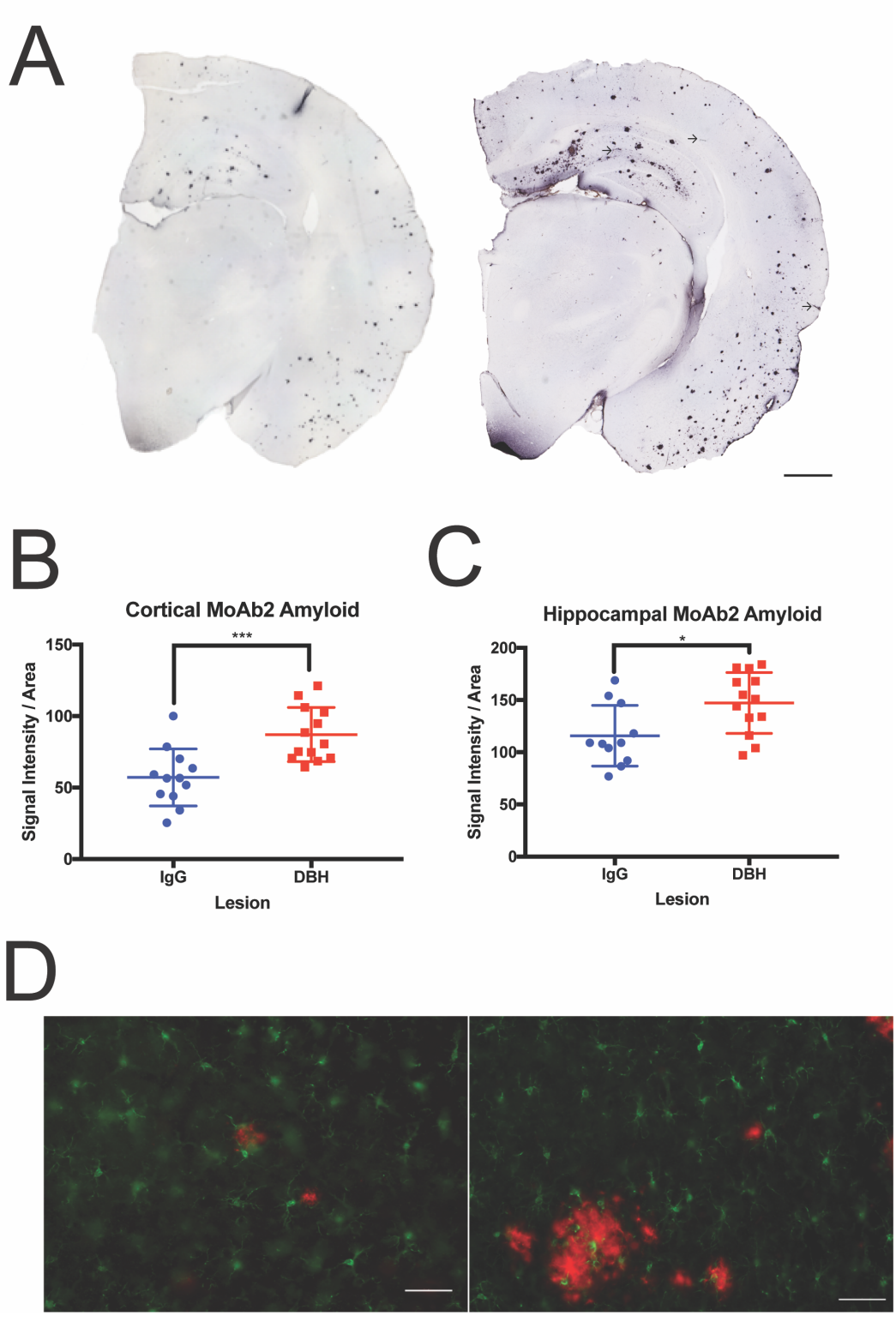

Figure 3.8 MOAB-2 is increased in both the cortex and hippocampus in DBH-sap lesioned TgF344 rats with accompanying microgliosis

Figure 3.8 (cont'd)

A. Representative image showing increased MOAB-2 immunostaining in both the cortex and hippocampus of DBH-sap lesioned TgF344 animals (*right*). Modest vascular MOAB2 deposition is observed in the DBH-sap lesioned cortex (arrows) (*scale bar = 1000um*). Increased amyloid burden quantified in the cortex (**B**; p=0.0008) and the hippocampus (**C**; p=0.0153) via LI-COR intensity measures. **D**. Fluorescence microscopy revealed larger MOAB-2 labeled plaques (red) in DBH-sap lesioned animals (*right panel*) compared to IgG-sap lesioned animals (*left panel*) accompanied by more ramified microglia labeled by Iba1 (green). Error bars=SEM.

Nogueira 2006; Amaral, Zorn, and Michelini 2000; Harazny et al. 2007). Arterioles that were perpendicular to the plane of view were measured in the NIS elements software. On average, arterioles in DBH-sap lesioned animals showed an increase in the WLR (**Figure 3.9 A- B;** $p<0.0001$) indicating a compensatory remodeling of the vessel structure (i.e. an increase in smooth muscle actin surrounding the vessel) as a result of the loss of NE-input to the vessels and vascular tone.

Evidence for astrocytic uptake of albumin following blood brain barrier disruption in DBH- sap lesioned TgF344 rats

To further investigate the impact of the DBH-sap lesion on the integrity of the blood brain barrier (BBB) we analyzed the PFC of DBH-sap or IgG-sap lesioned animals via anti-albumin IHC. Brightfield images showed an increase in albumin reactivity in DBH-sap lesioned animals (**Figure 3.10 A-B**). Notably, all animals were equally perfused so that little to no residual blood proteins should be present in the vessels. Therefore, the parenchymal or extravascular deposits of albumin indicate vessel leakage or BBB breakdown. This initial immunohistochemical observation was quantitatively confirmed with near-infrared signal measurements via LI-COR IHC (**Figure 3.10 C**; $p=0.0242$) and western blotting (**Figure 3.10 E**; $p=0.0052$). Further investigation with fluorescent immunohistochemistry revealed that the albumin observed in the DBH-sap lesioned animal colocalized with glial fibrillary acid protein (GFAP) a marker for astrocytes (**Figure 3.10 D**). Additionally, levels of GFAP in the PFC were also increased in DBH-sap lesioned animals indicating a glial immune response to BBB dysfunction/ albumin leakage ($p=0.011$; **Figure 3.10 F**).

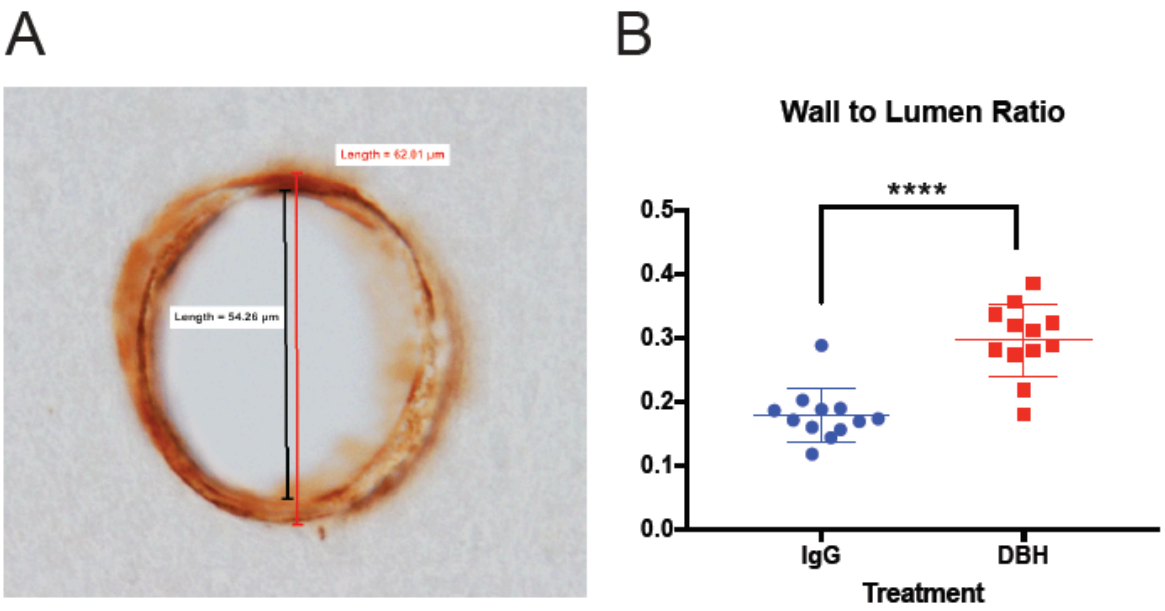

Figure 3.9 Wall to lumen ratio of parenchymal arterioles is increased in DBH-sap lesioned TgF344 rats

A. Representative image of Smooth Muscle Actin (ACTA2) labeled arteriole. Outside wall diameter measurement is compared to luminal diameter to produce Wall: Lumen Ratio value. **B.** DBH-sap lesioned animals displayed an approximately 0.5-fold increase in the Wall: Lumen ratio ($p<0.0001$). Error bars=SEM.

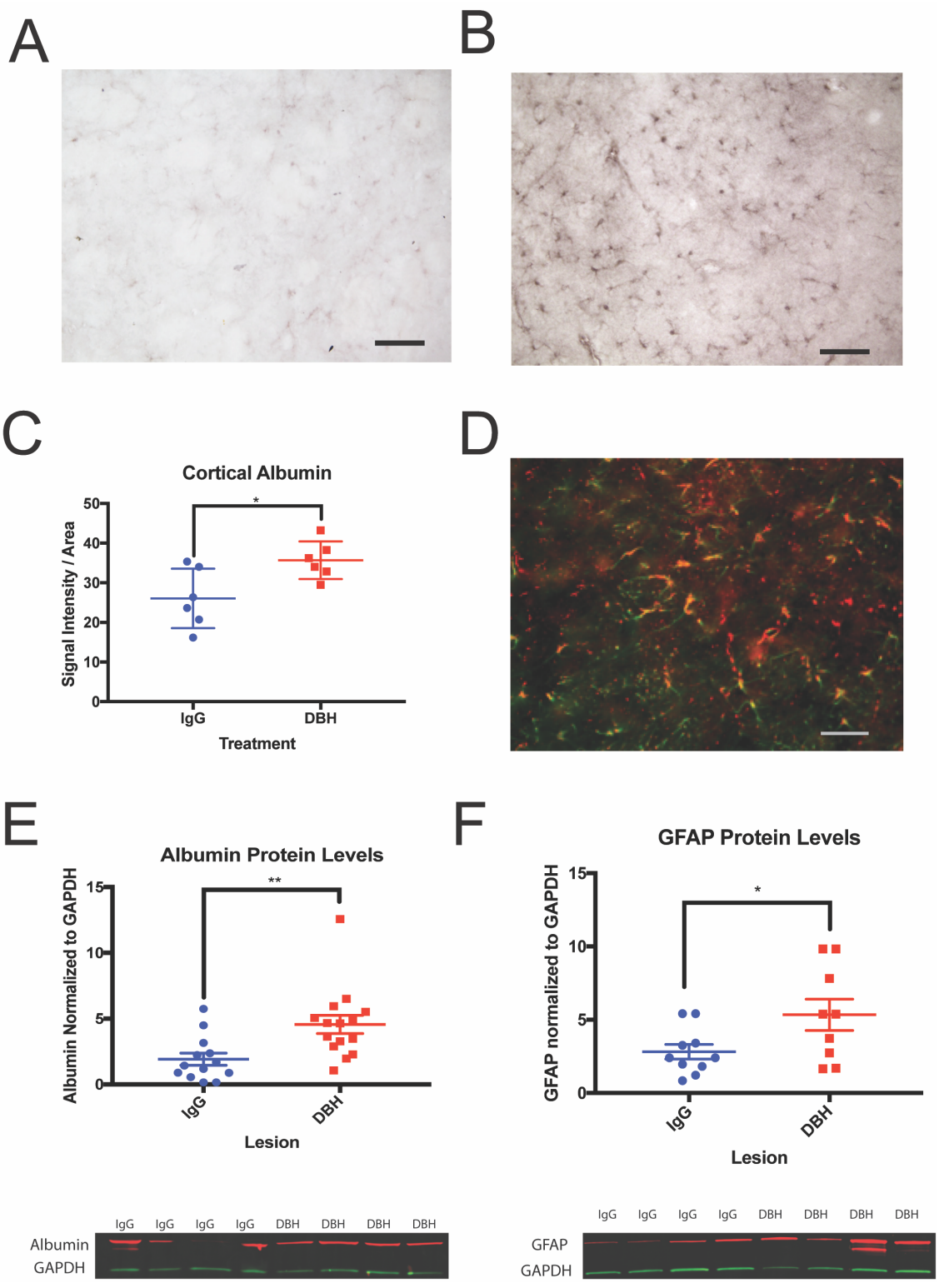

Figure 3.10 Intraparenchymal albumin levels are increased in DBH-sap lesioned TgF344 rats with evidence for albumin uptake by astrocytes

Figure 3.10 (cont'd)

A. DAB IHC for Albumin indicated an increase in parenchymal albumin deposition in DBH-sap animals (right). Scale bars =100um.**B.** Intensity analysis of LICOR IHC revealed increased Albumin reactivity in the cortex of DBH-sap lesioned animals. (p=0.0242) **C.** Fluorescence IHC revealed Albumin (red) co-labeled with GFAP (green) a marker for astrocytes. Scale bar =50um. Western blot analyses confirmed that both **D**. Albumin (p=0.0052) and **E.** GFAP (p=0.011) are increased in DBH-sap lesioned animals compared to controls (via Student's t-test). Error bars=SEM.

Discussion

The TgF344 rat was developed and characterized by Cohen and colleagues in 2013(Cohen et al. 2013) and a limited number of studies have utilized this model to date (Tsai et al. 2014; Rorabaugh et al. 2017; Daianu et al. 2015; Joo et al. 2017; Stoiljkovic et al. 2018; Bazzigaluppi et al. 2018). In this present study, we investigated the effects of lesioning the noradrenergic LC neurons and afferent fibers in the PFC of the Tgf344 (Cohen et al. 2013). To this end, we injected a noradrenergic immunotoxin into the PFC of 6-month-old TgF344 AD rats. The DBH-sap immunotoxin is advantageous over the other prominent noradrenergic lesion (N-(2-chloroethyl)-N-ethyl-2-bromobenzylamine) DSP4(Ross and Renyl 1976; Ross 1976). DSP4 administration leads to transient changes in NE tissue content, NE Transporter (NET) binding sites and α2-adrenergic binding sites in many forebrain regions, but these changes in forebrain regions occur without a loss of LC noradrenergic neurons (Szot et al. 2010). The DBH-sap immunotoxin leads to not only reduction in NE levels but sustained cell death of LC cells through ribosomal inactivation (Wrenn et al. 1996). Notably, this is the first study of its kind to have a direct injection into the cortex using a saporin immunotoxin in the context of AD and very few studies have utilized this type of specific immunotoxin in transgenic animals. Our DBH-sap lesioned rats displayed deficits in working and spatial memory, as well as increased amyloidosis and BBB breakdown consistent with a more severe AD phenotype as non-lesioned TgF344 rats are not impaired at this age (Cohen et al. 2013). Based on our present findings, the lesioned TgF344 rat uniquely meets the criteria for a suitable model of early LC dysfunction and its role in neural and vascular dysfunction in AD.

Contextual and spatial learning are corrupted in AD, and modulated by LC-NE transmission (Hagena, Hansen, and Manahan-Vaughan 2016). Behavior testing was completed at two weeks as well as six weeks post op to validate that behavioral phenotypes observed were not merely a product of the surgeries, but a sustained consequence of the loss of LC innervation. The exhibited spatial learning and working memory deficits align with the loss of LC innervation to the PFC and hippocampus as these cognitive functions depend greatly on NE (Gibbs, Hutchinson, and Summers 2010; Arnsten and Goldman-Rakic 1984, 1985) and further supported by the fact that β-adrenoreceptors are critically required for LTP-facilitated learning in the dentate gyrus (DG) of freely behaving rats (Hansen and Manahan-Vaughan 2015). NE fibers target the entire cerebral cortical mantle and acts to modulate PFC function especially in the context of attention and stress (Aston-Jones and Cohen 2005). The LC system is required for proper operation of prefrontal functions because a selective impairment in transmission within the PFC leads to disrupted working memory (Ramos and Arnsten 2007; Arnsten and Jin 2014). The highly bifurcated nature of LC neurons could lead to deafferentation be responsible for the off target (i.e. non-PFC) behavioral deficits including those in the hippocampus (Counts and Mufson 2012). To ensure locomotor or anxiolytic behavioral phenotypes were not also induced via this lesion, we conducted open field and elevated plus maze testing and observed no differences between lesioned and control animals.

Upon post-mortem evaluation, we validated the efficacy of our lesion and discovered increased Aβ deposition in the cortex and hippocampus of our lesioned animals as to be expected based on previous findings (Heneka et al. 2002; Heneka et

al. 2006; Jardanhazi-Kurutz et al. 2010). The resulting pathology in the lesioned animals was similar to that of several months-older TgF344 rats (Cohen et al. 2013). NE has been shown to have anti-amyloidogenic effects and thus, its removal could lead to an increase in plaque accumulation (Counts and Mufson 2010).

We also used numerous outcome measures to characterize vascular remodeling and BBB dysfunction that occurred as a result of our lesion. Using WLR measures, we found that DBH-sap lesioned animals have an increased WLR ratio in the PFC. This is indicative of vascular hypertrophy or vascular remodeling which is an underlying risk factor for hypertension. Vascular hypertrophy is of physiologic importance both in limiting blood flow during maximal vasodilatation and in increasing vascular responsiveness to constrictor stimuli (Hart, Heistad, and Brody 1980). It has also been demonstrated in patients with essential hypertension that the increase in media-lumen ratio is mainly due to a remodeling process (Schiffrin, Deng, and Larochelle 1992; Korsgaard et al. 1993; Heagerty, Bund, and Aalkjaer 1988; Hart, Heistad, and Brody 1980; Jacobsen, Hornbech, and Holstein-Rathlou 2011). This remodeling could be a direct compensatory response to the loss of the NE input to blood vessels provided by the LC which act on smooth muscle cells, endothelial cells and supporting astrocytic end feet to ensure proper blood flow to areas of higher order cognition (Bekar, Wei, and Nedergaard 2012; Cohen, Molinatti, and Hamel 1997; Szabadi 2013).

Additionally, we noted an increase in the extravasation of the blood protein albumin in the PFC of the DBH-sap lesioned animals. As all rats were equally perfused, there should be little to no residual albumin left in the vessels, so the residual albumin could be indicative of vascular hemorrhaging or microbleeds. The measurement of

plasma- or serum-derived molecules in the brain parenchyma has been widely used as a method to detect BBB disruption. Perivascular immunoreactivities of plasma proteins, albumin, and IgG, have been detected in microvascular segments associated with senile plaques and CAA in AD brains (Wisniewski and Kozlowski 1982; Wisniewski, Vorbrodt, and Wegiel 1997). AD patients have also been shown to possess an increased CSF/serum or CSF/plasma ratio of albumin, which has been long used as a proxy for BBB disruption (Alafuzoff et al. 1983; Skoog et al. 1998; Elovaara et al. 1985). Interestingly, immunohistochemical experiments showed that the extravascular and parenchymal albumin was being phagocytosed by surrounding astroglia. This is unsurprising as astrocytic end feet are generally surrounding the endothelium as first line of defense for infiltrating toxicants from the vasculature (Minagar et al. 2002). Astrocytes, as a significant component of the BBB, behave as one of the immune effector cells in the CNS as well. As a result, we also noted that GFAP was increased in the PFC of DBH-sap lesioned animals, most likely as a result of their recruitment to divide and wall off damaged areas (Abbott, Ronnback, and Hansson 2006; Bonkowski et al. 2011).

Notably, TgF344 rats do not express a human tau transgene but reportedly display age-dependent endogenous hyperphosphorylated tau in the hippocampus and medial PFC (Cohen et al. 2013; Rorabaugh et al. 2017). Compared to murine tau, rat tau is more similar to tau found in humans, and perhaps as a result, amyloid-based transgenic rats display unique phenotypes such as conversion of endogenous rat tau into hyperphosphorylated forms (Do Carmo and Cuello 2013; Cohen et al. 2013). Unfortunately, our cohort was not able to recapitulate the tau pathology that has been

previously reported in these animals (Cohen et al. 2013; Rorabaugh et al. 2017). No reactivity to AT8 or CP13 immunostaining was found in either the lesioned or control rats (data not shown). While our goal was to lesion animals at 6 months to model a "preclinical" AD related-LC degeneration, it is possible that our experimental rats could be too young to detect NFTs. Thus, aging out the animals or lesioning them at a later timepoint could elucidate such pathology. Further, while modest reductions of NE and MHPG (3-methoxy-4-hydroxyphenylglycol; a metabolite of NE) have been found in the hippocampus of TgF344 animals at this time point in other studies, LC loss is not evident, and reductions in noradrenergic fiber density and NE levels were not observed in the PFC at any age (Rorabaugh et al. 2017). This indicates that dysfunction is not universal across brain regions innervated by the LC in this model (Rorabaugh et al. 2017) making our lesioning paradigm, while perhaps too robust to replicate preclinical AD-related LC loss, more relevant to model human late-stage LC deafferentation than the TgF344 alone. Characterization of this lesioning paradigm to identify a dosing regimen that produces ~25-35% LC cell loss (Kelly et al, 2017, **Figure 2.1**) and associated fiber loss loss warrants investigation to replicate LC projection system loss observed in PCAD and MCI.

Rorabaugh and colleagues did find that DREADD-induced LC activation restored normal reversal learning to aged TgF344-AD rats, indicating that enhancing LC tone can improve cognition, even in the presence of AD pathology (Rorabaugh et al. 2017). This may be the result of increased perfusion from LC activation (Toussay et al. 2013), though this would need to be tested directly. Thus, modeling NE rescue in later stage TgF344 rats and DBH-sap lesioned animals could help test novel AD

pharmacotherapies targeting these pathways (Chalermpalanupap et al. 2013). Further characterization of the nascent TgF344 rat by Joo and colleagues has shown that at 9 months of age, these rats show significant amount of vascular Aβ deposits on the cortical penetrating arterioles, but they did not find significant differences between TgF344 and non-transgenics with regard to expressions of either occludin or GFAP (markers of the BBB). Again, our rats were most likely too young to see robust vascular Aβ deposits. However, modeling LC degeneration at later stages in the TgF344 life to understand how vascular Aβ is influenced by NE loss warrants further investigation.

LITERATURE CITED

LITERATURE CITED

Abbott, N. J., L. Ronnback, and E. Hansson. 2006. 'Astrocyte-endothelial interactions at the blood-brain barrier', *Nat Rev Neurosci*, 7: 41-53.

Alafuzoff, I., R. Adolfsson, G. Bucht, and B. Winblad. 1983. 'Albumin and immunoglobulin in plasma and cerebrospinal fluid, and blood-cerebrospinal fluid barrier function in patients with dementia of Alzheimer type and multi-infarct dementia', *J Neurol Sci*, 60: 465-72.

Alzheimer's. 2018. '2018 Alzheimer's disease facts and figures', *Alzheimer's & Dementia: The Journal of the Alzheimer's Association*, 14: 367-429.

Amaral, S. L., T. M. Zorn, and L. C. Michelini. 2000. 'Exercise training normalizes wall-to-lumen ratio of the gracilis muscle arterioles and reduces pressure in spontaneously hypertensive rats', *J Hypertens*, 18: 1563-72.

Arendt, T., M. K. Bruckner, M. Morawski, C. Jager, and H. J. Gertz. 2015. 'Early neurone loss in Alzheimer's disease: cortical or subcortical?', *Acta Neuropathol Commun*, 3.

Arnsten, A. F., and P. S. Goldman-Rakic. 1984. 'Selective prefrontal cortical projections to the region of the locus coeruleus and raphe nuclei in the rhesus monkey', *Brain Res*, 306.

———. 1985. 'Alpha 2-adrenergic mechanisms in prefrontal cortex associated with cognitive decline in aged nonhuman primates', *Science*, 230: 1273-6.

Arnsten, A. F., and L. E. Jin. 2014. 'Molecular influences on working memory circuits in dorsolateral prefrontal cortex', *Prog Mol Biol Transl Sci*, 122: 211-31.

Arvanitakis, Z., A. W. Capuano, S. E. Leurgans, D. A. Bennett, and J. A. Schneider. 2016. 'Relation of cerebral vessel disease to Alzheimer's disease dementia and cognitive function in elderly people: a cross-sectional study', *Lancet Neurol*, 15: 934-43.

Aston-Jones, G., and J. D. Cohen. 2005. 'An integrative theory of locus coeruleus-norepinephrine function: adaptive gain and optimal performance', *Annu Rev Neurosci*, 28.

Attar, A., T. Liu, W. T. Chan, J. Hayes, M. Nejad, K. Lei, and G. Bitan. 2013. 'A shortened Barnes maze protocol reveals memory deficits at 4-months of age in the triple-transgenic mouse model of Alzheimer's disease', *PLoS One*, 8: e80355.

Attems, J., and K. A. Jellinger. 2014. 'The overlap between vascular disease and Alzheimer's disease--lessons from pathology', *BMC Med*, 12: 206.

Bailey, T. L., C. B. Rivara, A. B. Rocher, and P. R. Hof. 2004. 'The nature and effects of cortical microvascular pathology in aging and Alzheimer's disease', *Neurol Res*, 26: 573-8.

Barnes, C. A. 1979. 'Memory deficits associated with senescence: a neurophysiological and behavioral study in the rat', *J Comp Physiol Psychol*, 93: 74-104.

Baumbach, G. L., and M. A. Hajdu. 1993. 'Mechanics and composition of cerebral arterioles in renal and spontaneously hypertensive rats', *Hypertension*, 21: 816-26.

Bazzigaluppi, P., T. L. Beckett, M. M. Koletar, A. Y. Lai, I. L. Joo, M. E. Brown, P. L. Carlen, J. McLaurin, and B. Stefanovic. 2018. 'Early-stage attenuation of phase-amplitude coupling in the hippocampus and medial prefrontal cortex in a transgenic rat model of Alzheimer's disease', *J Neurochem*, 144: 669-79.

Bekar, L. K., H. S. Wei, and M. Nedergaard. 2012. 'The locus coeruleus-norepinephrine network optimizes coupling of cerebral blood volume with oxygen demand', *J Cereb Blood Flow Metab*, 32: 2135-45.

Bonkowski, D., V. Katyshev, R. D. Balabanov, A. Borisov, and P. Dore-Duffy. 2011. 'The CNS microvascular pericyte: pericyte-astrocyte crosstalk in the regulation of tissue survival', *Fluids Barriers CNS*, 8: 8.

Braak, H., and K. Del Tredici. 2012. 'Where, when, and in what form does sporadic Alzheimer's disease begin?', *Curr Opin Neurol*, 25: 708-14.

Chalermpalanupap, T., B. Kinkead, W. T. Hu, M. P. Kummer, T. Hammerschmidt, M. T. Heneka, D. Weinshenker, and A. I. Levey. 2013. 'Targeting norepinephrine in mild cognitive impairment and Alzheimer's disease', *Alzheimers Res Ther*, 5: 21.

Cohen, R. M., K. Rezai-Zadeh, T. M. Weitz, A. Rentsendorj, D. Gate, I. Spivak, Y. Bholat, V. Vasilevko, C. G. Glabe, J. J. Breunig, P. Rakic, H. Davtyan, M. G. Agadjanyan, V. Kepe, J. R. Barrio, S. Bannykh, C. A. Szekely, R. N. Pechnick, and T. Town. 2013. 'A transgenic Alzheimer rat with plaques, tau pathology, behavioral impairment, oligomeric abeta, and frank neuronal loss', *J Neurosci*, 33: 6245-56.

Cohen, Z., G. Molinatti, and E. Hamel. 1997. 'Astroglial and vascular interactions of noradrenaline terminals in the rat cerebral cortex', *J Cereb Blood Flow Metab*, 17: 894-904.

Counts, S. E., and E. J. Mufson. 2010. 'Noradrenaline activation of neurotrophic pathways protects against neuronal amyloid toxicity', *J Neurochem*, 113: 649-60.

———. 2012. 'Locus coeruleus.' in J. K. Mai and G. Paxinos (eds.), *The human nervous system* (Academic: London).

Daianu, M., R. E. Jacobs, T. M. Weitz, T. C. Town, and P. M. Thompson. 2015. 'Multi-Shell Hybrid Diffusion Imaging (HYDI) at 7 Tesla in TgF344-AD Transgenic Alzheimer Rats', *PLoS One*, 10: e0145205.

Do Carmo, S., and A. C. Cuello. 2013. 'Modeling Alzheimer's disease in transgenic rats', *Mol Neurodegener*, 8: 37.

Dorrance, A. M., N. C. Rupp, and E. F. Nogueira. 2006. 'Mineralocorticoid receptor activation causes cerebral vessel remodeling and exacerbates the damage caused by cerebral ischemia', *Hypertension*, 47: 590-5.

Elovaara, I., A. Icen, J. Palo, and T. Erkinjuntti. 1985. 'CSF in Alzheimer's disease. Studies on blood-brain barrier function and intrathecal protein synthesis', *J Neurol Sci*, 70: 73-80.

Feinstein, D. L., M. T. Heneka, V. Gavrilyuk, C. Dello Russo, G. Weinberg, and E. Galea. 2002. 'Noradrenergic regulation of inflammatory gene expression in brain', *Neurochem Int*, 41.

Feinstein, D. L., S. Kalinin, and D. Braun. 2016. 'Causes, consequences, and cures for neuroinflammation mediated via the locus coeruleus: noradrenergic signaling system', *J Neurochem*, 139.

Gibbs, M. E., D. S. Hutchinson, and R. J. Summers. 2010. 'Noradrenaline release in the locus coeruleus modulates memory formation and consolidation; roles for alpha- and beta-adrenergic receptors', *Neuroscience*, 170: 1209-22.

Grinberg, L. T., and D. R. Thal. 2010. 'Vascular pathology in the aged human brain', *Acta Neuropathol*, 119: 277-90.

Grudzien, A., P. Shaw, S. Weintraub, E. Bigio, D. C. Mash, and M. M. Mesulam. 2007. 'Locus coeruleus neurofibrillary degeneration in aging, mild cognitive impairment and early Alzheimer's disease', *Neurobiol Aging*, 28: 327-35.

Hagena, H., N. Hansen, and D. Manahan-Vaughan. 2016. 'beta-Adrenergic Control of Hippocampal Function: Subserving the Choreography of Synaptic Information Storage and Memory', *Cereb Cortex*, 26: 1349-64.

Haglund, M., N. Friberg, E. J. Danielsson, J. Norrman, and E. Englund. 2016. 'A methodological study of locus coeruleus degeneration in dementing disorders', *Clin Neuropathol*, 35.

Hansen, N., and D. Manahan-Vaughan. 2015. 'Locus Coeruleus Stimulation Facilitates Long-Term Depression in the Dentate Gyrus That Requires Activation of beta-Adrenergic Receptors', *Cereb Cortex*, 25: 1889-96.

Harazny, J. M., M. Ritt, D. Baleanu, C. Ott, J. Heckmann, M. P. Schlaich, G. Michelson, and R. E. Schmieder. 2007. 'Increased wall:lumen ratio of retinal arterioles in male patients with a history of a cerebrovascular event', *Hypertension*, 50: 623-9.

Hart, M. N., D. D. Heistad, and M. J. Brody. 1980. 'Effect of chronic hypertension and sympathetic denervation on wall/lumen ratio of cerebral vessels', *Hypertension*, 2: 419-23.

Heagerty, A. M., S. J. Bund, and C. Aalkjaer. 1988. 'Effects of drug treatment on human resistance arteriole morphology in essential hypertension: direct evidence for structural remodelling of resistance vessels', *Lancet*, 2: 1209-12.

Heneka, M. T., E. Galea, V. Gavriluyk, L. Dumitrescu-Ozimek, J. Daeschner, M. K. O'Banion, G. Weinberg, T. Klockgether, and D. L. Feinstein. 2002. 'Noradrenergic depletion potentiates beta -amyloid-induced cortical inflammation: implications for Alzheimer's disease', *J Neurosci*, 22.

Heneka, M. T., M. Ramanathan, A. H. Jacobs, L. Dumitrescu-Ozimek, A. Bilkei-Gorzo, T. Debeir, M. Sastre, N. Galldiks, A. Zimmer, M. Hoehn, W. D. Heiss, T. Klockgether, and M. Staufenbiel. 2006. 'Locus ceruleus degeneration promotes Alzheimer pathogenesis in amyloid precursor protein 23 transgenic mice', *J Neurosci*, 26: 1343-54.

Holscher, C. 1999. 'Stress impairs performance in spatial water maze learning tasks', *Behav Brain Res*, 100: 225-35.

Jacobsen, J. C., M. S. Hornbech, and N. H. Holstein-Rathlou. 2011. 'Significance of microvascular remodelling for the vascular flow reserve in hypertension', *Interface Focus*, 1: 117-31.

Jardanhazi-Kurutz, D., M. P. Kummer, D. Terwel, K. Vogel, T. Dyrks, A. Thiele, and M. T. Heneka. 2010. 'Induced LC degeneration in APP/PS1 transgenic mice accelerates early cerebral amyloidosis and cognitive deficits', *Neurochem Int*, 57: 375-82.

Joo, I. L., A. Y. Lai, P. Bazzigaluppi, M. M. Koletar, A. Dorr, M. E. Brown, L. A. Thomason, J. G. Sled, J. McLaurin, and B. Stefanovic. 2017. 'Early neurovascular dysfunction in a transgenic rat model of Alzheimer's disease', *Sci Rep*, 7: 46427.

Karran, E., and J. Hardy. 2014. 'A critique of the drug discovery and phase 3 clinical programs targeting the amyloid hypothesis for Alzheimer disease', *Ann Neurol*, 76: 185-205.

Kelly, S. C., B. He, S. E. Perez, S. D. Ginsberg, E. J. Mufson, and S. E. Counts. 2017. 'Locus coeruleus cellular and molecular pathology during the progression of Alzheimer's disease', *Acta Neuropathol Commun*, 5: 8.

Kesby, J. P., J. J. Kim, M. Scadeng, G. Woods, D. M. Kado, J. M. Olefsky, D. V. Jeste, C. L. Achim, and S. Semenova. 2015. 'Spatial Cognition in Adult and Aged Mice Exposed to High-Fat Diet', *PLoS One*, 10: e0140034.

Korsgaard, N., C. Aalkjaer, A. M. Heagerty, A. S. Izzard, and M. J. Mulvany. 1993. 'Histology of subcutaneous small arteries from patients with essential hypertension', *Hypertension*, 22: 523-6.

Mather, M., and C. W. Harley. 2016. 'The Locus Coeruleus: Essential for Maintaining Cognitive Function and the Aging Brain', *Trends Cogn Sci*, 20: 214-26.

McCall, J. G., E. R. Siuda, D. L. Bhatti, L. A. Lawson, Z. A. McElligott, G. D. Stuber, and M. R. Bruchas. 2017. 'Locus coeruleus to basolateral amygdala noradrenergic projections promote anxiety-like behavior', *Elife*, 6.

Minagar, A., P. Shapshak, R. Fujimura, R. Ownby, M. Heyes, and C. Eisdorfer. 2002. 'The role of macrophage/microglia and astrocytes in the pathogenesis of three neurologic disorders: HIV-associated dementia, Alzheimer disease, and multiple sclerosis', *J Neurol Sci*, 202: 13-23.

Ostock, C. Y., D. Lindenbach, A. A. Goldenberg, E. Kampton, and C. Bishop. 2014. 'Effects of noradrenergic denervation by anti-DBH-saporin on behavioral responsivity to L-DOPA in the hemi-parkinsonian rat', *Behav Brain Res*, 270: 75-85.

Patrone, L. G. A., V. Biancardi, D. A. Marques, K. C. Bicego, and L. H. Gargaglioni. 2018. 'Brainstem catecholaminergic neurones and breathing control during postnatal development in male and female rats', *J Physiol*.

Pentkowski, N. S., L. E. Berkowitz, S. M. Thompson, E. N. Drake, C. R. Olguin, and B. J. Clark. 2018. 'Anxiety-like behavior as an early endophenotype in the TgF344-AD rat model of Alzheimer's disease', *Neurobiol Aging*, 61: 169-76.

Polinski, N. K., F. P. Manfredsson, M. J. Benskey, D. L. Fischer, C. J. Kemp, K. Steece-Collier, I. M. Sandoval, K. L. Paumier, and C. E. Sortwell. 2016. 'Impact of age and vector construct on striatal and nigral transgene expression', *Mol Ther Methods Clin Dev*, 3: 16082.

Price, J. L., and D. G. Amaral. 1981. 'An autoradiographic study of the projections of the central nucleus of the monkey amygdala', *J Neurosci*, 1.

Ramos, B. P., and A. F. Arnsten. 2007. 'Adrenergic pharmacology and cognition: focus on the prefrontal cortex', *Pharmacol Ther*, 113: 523-36.

Rorabaugh, J. M., T. Chalermpalanupap, C. A. Botz-Zapp, V. M. Fu, N. A. Lembeck, R. M. Cohen, and D. Weinshenker. 2017. 'Chemogenetic locus coeruleus activation restores reversal learning in a rat model of Alzheimer's disease', *Brain*, 140: 3023-38.

Rosenfeld, C. S., and S. A. Ferguson. 2014. 'Barnes maze testing strategies with small and large rodent models', *J Vis Exp*: e51194.

Ross, S. B. 1976. 'Long-term effects of N-2-chlorethyl-N-ethyl-2-bromobenzylamine hydrochloride on noradrenergic neurones in the rat brain and heart', *Br J Pharmacol*, 58: 521-7.

Ross, S. B., and A. L. Renyl. 1976. 'On the long-lasting inhibitory effect of N-(2-chloroethyl)-N-ethyl-2-bromobenzylamine (DSP 4) on the active uptake of noradrenaline', *J Pharm Pharmacol*, 28: 458-9.

Sara, S. J. 2009. 'The locus coeruleus and noradrenergic modulation of cognition', *Nat Rev Neurosci*, 10.

Schiffrin, E. L., L. Y. Deng, and P. Larochelle. 1992. 'Blunted effects of endothelin upon small subcutaneous resistance arteries of mild essential hypertensive patients', *J Hypertens*, 10: 437-44.

Schneider, J. A., Z. Arvanitakis, S. E. Leurgans, and D. A. Bennett. 2009. 'The neuropathology of probable Alzheimer disease and mild cognitive impairment', *Ann Neurol*, 66: 200-8.

Schulz, D., J. P. Huston, T. Buddenberg, and B. Topic. 2007. '"Despair" induced by extinction trials in the water maze: relationship with measures of anxiety in aged and adult rats', *Neurobiol Learn Mem*, 87: 309-23.

Skoog, I., A. Wallin, P. Fredman, C. Hesse, O. Aevarsson, I. Karlsson, C. G. Gottfries, and K. Blennow. 1998. 'A population study on blood-brain barrier function in 85-year-olds: relation to Alzheimer's disease and vascular dementia', *Neurology*, 50: 966-71.

Stoiljkovic, M., C. Kelley, B. Stutz, T. L. Horvath, and M. Hajos. 2018. 'Altered Cortical and Hippocampal Excitability in TgF344-AD Rats Modeling Alzheimer's Disease Pathology', *Cereb Cortex*.

Sun, M. K., and D. L. Alkon. 2004. 'Induced depressive behavior impairs learning and memory in rats', *Neuroscience*, 129: 129-39.

Szabadi, E. 2013. 'Functional neuroanatomy of the central noradrenergic system', *J Psychopharmacol*, 27: 659-93.

Szot, P., C. Miguelez, S. S. White, A. Franklin, C. Sikkema, C. W. Wilkinson, L. Ugedo, and M. A. Raskind. 2010. 'A comprehensive analysis of the effect of DSP4 on the locus coeruleus noradrenergic system in the rat', *Neuroscience*, 166: 279-91.

Theofilas, P., A. J. Ehrenberg, S. Dunlop, A. T. Di Lorenzo Alho, A. Nguy, R. E. P. Leite, R. D. Rodriguez, M. B. Mejia, C. K. Suemoto, R. E. L. Ferretti-Rebustini, L. Polichiso, C. F. Nascimento, W. W. Seeley, R. Nitrini, C. A. Pasqualucci, W.

Jacob Filho, U. Rueb, J. Neuhaus, H. Heinsen, and L. T. Grinberg. 2017. 'Locus coeruleus volume and cell population changes during Alzheimer's disease progression: A stereological study in human postmortem brains with potential implication for early-stage biomarker discovery', *Alzheimers Dement*, 13: 236-46.

Toussay, X., K. Basu, B. Lacoste, and E. Hamel. 2013. 'Locus coeruleus stimulation recruits a broad cortical neuronal network and increases cortical perfusion', *J Neurosci*, 33: 3390-401.

Tsai, Y., B. Lu, A. V. Ljubimov, S. Girman, F. N. Ross-Cisneros, A. A. Sadun, C. N. Svendsen, R. M. Cohen, and S. Wang. 2014. 'Ocular changes in TgF344-AD rat model of Alzheimer's disease', *Invest Ophthalmol Vis Sci*, 55: 523-34.

Walf, A. A., and C. A. Frye. 2007. 'The use of the elevated plus maze as an assay of anxiety-related behavior in rodents', *Nat Protoc*, 2: 322-8.

Weinshenker, D. 2008. 'Functional consequences of locus coeruleus degeneration in Alzheimer's disease', *Curr Alzheimer Res*, 5.

Wilson, R. S., S. Nag, P. A. Boyle, L. P. Hizel, L. Yu, A. S. Buchman, J. A. Schneider, and D. A. Bennett. 2013. 'Neural Reserve, Neuronal Density in the Locus Coeruleus, and Cognitive Decline', *Neurology*, 80.

Wisniewski, H. M., and P. B. Kozlowski. 1982. 'Evidence for blood-brain barrier changes in senile dementia of the Alzheimer type (SDAT)', *Ann N Y Acad Sci*, 396: 119-29.

Wisniewski, H. M., A. W. Vorbrodt, and J. Wegiel. 1997. 'Amyloid angiopathy and blood-brain barrier changes in Alzheimer's disease', *Ann N Y Acad Sci*, 826: 161-72.

Wrenn, C. C., M. J. Picklo, D. A. Lappi, D. Robertson, and R. G. Wiley. 1996. 'Central noradrenergic lesioning using anti-DBH-saporin: anatomical findings', *Brain Res*, 740: 175-84.

Yang, S., A. F. Smit, S. Schwartz, F. Chiaromonte, K. M. Roskin, D. Haussler, W. Miller, and R. C. Hardison. 2004. 'Patterns of insertions and their covariation with substitutions in the rat, mouse, and human genomes', *Genome Res*, 14: 517-27.

Youmans, K. L., L. M. Tai, T. Kanekiyo, W. B. Stine, Jr., S. C. Michon, E. Nwabuisi-Heath, A. M. Manelli, Y. Fu, S. Riordan, W. A. Eimer, L. Binder, G. Bu, C. Yu, D. M. Hartley, and M. J. LaDu. 2012. 'Intraneuronal Abeta detection in 5xFAD mice by a new Abeta-specific antibody', *Mol Neurodegener*, 7: 8.

Chapter 4: Discussion

Introduction

In this present dissertation, we tested the hypothesis that significant LC degeneration occurred prior to the onset of cognitive impairment linked to AD and thus influenced a broad range of neuronal and vascular pathophysiology observed in later stages of disease severity. My first goal was to examine the extent of LC degeneration prior to the onset of MCI using postmortem tissue from UKADC subjects who were diagnosed with NCI (Braak neuropathological stages 0-II), PCAD (Braak III/IV), MCI, or mild AD, and correlate these findings with measures of cognition, AD pathology and vascular pathology. To better understand the mechanisms linking LC degeneration, neurovascular pathology, and cognition, my second goal was to lesion the LC projection system in a rat model of AD to test its effects on cognitive behaviors and markers of AD-related neuropathology and vascular dysfunction. Taken together, these goals formed the foundation of my Specific Aims, which were designed to fill a knowledge gap on the extent to which LC NE projection system degeneration contributes to neuronal and vascular pathology during the transition from normal cognition to incipient disease. Given the renewed interest in vascular contributions to AD (Kisler et al. 2017; Snyder et al. 2015), our hope was that the results of this dissertation project would reveal a novel role for noradrenergic signaling loss in driving cognitive impairment in AD through its effects on cerebrovascular integrity in target fields, thus providing new insights into molecular pathogenic mechanisms and therapeutic targets of disease.

Chapter 2: Characterizing LC vascular and AD pathology in PCAD

Aim 1 findings, in brief

In **Chapter 2,** we quantified and analyzed the pathology of LC neurons in individuals classified as NCI, PCAD, MCI or AD. We noted a significant decrease in TH-positive LC cells in MCI and AD, and also observed marked differences in the topography of cell loss in individuals classified as PCAD. This cell loss was also significantly correlated with global cognition as measured by the MMSE. Further, we noted that arteriosclerosis in areas surrounding the pons was increased in MCI and AD compared to both NCI and PCAD groups, indicating that arteriosclerosis and vessel health of the pons may be related to LC vulnerability and cognitive status. IHC studies of AT8 tau reactivity in the LC revealed significantly increased LC-tangle burden in PCAD, MCI and AD cases compared to control and these measures significantly correlated with global Braak stage and TH-positive LC number. Additionally, DNA/RNA oxidative damage was significantly increased in MCI and AD and the ratio of LC neurons bearing this oxidative stress marker negatively associated with both LC number and MMSE score. Together, this chapter elucidated that while subjects classified as PCAD show increased pre-tangle pathology, they significantly differ from NCI subjects only in the topography of progressive LC cell loss during AD.

Study limitations

Due to the nature of the pontine tissue that we received from the UKADC, we could not perform unbiased stereology for these samples. Formalin fixed, paraffin-embedded tissue sectioned at 20μm does not allow for establishing guard heights necessary to

properly utilize the optical dissector probe. This could have impacted how accurate our estimates were, but nevertheless, our counts were consistent with previous reports from our lab and others, although the PCAD group was not systematically examined as in the present study (Kelly et al. 2017; Arendt et al. 2015; Theofilas et al. 2017). Further, the paraffin embedded form of our tissue did not allow us to investigate certain conformational isoforms of tau (e.g. TNT1, TOC1, etc.; Combs, Hamel, and Kanaan 2016) due to the nature of retrieval necessary to unmask antigenicity. Free floating tissue would have enabled us to examine these epitopes, thus enabling us to further character LC NFT formation, in addition to giving us the required thickness for unbiased stereology. However, we can now appreciate that the biggest hindrance to our study was the sample size due to the limited number of cases for each diagnostic group that met the appropriate clinical neuropathologic criteria and tissue integrity requirements for case selection. Whereas our initial power calculation suggested that even 6 cases would be sufficient for the detetion of moderate effect sizes, our data now indicate an n> 20 cases/ sample set would be powered to elucidate differences between NCI and PCAD classifications due to the heterogeneity of the two groups.

Study implications and future directions

Here we demonstrated that TH-positive, noradrenergic LC neurons are vulnerable during the onset of dementia as evidenced by their differential pathological patterns in PCAD compared to NCI, neuron loss in MCI and AD, and the association of this loss with measures of cognitive deterioration and neuropathological accumulation. For instance, while our TH-positive LC counts did not correlate with Braak staging, AT8

immunoreactivity in the LC did. This is interesting as Braak staging does not consider the brainstem in its pathological assessment (Braak and Braak 1991) and thus LC NFT burden may be a better indicator of disease severity than global NFT burden (Braak and Del Tredici 2012). Further, the discovery that PCAD subjects display no differences between NCI individuals other than topography of LC cell loss and NFT burden, indicates that these subjects may represent a population of cognitively resilient individuals (i.e. capable of withstanding higher AD pathology).

The concept of "cognitive resilience" attempts to explain how some individuals are able to maintain normal cognitive performance despite pathological disease burden (Katzman 1993; Stern 2012), thus possibly delaying or reducing the risk of developing clinical presentation of dementia. Based on advances in positron emission tomography (PET) using radiotracers that bind to Aβ (Klunk et al. 2004), along with postmortem pathological assessments (Sperling et al. 2011), we now understand that AD includes a long preclinical stage whereby cognitively normal individuals may display certain biomarker abnormalities approximately 15 years prior to the onset of dementia (Bateman et al. 2012; Rowe et al. 2010; Sperling et al. 2011). Recent studies by Bennett and colleagues found that both Aβ and NFTs are related to cognition in persons without dementia (Bennett et al. 2012; Boyle et al. 2013). As the field moves toward the identification and possible intervention of individuals with PCAD, the factors that influence the relationships among cognition and pathologic burden have important implications.

To further investigate the PCAD population it would be of interest to characterize and possibly subdivide the heterogenous population. Separating PCAD individuals with

vascular risk factors or vascular comorbidities from those without and comparing their LC populations could help us further understand if the PCAD group is, in fact, a pre-MCI population and if LC dysfunction is truly an initiating site of vascular pathology. Further, as degeneration of cholinergic NB is a well-known hallmark of AD, characterizing its degeneration in the PCAD population alongside the LC could help to shed light on disease progression. This information would be aided by including additional neurodegenerative disorders such as Parkinson's disease, vascular dementia, and Lewy body dementia as neurologic controls for the specificity and sensitivity of our observations for AD pathogenesis. Additionally, LC dysfunction has been implicated in psychiatric disorders such as schizophrenia, anxiety, and depression, and demyelinating conditions such as multiple sclerosis. Comparing the LC cell populations of these groups with not only stereological methods, but topographical analyses could help shed light on LC subpopulations sub-serving cognition and behavior, especially in preclinical populations.

A novel aspect of our study looked at arteriosclerosis specifically in the pons and noted increased arteriosclerosis in MCI and AD. Looking even more in depth at pontine vascular health could elucidate mechanisms of LC toxicant burden (Pamphlett 2014), and metabolic deficits (Kelly et al. 2017). Furthermore, the trending relationship between LC cell number and arteriosclerosis severity indicates that survival of LC cells could be in part related to the vascular health of surrounding LC vessels. As the LC sits on one of the biggest capillary beds in the CNS (Finley 1940), toxicants could enter LC neurons aided by the extensive exposure these neurons have to the vasculature, as well as by stressors that upregulate LC activity (Pamphlett 2014; Kelly et al. 2017;

Kalinin et al. 2006). Investigating other measures of vascular dysfunction such as hemorrhages in the pons could be of added value. Of note, some UKADC blocks did have observable hemorrhaging in the LC and investigating the consequence of LC microbleeds warrants further investigation with larger cohorts **(Figure 4.1**).

In the UKADC cohort we also investigated markers of LC DNA/RNA damage and noticed a profound increase in the damage ratio of MCI and AD individuals. Previous reports have indicated both molecular dysregulation of mitochondrial function and neuritic/structural plasticity coinciding with the loss of LC neurons prior to the transition from NCI to prodromal AD (Kelly et al. 2017). It has also been shown that insulin resistance impairs glucose metabolism and mitochondrial function, thus increasing production of reactive oxygen species (Abolhassani et al. 2017). Additionally, in MCI, mitochondrial dysfunction and oxidative damage may induce synaptic dysfunction due to energy failures in neurons thus resulting in impaired cognitive function (Leon et al. 2016). Therefore, the previously observed mitochondrial dysfunction in MCI could lead to the presently described increases in DNA and RNA oxidative damage in the LC, with subsequent implications for cognitive impairment.

Notably, NE, the primary neurotransmitter of LC neurons, may in itself be a risk factor (Weinshenker 2018). NE is sequestered inside synaptic vesicles by the vesicular monoamine transporter 2 (VMAT2), but after synaptic release, it is taken up into the cytoplasm by the NE transporter (NET). Alternately, cytoplasmic NE can autoxidize or be converted to chemically reactive and toxic metabolites [e.g., 3,4 dihydroxyphenylglycolaldehyde (DOPEGAL)] by monoamine oxidase (MAO), which can then cause subsequent damage to proteins, lipids, and nucleotides (Goldstein 2013).

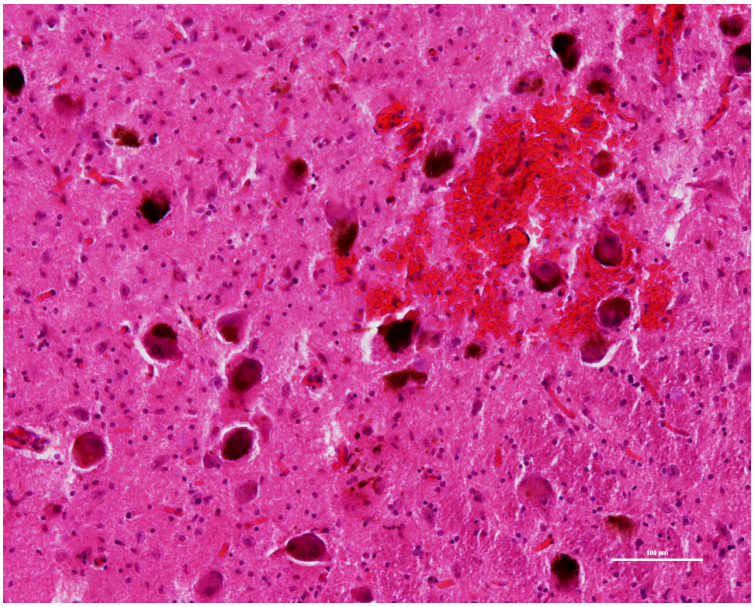

Figure 4.1 Pontine microbleed in UKADC tissue

Hemorrhaging in/around the LC is evident in select cases of the UKADC cohort and warrants further investigation. LC cells visualized via black-brown neuromelanin pigmentation. Sale bar = 100um.

Thus, if LC hyperactivity is a putative preclinical phenomenon in AD similar to that proposed for the medial temporal lobe (Kircher et al. 2007), then increased NE turnover and DOPEGAL production could lead to further cellular stress. This concept is ripe for future exploration.

Finally, relating LC cell pathology to corresponding target field alterations in LC afferents could help further illuminate the connection between LC cell pathology or number, and cognition. Studies have shown that while the LC may be an initiating site of degeneration, these cells may be able to withstand pathologies for decades before having any symptomatic presentation. For example, hyperphosphorylated tau can be detected in the LC before anywhere else in the brain, sometimes during the first few decades of life, (Braak and Del Tredici 2012, 2011; Braak et al. 2011). Similarly, α-synuclein pathology appears in LC neurons before the substantia nigra pars compacta, the canonical midbrain dopaminergic nucleus that controls motor function (Braak and Del Tredici 2017; Braak et al. 2003). Hence, understanding the extent of LC afferent degeneration and firing dysregulation as LC pathology and cell loss accrues during PCAD and MCI could provide valuable therapeutic insights for strategies aimed at maintaining proper LC function during AD and related dementias.

Chapter 3: Consequences of LC deafferentation in a rat model of AD

Aim 2 findings, in brief

In **Chapter 3**, we lesioned LC noradrenergic afferents of the PFC, with accompanying LC call loss, using a NE specific immunotoxin DBH-sap in the TgF344 rat model of AD at 6 months of age. This lesion produced stark differences in spatial and working memory at 2 weeks post-op that was sustained 6 weeks post-op. We quantified the

intensity of fiber loss and this was accompanied with increased amyloid burden in both the cortex and hippocampus and accompanying microgliosis. Interestingly, DBH-sap lesioned rats exhibited increased WLR in cortical arterioles indicating a loss of vascular tone as a result of LC deafferentation. This was accompanied by evidence of BBB disruption indicated by parenchymal albumin deposition and astrogliosis.

Study limitations

While the novel TgF344 rat offered the ability to investigate the mechanisms of LC cell loss in AD, we were limited in our ability to claim a truly “preclinical model” due to the acute onset and robust nature of our lesion. Further studies with more diffuse lesions may be able to better model subtle changes in LC cell loss over time, perhaps using comprehensive pretesting of animals with various dose and time titrations of DBH-sap. In addition, we are cognizant that a caveat to the Barnes Maze task is that it is often thought to lack sufficient motivating factors (i.e. negative stimuli), however, the Morris water maze is undoubtedly more stressful compared to the Barnes Maze, and motivation can be increased with noise and lighting intensity during training. Since mice and rats are more physiologically adapted to dry land tasks, this confers an advantage to the Barnes Maze task to better elucidate certain learning/navigation behaviors in these animals (Whishaw and Tomie 1996). Furthermore, our rats were not able to replicate previously reported endogenous tau pathology (Cohen et al. 2013; Rorabaugh et al. 2017) but this may be because they were too young. True preclinical modeling would hopefully have some LC NFT pathology at this stage based on previous neuropathological examinations in humans (Braak and Del Tredici 2011; Braak et al.

2011). Finally, we were unable to perform studies of LC effects on *in vivo* neurovascular coupling/functional hyperemia (Bekar, Wei, and Nedergaard 2012), which would have involved separate cohorts and two-photon microscopic procedures. Finally, we are aware of the evidence that LC projection neurons release other neurochemical transmitters along with NE, albeit at much lower levels, such as neuropeptide Y, galanin, dopamine, and even BDNF (Holets et al. 1988; Fawcett et al. 1998; Kempadoo et al. 2016; Counts et al. 2006), suggesting that loss of these molecules with LC degeneration may also contribute to our outcomes. This could be addressed in future studies using LC-targeted RNA interference prior to the lesion.

Study implications and future directions

In this chapter we showed that lesioning the LC can produce profound behavioral deficits on tests designed to measure spatial and working/procedural memory function in TgF344 AD rats. Previous studies have shown that LC lesions exacerbate cognitive deficits in APP transgenic mouse models of AD, while enhancement of NE transmission via increasing NE synthesis or inhibiting reuptake can ameliorate these deficits (Jardanhazi-Kurutz et al. 2010; Kalinin et al. 2012; Hammerschmidt et al. 2013; Kummer et al. 2014; Totah, Logothetis, and Eschenko 2015). Additionally, LC stimulation or pharmacological increases in NE levels have been shown to enhance performance in spatial learning and reversal learning in multiple behavioral tasks (Hansen and Manahan-Vaughan 2015; Totah, Logothetis, and Eschenko 2015; Rorabaugh et al. 2017). To this end, using our DBH-sap lesioned TgF344 (or a variant thereof) in conjunction with NE replacement therapies could help gain insight into

mechanisms of NE based pharmacologic intervention on our outcomes, particularly the forebrain vascular pathology induced by LC projection system degeneration (Biaggioni and Robertson 1987). Of note, L-Dihydroxyphenylserine (L-DOPS), a synthetic catecholamine acid that when ingested is converted to NE via decarboxylation catalyzed by L-aromatic-amino-acid decarboxylase (LAAAD)(Goldstein 2006) and has already been approved for use in the treatment of hypotension, could be used to address this question as preclinical proof of principle.

For other further studies it could be of value to clarify if vascular insults alone, could amplify AD pathology and behavior in these TgF344 animals or if these are merely a result of NE loss as NE has been shown to be a mediator of vascular tone and neurovascular coupling (Cohen, Molinatti, and Hamel 1997; Bekar, Wei, and Nedergaard 2012). Specifically, inducing strokes or hypertension in the “preclinical” stage (<9months old) via endothelin, middle cerebral artery occlusion or bilateral carotid artery stenosis could help shed light on other mechanisms of CVD and AD related neurodegeneration as LC cell loss may not be the “initiating event”. Alternatively, modeling dietary risk factors through high fat or high salt diet could provide insights into the relative roles of CVD and LC cell loss on cognition and AD pathogenesis (Liu et al. 2014).

Finally, studies have shown success using another saporin (192-sap) which is specific to cholinergic cells like those of the nucleus basalis of Meynert (NB) of the basal forebrain (Turnbull, Boskovic, and Coulson 2018; Berger-Sweeney et al. 2001). The immunotoxin is specific to the p75NTR pan-neurotrophin receptor. As it is well known that the NB also degenerates in MCI and AD (Mufson et al. 2002; Mufson et al. 2000;

Price et al. 1991; Tiernan et al. 2016), lesioning the LC and the NB in parallel could produce an even more complete model of the early neurodegeneration seen in AD. Preliminary studies in our lab have noted distinct behavioral phenotypes between wild type F344 rats lesioned with DBH-sap or 192-sap (**Figure 4.2**), so a combined lesion may produce a more severe phenotype more attributable to that observed in AD. Furthermore, given the known central regulatory effects of both NE and acetylcholine on cerebrovascular integrity (Sato, Sato, and Uchida 2004; Radu et al. 2017; Librizzi, Folco, and de Curtis 2000; Bekar, Wei, and Nedergaard 2012; Cohen, Molinatti, and Hamel 1997; Szabadi 2013), moderate lesioning of both of these nuclei could produce profound vascular pathology in the TgF344 rat that better replicates the complex interplay of neuronal and vascular pathology postulated to impact the progression of AD (Iadecola and Dirnagl 2013).

Final remarks

Collectively the results in this dissertation support the hypothesis that LC dysfunction and degeneration may be an initiating event in the transition of preclinical AD to incipient disease through its dual effects on vascular and neuropathology **(Figure 4.3).** Completion of the Specific Aims of this dissertation supports the hypothesis that vascular dysfunction accompanies LC cell loss both in the local pontine environment (Chapter 2, observed as arteriosclerosis) or in LC projection zones (Chapter 3, observed as BBB remodeling/leakage in the PFC). Additional support of this hypothesis would be provided by a more comprehensive study of the pathological differences between NCI, PCAD, and MCI using larger sample sizes and tissue from both the LC

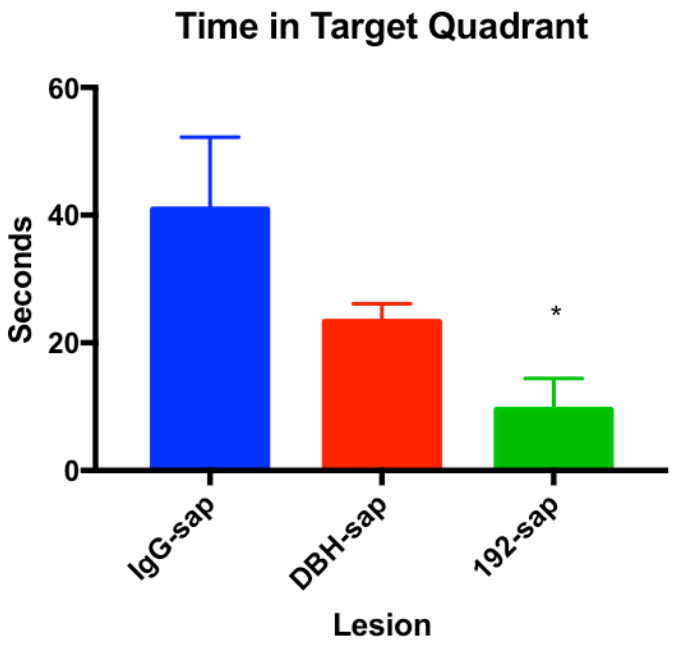

Figure 4.2 Saporin lesion differences in Barnes maze performance

Preliminary data showing impaired performance of WT F344 rats lesioned with DBH sap (trending p=0.12) and 192(p=0.0398) during probe trial of Barnes maze task via ANOVA with Tukey's *post hoc* (see **Table 3.1** for protocol). Error bars=SEM, n=3/group.

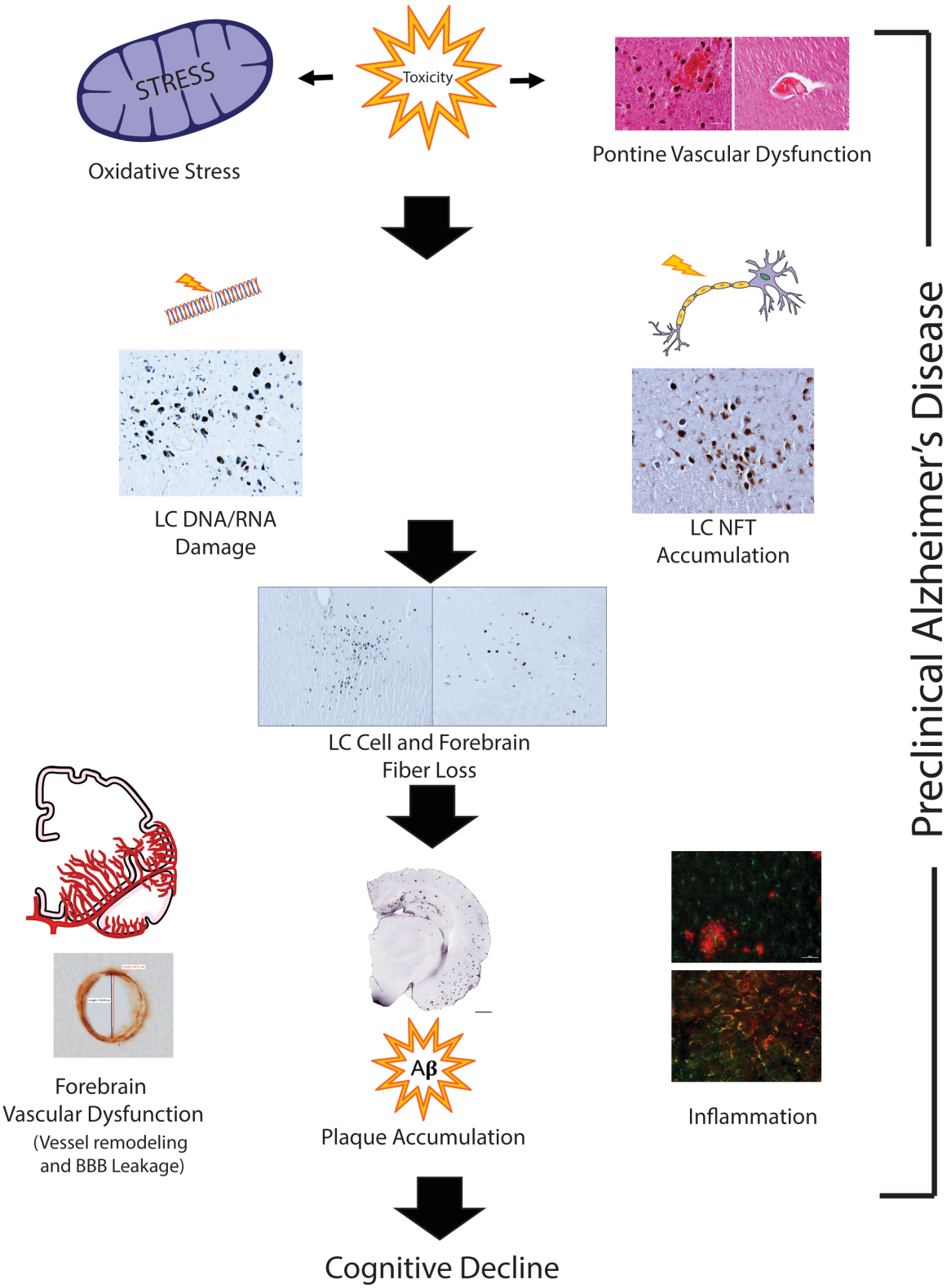

Figure 4.3 LC dysfunction and degeneration may be a critical event in the transition of preclinical AD to incipient disease

Figure 4.3 (cont'd)

Initiating events such as oxidative stress and vascular dysfunction (e.g., reduced CBF) surrounding the LC along with other possible mechanisms of LC toxicity may alter key cellular and molecular pathways within noradrenergic neurons via increased DNA/RNA oxidative damage and other insults, potentially leading to NFT formation and tau-mediated cell toxicity. This may lead to LC cell death and subsequent deafferentation of LC forebrain target fields. Loss of the LC-NE projection system could then cause a loss in vascular tone, leading to vessel remodeling, plaque accumulation, BBB dysfunction and associated neuroinflammation. Evidence in this dissertation suggests that all of these pathologies occur in some form before the onset of cognitive decline (i.e., MCI, AD).

and PFC of the same subjects. Characterization of the vascular comorbidities commonly seen in AD is also necessary to determine if they are a cause/ consequence of LC degeneration, or simply act in parallel to this degeneration. Moreover, further characterization (e.g., neurovascular coupling effects) and optimization of the DBH-sap lesion in TgF344 rat would be beneficial for providing much needed preclinical models of AD. The results of this dissertation provide compelling rationale for using these improved models to test treatments based on modulating forebrain NE levels or LC neuroprotection (Chamberlain and Robbins 2013) as a mechanism of disease modification for AD and possibly other dementias.

LITERATURE CITED

LITERATURE CITED

Abolhassani, N., J. Leon, Z. Sheng, S. Oka, H. Hamasaki, T. Iwaki, and Y. Nakabeppu. 2017. 'Molecular pathophysiology of impaired glucose metabolism, mitochondrial dysfunction, and oxidative DNA damage in Alzheimer's disease brain', *Mech Ageing Dev*, 161: 95-104.

Arendt, T., M. K. Bruckner, M. Morawski, C. Jager, and H. J. Gertz. 2015. 'Early neurone loss in Alzheimer's disease: cortical or subcortical?', *Acta Neuropathol Commun*, 3: 10.

Bateman, R. J., C. Xiong, T. L. Benzinger, A. M. Fagan, A. Goate, N. C. Fox, D. S. Marcus, N. J. Cairns, X. Xie, T. M. Blazey, D. M. Holtzman, A. Santacruz, V. Buckles, A. Oliver, K. Moulder, P. S. Aisen, B. Ghetti, W. E. Klunk, E. McDade, R. N. Martins, C. L. Masters, R. Mayeux, J. M. Ringman, M. N. Rossor, P. R. Schofield, R. A. Sperling, S. Salloway, J. C. Morris, and Network Dominantly Inherited Alzheimer. 2012. 'Clinical and biomarker changes in dominantly inherited Alzheimer's disease', *N Engl J Med*, 367: 795-804.

Bekar, L. K., H. S. Wei, and M. Nedergaard. 2012. 'The locus coeruleus-norepinephrine network optimizes coupling of cerebral blood volume with oxygen demand', *J Cereb Blood Flow Metab*, 32: 2135-45.

Bennett, D. A., R. S. Wilson, P. A. Boyle, A. S. Buchman, and J. A. Schneider. 2012. 'Relation of neuropathology to cognition in persons without cognitive impairment', *Ann Neurol*, 72: 599-609.

Berger-Sweeney, J., N. A. Stearns, S. L. Murg, L. R. Floerke-Nashner, D. A. Lappi, and M. G. Baxter. 2001. 'Selective immunolesions of cholinergic neurons in mice: effects on neuroanatomy, neurochemistry, and behavior', *J Neurosci*, 21: 8164-73.

Biaggioni, I., and D. Robertson. 1987. 'Endogenous restoration of noradrenaline by precursor therapy in dopamine-beta-hydroxylase deficiency', *Lancet*, 2: 1170-2.

Boyle, P. A., L. Yu, R. S. Wilson, J. A. Schneider, and D. A. Bennett. 2013. 'Relation of neuropathology with cognitive decline among older persons without dementia', *Front Aging Neurosci*, 5: 50.

Braak, H., and E. Braak. 1991. 'Neuropathological stageing of Alzheimer-related changes', *Acta Neuropathol*, 82.

Braak, H., and K. Del Tredici. 2011. 'The pathological process underlying Alzheimer's disease in individuals under thirty', *Acta Neuropathol*, 121: 171-81.

———. 2012. 'Where, when, and in what form does sporadic Alzheimer's disease begin?', *Curr Opin Neurol*, 25: 708-14.

———. 2017. 'Neuropathological Staging of Brain Pathology in Sporadic Parkinson's disease: Separating the Wheat from the Chaff', *J Parkinsons Dis*, 7: S71-S85.

Braak, H., K. Del Tredici, U. Rub, R. A. de Vos, E. N. Jansen Steur, and E. Braak. 2003. 'Staging of brain pathology related to sporadic Parkinson's disease', *Neurobiol Aging*, 24: 197-211.

Braak, H., D. R. Thal, E. Ghebremedhin, and K. Del Tredici. 2011. 'Stages of the pathologic process in Alzheimer disease: age categories from 1 to 100 years', *J Neuropathol Exp Neurol*, 70: 960-9.

Chamberlain, S. R., and T. W. Robbins. 2013. 'Noradrenergic modulation of cognition: therapeutic implications', *J Psychopharmacol*, 27: 694-718.

Cohen, R. M., K. Rezai-Zadeh, T. M. Weitz, A. Rentsendorj, D. Gate, I. Spivak, Y. Bholat, V. Vasilevko, C. G. Glabe, J. J. Breunig, P. Rakic, H. Davtyan, M. G. Agadjanyan, V. Kepe, J. R. Barrio, S. Bannykh, C. A. Szekely, R. N. Pechnick, and T. Town. 2013. 'A transgenic Alzheimer rat with plaques, tau pathology, behavioral impairment, oligomeric abeta, and frank neuronal loss', *J Neurosci*, 33: 6245-56.

Cohen, Z., G. Molinatti, and E. Hamel. 1997. 'Astroglial and vascular interactions of noradrenaline terminals in the rat cerebral cortex', *J Cereb Blood Flow Metab*, 17: 894-904.

Combs, B., C. Hamel, and N. M. Kanaan. 2016. 'Pathological conformations involving the amino terminus of tau occur early in Alzheimer's disease and are differentially detected by monoclonal antibodies', *Neurobiol Dis*, 94: 18-31.

Counts, S. E., E. Y. Chen, S. Che, M. D. Ikonomovic, J. Wuu, S. D. Ginsberg, S. T. Dekosky, and E. J. Mufson. 2006. 'Galanin fiber hypertrophy within the cholinergic nucleus basalis during the progression of Alzheimer’s disease', *Dement Geriatr Cogn Disord*, 21.

Fawcett, J. P., S. X. Bamji, C. G. Causing, R. Aloyz, A. R. Ase, T. A. Reader, J. H. McLean, and F. D. Miller. 1998. 'Functional evidence that BDNF is an

Finley, Cobb. 1940. 'The capillary bed of the locus coeruleus', *Journal of comparative neurology*, 73: 49-58.

Goldstein, D. S. 2006. 'L-Dihydroxyphenylserine (L-DOPS): a norepinephrine prodrug', *Cardiovasc Drug Rev*, 24: 189-203.

———. 2013. 'Biomarkers, mechanisms, and potential prevention of catecholamine neuron loss in Parkinson disease', *Adv Pharmacol*, 68: 235-72.

Hammerschmidt, T., M. P. Kummer, D. Terwel, A. Martinez, A. Gorji, H. C. Pape, K. S. Rommelfanger, J. P. Schroeder, M. Stoll, J. Schultze, D. Weinshenker, and M. T. Heneka. 2013. 'Selective loss of noradrenaline exacerbates early cognitive dysfunction and synaptic deficits in APP/PS1 mice', *Biol Psychiatry*, 73: 454-63.

Hansen, N., and D. Manahan-Vaughan. 2015. 'Locus Coeruleus Stimulation Facilitates Long-Term Depression in the Dentate Gyrus That Requires Activation of beta-Adrenergic Receptors', *Cereb Cortex*, 25: 1889-96.

Holets, V. R., T. Hokfelt, A. Rokaeus, L. Terenius, and M. Goldstein. 1988. 'Locus coeruleus neurons in the rat containing neuropeptide Y, tyrosine hydroxylase or galanin and their efferent projections to the spinal cord, cerebral cortex and hypothalamus', *Neuroscience*, 24: 893-906.

Iadecola, C., and U. Dirnagl. 2013. 'The microcircualtion--fantastic voyage: introduction', *Stroke*, 44: S83.

Jardanhazi-Kurutz, D., M. P. Kummer, D. Terwel, K. Vogel, T. Dyrks, A. Thiele, and M. T. Heneka. 2010. 'Induced LC degeneration in APP/PS1 transgenic mice accelerates early cerebral amyloidosis and cognitive deficits', *Neurochem Int*, 57: 375-82.

Kalinin, S., D. L. Feinstein, H. L. Xu, G. Huesa, D. A. Pelligrino, and E. Galea. 2006. 'Degeneration of noradrenergic fibres from the locus coeruleus causes tight-junction disorganisation in the rat brain', *Eur J Neurosci*, 24: 3393-400.

Kalinin, S., P. E. Polak, S. X. Lin, A. J. Sakharkar, S. C. Pandey, and D. L. Feinstein. 2012. 'The noradrenaline precursor L-DOPS reduces pathology in a mouse model of Alzheimer’s disease', *Neurobiol Aging*, 33.

Katzman, R. 1993. 'Education and the prevalence of dementia and Alzheimer's disease', *Neurology*, 43: 13-20.

Kelly, S. C., B. He, S. E. Perez, S. D. Ginsberg, E. J. Mufson, and S. E. Counts. 2017. 'Locus coeruleus cellular and molecular pathology during the progression of Alzheimer's disease', *Acta Neuropathol Commun*, 5: 8.

Kempadoo, K. A., E. V. Mosharov, S. J. Choi, D. Sulzer, and E. R. Kandel. 2016. 'Dopamine release from the locus coeruleus to the dorsal hippocampus promotes spatial learning and memory', *Proc Natl Acad Sci U S A*, 113: 14835-40.

Kircher, T. T., S. Weis, K. Freymann, M. Erb, F. Jessen, W. Grodd, R. Heun, and D. T. Leube. 2007. 'Hippocampal activation in patients with mild cognitive impairment

is necessary for successful memory encoding', *J Neurol Neurosurg Psychiatry*, 78: 812-8.

Kisler, K., A. R. Nelson, A. Montagne, and B. V. Zlokovic. 2017. 'Cerebral blood flow regulation and neurovascular dysfunction in Alzheimer disease', *Nat Rev Neurosci*, 18: 419-34.

Klunk, W. E., H. Engler, A. Nordberg, Y. Wang, G. Blomqvist, D. P. Holt, M. Bergstrom, I. Savitcheva, G. F. Huang, S. Estrada, B. Ausen, M. L. Debnath, J. Barletta, J. C. Price, J. Sandell, B. J. Lopresti, A. Wall, P. Koivisto, G. Antoni, C. A. Mathis, and B. Langstrom. 2004. 'Imaging brain amyloid in Alzheimer's disease with Pittsburgh Compound-B', *Ann Neurol*, 55: 306-19.

Kummer, M. P., T. Hammerschmidt, A. Martinez, D. Terwel, G. Eichele, A. Witten, S. Figura, M. Stoll, S. Schwartz, H. C. Pape, J. L. Schultze, D. Weinshenker, M. T. Heneka, and I. Urban. 2014. 'Ear2 deletion causes early memory and learning deficits in APP/PS1 mice', *J Neurosci*, 34: 8845-54.

Leon, J., K. Sakumi, E. Castillo, Z. Sheng, S. Oka, and Y. Nakabeppu. 2016. '8-Oxoguanine accumulation in mitochondrial DNA causes mitochondrial dysfunction and impairs neuritogenesis in cultured adult mouse cortical neurons under oxidative conditions', *Sci Rep*, 6: 22086.

Librizzi, L., G. Folco, and M. de Curtis. 2000. 'Nitric oxide synthase inhibitors unmask acetylcholine-mediated constriction of cerebral vessels in the in vitro isolated guinea-pig brain', *Neuroscience*, 101: 283-7.

Liu, Y. Z., J. K. Chen, Z. P. Li, T. Zhao, M. Ni, D. J. Li, C. L. Jiang, and F. M. Shen. 2014. 'High-salt diet enhances hippocampal oxidative stress and cognitive impairment in mice', *Neurobiol Learn Mem*, 114: 10-5.

Mufson, E. J., S. Y. Ma, E. J. Cochran, D. A. Bennett, L. A. Beckett, S. Jaffar, H. U. Saragovi, and J. H. Kordower. 2000. 'Loss of nucleus basalis neurons containing trkA immunoreactivity in individuals with mild cognitive impairment and early Alzheimer's disease', *J Comp Neurol*, 427: 19-30.

Mufson, E. J., S. Y. Ma, J. Dills, E. J. Cochran, S. Leurgans, J. Wuu, D. A. Bennett, S. Jaffar, M. L. Gilmor, A. I. Levey, and J. H. Kordower. 2002. 'Loss of basal forebrain P75(NTR) immunoreactivity in subjects with mild cognitive impairment and Alzheimer's disease', *J Comp Neurol*, 443: 136-53.

Pamphlett, R. 2014. 'Uptake of environmental toxicants by the locus ceruleus: a potential trigger for neurodegenerative, demyelinating and psychiatric disorders', *Med Hypotheses*, 82: 97-104.

Price, J. L., P. B. Davis, J. C. Morris, and D. L. White. 1991. 'The distribution of tangles, plaques and related immunohistochemical markers in healthy aging and Alzheimer's disease', *Neurobiol Aging*, 12: 295-312.

Radu, B. M., A. M. M. Osculati, E. Suku, A. Banciu, G. Tsenov, F. Merigo, M. Di Chio, D. D. Banciu, C. Tognoli, P. Kacer, A. Giorgetti, M. Radu, G. Bertini, and P. F. Fabene. 2017. 'All muscarinic acetylcholine receptors (M1-M5) are expressed in murine brain microvascular endothelium', *Sci Rep*, 7: 5083.

Rorabaugh, J. M., T. Chalermpalanupap, C. A. Botz-Zapp, V. M. Fu, N. A. Lembeck, R. M. Cohen, and D. Weinshenker. 2017. 'Chemogenetic locus coeruleus activation restores reversal learning in a rat model of Alzheimer's disease', *Brain*, 140: 3023-38.

Rowe, C. C., K. A. Ellis, M. Rimajova, P. Bourgeat, K. E. Pike, G. Jones, J. Fripp, H. Tochon-Danguy, L. Morandeau, G. O'Keefe, R. Price, P. Raniga, P. Robins, O. Acosta, N. Lenzo, C. Szoeke, O. Salvado, R. Head, R. Martins, C. L. Masters, D. Ames, and V. L. Villemagne. 2010. 'Amyloid imaging results from the Australian Imaging, Biomarkers and Lifestyle (AIBL) study of aging', *Neurobiol Aging*, 31: 1275-83.

Sato, A., Y. Sato, and S. Uchida. 2004. 'Activation of the intracerebral cholinergic nerve fibers originating in the basal forebrain increases regional cerebral blood flow in the rat's cortex and hippocampus', *Neurosci Lett*, 361: 90-3.

Snyder, H. M., R. A. Corriveau, S. Craft, J. E. Faber, S. M. Greenberg, D. Knopman, B. T. Lamb, T. J. Montine, M. Nedergaard, C. B. Schaffer, J. A. Schneider, C. Wellington, D. M. Wilcock, G. J. Zipfel, B. Zlokovic, L. J. Bain, F. Bosetti, Z. S. Galis, W. Koroshetz, and M. C. Carrillo. 2015. 'Vascular contributions to cognitive impairment and dementia including Alzheimer's disease', *Alzheimers Dement*, 11: 710-7.

Sperling, R. A., P. S. Aisen, L. A. Beckett, D. A. Bennett, S. Craft, A. M. Fagan, T. Iwatsubo, C. R. Jack, Jr., J. Kaye, T. J. Montine, D. C. Park, E. M. Reiman, C. C. Rowe, E. Siemers, Y. Stern, K. Yaffe, M. C. Carrillo, B. Thies, M. Morrison-Bogorad, M. V. Wagster, and C. H. Phelps. 2011. 'Toward defining the preclinical stages of Alzheimer's disease: recommendations from the National Institute on Aging-Alzheimer's Association workgroups on diagnostic guidelines for Alzheimer's disease', *Alzheimers Dement*, 7: 280-92.

Stern, Y. 2012. 'Cognitive reserve in ageing and Alzheimer's disease', *Lancet Neurol*, 11: 1006-12.

Szabadi, E. 2013. 'Functional neuroanatomy of the central noradrenergic system', *J Psychopharmacol*, 27: 659-93.

Theofilas, P., A. J. Ehrenberg, S. Dunlop, A. T. Di Lorenzo Alho, A. Nguy, R. E. P. Leite, R. D. Rodriguez, M. B. Mejia, C. K. Suemoto, R. E. L. Ferretti-Rebustini, L. Polichiso, C. F. Nascimento, W. W. Seeley, R. Nitrini, C. A. Pasqualucci, W. Jacob Filho, U. Rueb, J. Neuhaus, H. Heinsen, and L. T. Grinberg. 2017. 'Locus coeruleus volume and cell population changes during Alzheimer's disease

progression: A stereological study in human postmortem brains with potential implication for early-stage biomarker discovery', *Alzheimers Dement*, 13: 236-46.

Tiernan, C. T., S. D. Ginsberg, A. L. Guillozet-Bongaarts, S. M. Ward, B. He, N. M. Kanaan, E. J. Mufson, L. I. Binder, and S. E. Counts. 2016. 'Protein homeostasis gene dysregulation in pretangle bearing nucleus basalis neurons during the progression of Alzheimer's disease', *Neurobiol Aging*, 42.

Totah, N. K., N. K. Logothetis, and O. Eschenko. 2015. 'Atomoxetine accelerates attentional set shifting without affecting learning rate in the rat', *Psychopharmacology (Berl)*, 232: 3697-707.

Turnbull, M. T., Z. Boskovic, and E. J. Coulson. 2018. 'Acute Down-regulation of BDNF Signaling Does Not Replicate Exacerbated Amyloid-beta Levels and Cognitive Impairment Induced by Cholinergic Basal Forebrain Lesion', *Front Mol Neurosci*, 11: 51.

Weinshenker, D. 2018. 'Long Road to Ruin: Noradrenergic Dysfunction in Neurodegenerative Disease', *Trends Neurosci*, 41: 211-23.

Whishaw, I. Q., and J. Tomie. 1996. 'Of mice and mazes: similarities between mice and rats on dry land but not water mazes', *Physiol Behav*, 60: 1191-7.